

Master's thesis

2019

Master's thesis

Erling Vingelsgård

**NTNU**  
Norwegian University of  
Science and Technology  
Faculty of Engineering  
Department of Energy and Process Engineering

Erling Vingelsgård

# Design and simulation of adsorption based solar ice maker

July 2019





Norwegian University of  
Science and Technology

# Design and simulation of adsorption based solar ice maker

**Erling Vingelsgård**

Energy and environment - Industrial process engineering

Submission date: July 2019

Supervisor: Trygve Magne Eikevik

Co-supervisor: Sourav Mitra, Ignat Tolstorebrov, Kristina Widell

Norwegian University of Science and Technology  
Department of Energy and Process Engineering





---

*Dedication*

*To my beloved parents, brothers, sister, friends, and girlfriend*

---

---

---

---

# Summary

Food waste and refrigerating systems with harmful working fluids are some of the most critical problems to address in the world concerning global warming and population increase. Currently, one-third of the food is wasted, and in developing countries such as India, the main problem is lack of a functional supply and cold chain. A possible solution for some of the cold chains is a solar-based adsorption ice maker. There are many small farmers, fishermen etc. living in rural areas suffering economic losses due to non-availability of suitable storage systems for their produce. Availability of reliable electrical power is one of the major issues for these people. Hence a simple system relying on renewable energy sources such as solar could be useful. An adsorption system operating intermittently will produce ice during the night and use solar energy during the day to drive the system.

The operation and dimensions of a small solar-based adsorption ice maker have been studied. Maxsorb III is currently the best adsorbent on the market and three working fluids (methanol, ethanol, R134a) have been simulated. The simulations are in three parts. Part one carried out a thermodynamic analysis of the most important parameters, part two looks at the thickness of the bed, and part three looks at the operation through a whole day. The calculations are based on climatic data from India and based on energy balances of the components of the system. R134a and Maxsorb III turn out not to be a good combination for intermittent operation, while methanol and ethanol show promising results in the thermodynamic analysis and simulation through the day. Methanol is the best working fluid for adsorption temperatures below 28°C and ethanol is the best working fluid for above 28°C. The thickness of the bed is calculated to a maximum of 7.5 cm to have a tolerant cooling time. The results show that a small scale adsorption ice maker with the dimensions of 1 m<sup>2</sup> solar collector, 20 kg of adsorbent and Indian solar conditions can provide cooling to people who previously did not have access to cooling almost all year round.

The work was partly done in India and Norway. A two and half month stay at IIT (Indian Institute of Technology) Kharagpur was completed to investigate the status and explore the possibilities of improving the cold chain. During the stay, a survey was made to map the knowledge and awareness of the cold chain. Most people are aware of the need for cooling produce, but most people did not care if the food they bought was cooled.

---

# Sammendrag

Matsvinn og kjølesystemer med miljøskadelige arbeidsfluider er noen av de største problemene verden står ovenfor med hensyn til global oppvarming og populasjonsvekst. En tredel av produsert mat blir kastet, og et av problemene er en mangel på kuldekjede i utviklingsland som India. En mulig løsning for noen av kuldekjedene kan være en sol-basert adsorpsjons ismaskin. Det er mange små bønder og fiskere boende i rurale områder som lider økonomiske tap på grunn av mangel på tilgjengelig kjøling for deres produkter. Tilgang på elektrisitet er et stort problem, derfor kan et enkelt system basert på solenergi være nyttig. Et adsorpsjonssystem som operer over en periode på en dag, vil produsere is på natten ved å bruke solvarmen på dagen for å drive systemet.

Dimensjoneringen av et system som produserer 10 kg is og driften av systemet har blitt studert. Maxsorb III er den beste adsorbenten på markedet i dag og tre forskjellige kjølemedier (metanol, etanol og R134a) har blitt sammenlignet. Simuleringen er i tre deler. Del en er en termodynamisk analyse av systemet, del to ser på tykkelsen på adsorpsjonssengen, og del tre ser på driften gjennom en hel dag. Beregningene er basert på klimatiske data fra India og energibalanser for komponenter i systemet. I den termodynamiske analysen viser det seg at R134a og Maxsorb III ikke egner seg som en god kombinasjon for drift av et system med en periode for en dag. Metanol og etanol viser lovende resultater i den termodynamiske analysen og simulasjonen gjennom en hel dag. Metanol viser seg å være det beste arbeidsmediet for adsorpsjonstemperaturer under 28°C, mens etanol er bedre for temperaturer høyere enn 28°C. Tykkelsen på sengen er beregnet til å være maksimalt 7.5 cm tykk, for å ha en relativt rask nedkjøling. Et lite system med en solfanger på 1m<sup>2</sup> og 20 kg med adsorbent vil gi mennesker som før ikke hadde tilgang på kjøling mulighet til å bruke is for å kjøle produktene sine.

Arbeidet ble delvis gjennomført i India og Norge. Et to og et halvt måneds opphold ble gjennomført ved IIT Kharagpur, hvor status og mulighetene for å forbedre kuldekjeden ble utforsket. Under oppholdet ble en undersøkelse, om kunnskapen og betydningen av kuldekjeden, gjennomført. Den viste blant annet at mange er klar over at det er viktig å ha en kuldekjede, men de brydde seg ikke noe om at den maten de selv spiste hadde vært en del av kuldekjeden.

---

# Preface

This master thesis has been completed at Indian Institute of Technology (IIT) Kharagpur and the Norwegian University of Science and Technology spring semester 2019. The thesis consists of a literature study of different food cold chains in India and explores the possibilities of using a solar-based adsorption system as refrigeration system in India, thus improving and developing the cold chain. The master thesis is done in cooperation with SINTEF Ocean and is a part of the Re-FOOD project, which is an international partnership between Norway and India. Two fellow students, Benjamin Hammer Espedalen and Tom Andr Bredesen, and I spend two and a half months in India.

My supervisor in Norway, Trygve Magne Eikevik, deserve a thank, I greatly appreciate the opportunity to travel to India. So do my supervisor in India, Sourva Mitra, you helped me with the academics in India, and I really appreciated the conversations we had. My co-supervisor, Ignat Tolstorebrov, helped me with any question I have had, and I appreciate Armin Hafner and Norsk Kjøleteknisk Forening trust in giving us the Gustav Lorentzen grant. Kristina Wiedell set us in contact with SINTEF ocean, and I appreciate the good sources and advice.

Erling Vingelsgård

---

# Table of Contents

<b>Summary</b>	<b>i</b>
<b>Preface</b>	<b>iii</b>
<b>Table of Contents</b>	<b>vii</b>
<b>List of Tables</b>	<b>ix</b>
<b>List of Figures</b>	<b>xii</b>
<b>Abbreviations</b>	<b>xiii</b>
<b>1 Introduction</b>	<b>1</b>
1.1 Background and motivation . . . . .	1
1.2 Problem description . . . . .	2
<b>2 The Cold Chain</b>	<b>3</b>
2.1 Primary cooling . . . . .	4
2.2 Secondary cooling . . . . .	4
2.3 Optimal target temperature - product segmentation . . . . .	5
2.4 Temperature management of the cold chain . . . . .	5
2.5 Consequences with bad cold chains . . . . .	6
2.6 Environmental impact . . . . .	6
2.7 Summary of general cold chain . . . . .	7
<b>3 Cold chains in India</b>	<b>9</b>
3.1 Current status in India . . . . .	9
3.2 Fruit and vegetable . . . . .	10
3.2.1 Domestic supply chain for fruit . . . . .	10
3.2.2 Domestic supply chain for vegetable . . . . .	11
3.3 Inland and marine fisheries . . . . .	12
3.3.1 Stakeholders in domestic seafood industries . . . . .	12

---

3.3.2	Export seafood . . . . .	12
3.4	Diary . . . . .	13
3.5	Poultry . . . . .	14
3.6	Challenges facing the Indian supply and cold chain . . . . .	15
3.7	Survey . . . . .	17
3.8	Climate in India . . . . .	20
3.9	Summary cold chain in India . . . . .	22
<b>4</b>	<b>Adsorption systems</b>	<b>23</b>
4.1	Why adsorption systems? . . . . .	23
4.2	Adsorption technology . . . . .	24
4.3	Possible adsorption working pairs . . . . .	25
4.4	Activated carbon . . . . .	28
4.5	Previous adsorption solar based ice making system . . . . .	30
<b>5</b>	<b>Theory</b>	<b>31</b>
5.1	Cold production - Heat pump theory . . . . .	31
5.2	Ice production . . . . .	34
5.3	Solar irradiation as heat source . . . . .	35
5.4	Adsorption . . . . .	36
5.5	Heat loss . . . . .	37
<b>6</b>	<b>System operation</b>	<b>39</b>
6.1	System overview . . . . .	39
6.2	Thermodynamic description . . . . .	40
6.3	Pressure levels and temperature variation . . . . .	43
6.4	Components of the system . . . . .	46
6.4.1	Collector . . . . .	46
6.4.2	Condenser . . . . .	47
6.4.3	Evaporator and water tank . . . . .	48
6.4.4	Reservoir and valves . . . . .	48
6.5	Economics . . . . .	49
<b>7</b>	<b>Modeling</b>	<b>51</b>
7.1	6-point analysis . . . . .	51
7.2	Temperature distribution through the bed . . . . .	54
7.3	Simulation through the day . . . . .	55
<b>8</b>	<b>Results and discussion</b>	<b>57</b>
8.1	Thermodynamic analysis . . . . .	57
8.1.1	Validation of the code . . . . .	57
8.1.2	Effect of main factors . . . . .	58
8.1.3	Comparing working pairs with Maxsorb III as adsorbent . . . . .	60
8.1.4	Simple 6 point comparison . . . . .	62

---



---

8.1.5	Summary of thermodynamic analysis . . . . .	65
8.2	Transient analysis - cooling time . . . . .	66
8.2.1	Flat plate design . . . . .	66
8.2.2	Cylinder design . . . . .	69
8.2.3	Summary of transient analysis . . . . .	71
8.3	Simulation through a day . . . . .	72
8.3.1	Solar irradiation - heating . . . . .	72
8.3.2	Heat losses . . . . .	72
8.3.3	Time frame . . . . .	73
8.3.4	Varying solar irradiating . . . . .	74
8.3.5	Varying ambient temperature . . . . .	75
8.3.6	Mass flow . . . . .	77
8.3.7	Summary of simulation through a day . . . . .	78
<b>9</b>	<b>Conclusion and further work</b>	<b>79</b>
	<b>Bibliography</b>	<b>80</b>
<b>A</b>	<b>India</b>	<b>A-1</b>
A.1	Optimal tilt angle of the collector . . . . .	A-1
A.2	Solar irradiation in India . . . . .	A-2
A.3	Previous system . . . . .	A-3
A.4	Potato cold storage . . . . .	A-4
A.5	Local fruit and vegetable market & local fish market . . . . .	A-6
<b>B</b>	<b>EES code</b>	<b>B-1</b>
B.1	6-point analysis model . . . . .	B-1
B.2	Transient analysis model . . . . .	B-4
B.3	Simulation through one day . . . . .	B-6
<b>C</b>	<b>Hazardous activity identification process</b>	<b>C-1</b>



# List of Tables

2.1	Overview of temperature classification. Source: NCCD (2015) . . . . .	5
3.1	Developed cold chain infrastructure and infrastructure gap in India. Source NCCD (2015) . . . . .	9
3.2	Monthly climate indicators for Kolkata and Jaipur . . . . .	21
4.1	Experimental data for activated carbon with methanol as working fluid . . . . .	26
4.2	Experimental data for Ethanol . . . . .	26
4.3	Experimental data for R134a . . . . .	27
4.4	Possible working pairs and temperature range. Source (Choudhury et al., 2013) . .	28
4.5	Maxsorb properties . . . . .	30
5.1	Experimental data for Maxsorb III . . . . .	36
6.1	Relevant condensing temperatures and their corresponding saturated pressures. Data from EES . . . . .	43
6.2	Relevant evaporator temperatures and their corresponding saturated pressures. Data from EES . . . . .	43
6.3	Cost of an electric small scale ice maker . . . . .	49
6.4	Approximately cost of components in the system . . . . .	49
8.1	Wang et al. (2000) values of COP and kg ice produce . . . . .	58
8.2	Parameters used in simulation . . . . .	58
8.3	Parameters used in simulation . . . . .	63
8.4	Dimensions of possible tube bed design . . . . .	70



# List of Figures

2.1	Optimal temperature along the cold chain. Source: (Mercier et al., 2017) . . . . .	3
2.2	Holding life for perishable products. Source: NCCD (2015) . . . . .	4
3.1	Supply and cold chain structures for vegetables and fruits with the current status . .	11
3.2	Supply and cold chain structures for fish with the current status . . . . .	13
3.3	Supply and cold chain structures for dairy products with the current status . . . . .	14
3.4	Example of an efficient supply chain . . . . .	15
3.5	Survey question 1 . . . . .	17
3.6	Survey question 2 . . . . .	18
3.7	Survey question 3 . . . . .	18
3.8	Survey question 4 . . . . .	18
3.9	Survey question 5 . . . . .	19
3.10	Survey question 6 . . . . .	19
3.11	Survey question 7 . . . . .	20
4.1	Physical vs chemical adsorption . . . . .	24
4.2	Pressure-enthalpy plots of Methanol, ethanol and R134a. Working temperature -5°C and 30 °C . . . . .	27
4.3	Schematic representation of adsorbent pore structure (Hassan et al., 2015) . . . . .	29
5.1	Heat flow evaporation and condensation. Source:(Eikevik, 2018) . . . . .	31
5.2	Heat pump system with high and low temperature. Source: (Eikevik, 2018) . . . . .	32
5.3	Pressure-enthalpy diagram for a methanol refrigeration cycle . . . . .	33
5.4	Temperature-time plot of freezing process of water . . . . .	34
5.5	Solar angles and tilt of the earth . . . . .	35
6.1	Components of the system . . . . .	39
6.2	Pressure-temperature diagram for a cycle through one day . . . . .	40
6.3	Stage 1 and 2 of the system cycle . . . . .	41
6.4	Stage 3 and 4 of the system cycle . . . . .	42
6.5	Adsorbent uptake - bed temperature diagram with varying condensing temperature	44
6.6	Influence of increasing desorption/maximal bed temperature . . . . .	45

---

6.7	Influence of decrease the adsorption/minimal bed temperature . . . . .	45
6.8	Components on the bed . . . . .	46
6.9	Possible tubular and rectangular adsorption bed . . . . .	47
6.10	Condenser, evaporator, valve and reservoir . . . . .	48
6.11	Operational cost of commercial and adsorption system over 10 year . . . . .	50
7.1	Simulation structure for the operation through one day . . . . .	56
8.1	Effect of increasing ambient/condenser temperature. . . . .	59
8.2	Effect of increasing bed temperature/desorption temperature . . . . .	59
8.3	Blue field - possible adsorption temperatures, Red field - possible desorption temperatures. . . . .	60
8.4	Blue field - possible adsorption temperatures, Red field - possible desorption temperatures. . . . .	61
8.5	Blue field - possible adsorption temperatures, Red field - possible desorption temperatures. . . . .	62
8.6	Working fluid with increasing desorption temperature . . . . .	63
8.7	Working fluid with increasing adsorption temperature . . . . .	64
8.8	Working fluid with increasing adsorption and desorption temperature . . . . .	65
8.9	Temperature profile of four points on a flat plate . . . . .	66
8.10	Change in transient temperature profile with varying conductivity . . . . .	67
8.11	Change in transient temperature profile with varying external heat transfer coefficient . . . . .	68
8.12	Change in transient temperature profile with varying density . . . . .	68
8.13	Change in transient temperature profile with bed thickness of 2.5 and 5 cm . . . . .	69
8.14	Change in transient temperature profile with bed thickness of 7.5 and 10 cm . . . . .	69
8.15	Cross section of adsorbent tube . . . . .	70
8.16	Change in transient temperature profile with tubular radius increase . . . . .	70
8.17	Cylinder design - Transient temperature profile of 20 kg Maxsorb III . . . . .	71
8.18	Solar irradiation and heat loss . . . . .	72
8.19	Heat loss through the top and the back/sides of the collector . . . . .	73
8.20	Bed and ambient temperature through a day . . . . .	73
8.21	Ice production through the day . . . . .	74
8.22	Solar irradiation effect on bed temperature . . . . .	75
8.23	Solar irradiation effect on ice production . . . . .	75
8.24	Condenser/ambient temperature effect on bed temperature . . . . .	76
8.25	Condenser/ambient temperature effect ice production . . . . .	76
8.26	Desorped and adsorbed working fluid through the day . . . . .	77
8.27	Mass flow rate through the day . . . . .	77

---

# Abbreviations

## Symbols

$T$	=	Temperature
$P$	=	Pressure
$t$	=	Time
$X_0$	=	Maximum adsorbent uptake
$I$	=	Solar irradiation
$C_p$	=	Specific heat
$m$	=	Mass
$\rho$	=	Density
$q_{st}$	=	Desorption heat
$\Delta x$	=	Amount desorbed per kg/kg
$d_p$	=	Particle diameter
$k$	=	Thermal conductivity
$h$	=	Enthalpy
$A$	=	Areal
$\beta$	=	Elevation angle of solar collector
$D$	=	Characteristic adsorption parameter
$n$	=	Characteristic adsorption parameter
$U_L$	=	Overall heat transfer coefficient
$\theta$	=	Dimensionless temperature
$\mu$	=	Root of parametric equation
$y'$	=	Liquid fraction
$L$	=	Length
$a$	=	Thermal diffusivity
$b$	=	External heat transfer coefficient

## Subscript

amb	=	Ambient
evap	=	Evaproatation
cond	=	Condensation
ads	=	Adsorption
des	=	Desorption
eq	=	Equilibrium
iw	=	Initial water temperature
w	=	Walls of container
AC	=	Activated carbon
wf	=	Working fluid
abs	=	Absolute

---

Others

AC	=	Activated carbon
GWP	=	Global warming potential
ODP	=	Ozone depletion potential
MT	=	Metric tonnes
Bi	=	Biot number
Fo	=	Fourier number
SCOP	=	Solar coefficient of performance



# Introduction

## 1.1 Background and motivation

The world's population is increasing every day and is not going to stagnate or decrease in the near future. China is the most populous country with 1.418 billion followed by India with 1.365 billion in 2019 (UN, 2019). It is predicted that India is going to take over China as the most populous country by 2022 (bbc.com, 2015). A big proportion of the population is undernourished (14.8%) (FAO, 2019), and that number is going to increase with an increasing population if nothing is done to improve the situation. On the other hand, it is estimated that nearly one-third of the food in the world for human consumption every year gets lost or wasted. A significant portion of this occurs upstream, at harvest and post-harvest handling mainly due to lack of refrigeration system. Many places in the world have the food cold chain significant gaps or are non-existent. Lack of resources for investment, information about food safety, and technical skills is some of the challenges facing India and similar countries.

There are several issues with the refrigeration system from an environmental perspective. Many of the refrigerating units operating today are using chlorofluorocarbons (CFCs), hydrochlorofluorocarbons (HCFCs) or hydrofluorocarbons (HFCs) as working fluids. These working fluids have high global warming potential (GWP), up to thousands or tens of thousands of times greater than CO<sub>2</sub> (epa.gov, 2019), and contribute to the increasing temperature of the planet. Refrigeration system using these harmful working fluids are being phased out from industrial countries according to the Paris Agreement. However, these systems are the cheapest and for developing countries price is very important. The introduction of refrigeration system using CFCs or HCFCs for 1.3 billion people would be a climatic disaster. Therefore, it is important to introduce environmental friendly working fluids such as natural refrigerants worldwide.

## 1.2 Problem description

Globally, 1.3 billion tonnes of food is lost every year. In order to enable sustainable development of the food system, EU and the member states adopted the Sustainable Development Goals (SDG) in September 2015, which include a target to halve per capita food waste at the retail and consumer level by 2030 and reduce food losses along the food production and supply chains. A majority of food waste occurs at the consumption stage in Europe, but in India, most of the loss occurs at the post-harvest stage due to improper handling and cold chain management (FAO, 2019). India is a major producer and exporter of food products (ranking 6th in the world in 2013). There are many small farmers, fishermen etc. living in rural areas suffering economic losses due to non-availability of suitable storage systems for their produce. Availability of reliable electrical power is one of the major issues for these people. Hence simple solutions relying on renewable energy sources such as solar and biomass could be effective. An adsorption system operating intermittent will produce ice during the night using the solar energy available during the day. In recent years improvements in material and reactor front could pave the way for successful development of these systems. These systems will make it possible for small farmers, fishermen, etc. to start the cold chain right after harvest. The following tasks are considered:

1. Literature review of the cold chain
2. Mapping the different cold chains in India and inspect the needs of potential farmers and fishermen using the system
3. Thermodynamic analysis of intermittent adsorption refrigeration systems suitable for ice making considering different adsorbents and adsorbates
4. Select suitable adsorbent and adsorbate for ice making applications and make preliminary estimation of required adsorbent and adsorbate mass for 10 kg ice per day
5. Develop simple mathematical models for predicting charge-discharge characteristics of adsorbent beds of suitable geometry using solar energy as heat source and ambient air as heat sink
6. Simulate the performance of the entire system consisting of the solar collector, adsorbent beds and evaporator/condenser for ice making applications through one day
7. Identification of the best adsorption pair based on key performance parameters
8. Preparation of a scientific paper from the main results of the Master Thesis
9. Suggestions for further work

## The Cold Chain

The cold chain refers to the chilled stages the product goes through from harvest to consumer (Brijesh K. Tiwari, 2013). From the moment fruits or vegetables are harvested, the product starts to decay. Delaying this process is the aim of the cold chain, and an efficient cold chain is designed to slow down this process as much as possible. The same applies to animals and fish after slaughtering.

The food cold chain consists of two parts: primary and secondary cooling. The primary cooling is the process of removing heat from the product, thus lowering the temperature of the product to the desired temperature. Removing heat from food is difficult, time-consuming and in some cases expensive. Therefore, is this a critical part of the cold chain. The secondary cooling is the process of maintaining the right temperature through all the stages to the consumer. The main stages are distribution, storage, retail display, and domestic storage.

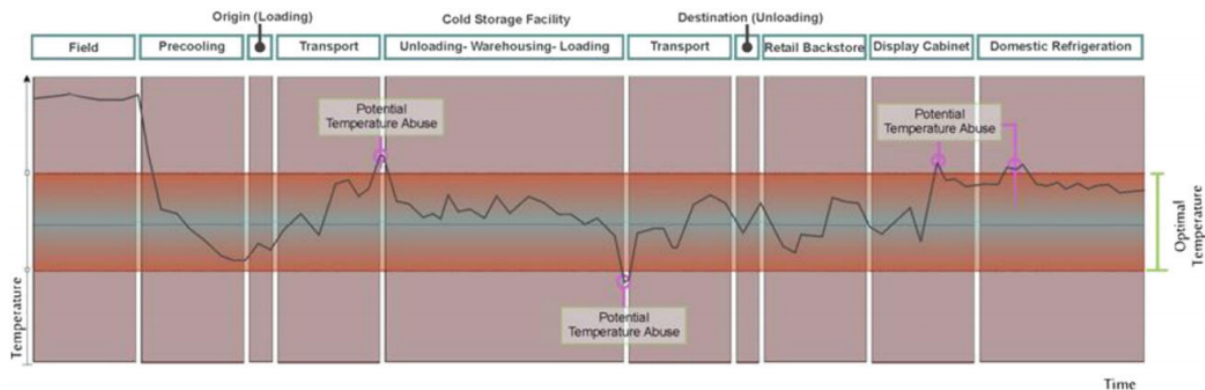


**Figure 2.1:** Optimal temperature along the cold chain. Source: (Mercier et al., 2017)

All foods have an optimum storage temperature and relative humidity that ensure the freshness of the product for the longest possible time (Cohen and Levin, 2011). For some fruits, ethylene production affects the rate of maturing, and some fruits are more sensitive than others. Apples, for example, have a very high production of ethylene, while bananas have a high sensitivity to ethylene (Cantwell, 2011). Therefore should long-term storage of products that influences each other be avoided. Ethylene sensitivity is one example that shows the importance of product segmentation.

Mishandling of product could lead to product loss, economic loss, and put human health at risk. Therefore is the study of cold chain very interesting. The next chapter will highlight the main challenges with a functional cold chain. The following description of the cold chain comes from the National Centre of Cold-chain Development (NCCD, 2015).

## 2.1 Primary cooling

The primary cooling process begins the moment the product is harvested and started to cool down. After the harvest, the product is sent to a packing-house, preferably close to the farm. The first step in the packing-house is sorting, which is the process of categorizing products in different value-based flows. The next step is washing and drying. Products meeting quality standards are packed and precooled. The precooling type varies with the product, and all modalities are designed to rapidly remove heat from the product, thus lowering the temperature to the optimal state. Packing-houses is the first step in organized post-harvest management.

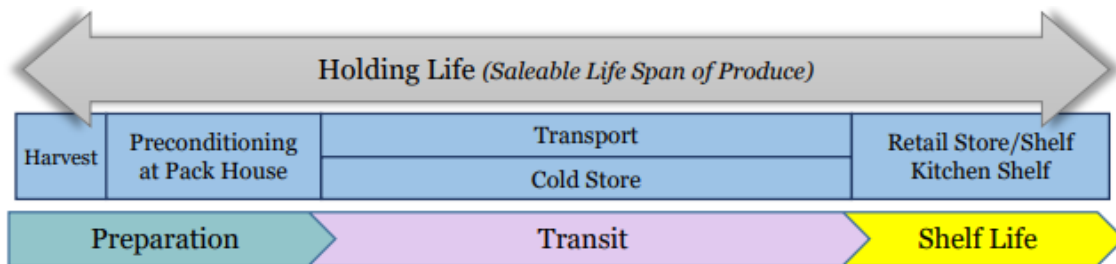


**Figure 2.2:** Holding life for perishable products. Source: NCCD (2015)

## 2.2 Secondary cooling

The purpose of secondary cooling is to maintain the optimal temperature from primary cooling until consumption. This process includes many different steps, depending on the product. Some products may be transported to cold storage for long-term storage, whereas other products consumed as soon as possible. After the precooling process, products are usually placed in cold rooms or cold storage for temporary storage at the packing-house. Then reefers (refrigerated trucks) transports the goods to big cold storage with multiple chambers with different temperatures levels. These storages are often referred to as bulk cold storage and are generally close to the farmers. Products with a long holding life could stay for a long time in these storages if necessary. Next in the cold chain is transportation to the next cold storage, often referred to as hub cold storage and are generally close to consumers. Hubs are effective at distributing products and a vital part of an effective cold chain.

Further, the products are transported to stores and put on displays or in the store cold storage. Consumers could freely pick the product they want and put it in the fridge at home. The domestic fridge is the final part of the cold chain. Cold chains vary by the product. Some products, for example, bananas, get harvested before fully matured. Instead the bananas mature on the way to the consumer. So, an extra stage – a ripening unit – are a part of this particular cold chain.

## 2.3 Optimal target temperature - product segmentation

In a supermarket store, almost 40% of the product is perishable or semi-perishable and should be refrigerated (James and James, 2010). There are mainly four different temperature classifications, as seen in Table 2.1. These categories are divided into 10 °C intervals, and below 18 °C and above 20 °C, that is rough classification compared to the optimal temperature. At many hubs and bulk cold storage, there is a more detailed classification with intervals down to  $\pm 1^{\circ}\text{C}$  (Paludetti et al., 2018).

<b>Frozen</b> < -10 °C	<b>Chill</b> 0 °C -10 °C	<b>Mild chill</b> 10 °C - 20 °C	<b>Normal</b> > 20 °C
Frozen vegetables	Fresh fruit	Sub-tropical fruits	Dehydrated foods
Frozen fish	Fresh vegetable	Seeds	Pickle, jams, jelly
Ice cream	Milk, butter, eggs	Chocolate	Oils and extracts

**Table 2.1:** Overview of temperature classification. Source: NCCD (2015)

## 2.4 Temperature management of the cold chain

The world gets more globalized, and there is an increase in the distance from producer to consumer. Consumers with purchasing power prefer fresh and ripe products from other parts of the world. Sadly, for some fruits and vegetables, up to 40 % of them go uneaten, mostly due to insufficient temperature control (Pang, 2012). Those numbers are not only bad economically for farmers and producers, but it is a great issue associated with global food security. Fruits and vegetable are some of the most perishable foods in the market with a short shelf life compared to other products, and any small temperature deviation could lead to all the efforts in the whole cold chain goes to waste (Mahajan et al., 2014).

In places lacking refrigeration, too high temperature is the main problem. However, too low temperature could cause just as much damage, in the form of freezing damages. As mentioned earlier, products must maintain an optimum temperature and relative humidity to keep the freshness. With long transport distances, especially in places like seaports or airports, the control is difficult to maintain (Derens-Bertheau et al., 2015). This is especially true for temperature management in cold rooms with on-off cycles. These systems have a commercial desired set point, and keeping the temperature constant in the whole cold room is almost impossible. A study by Ruiz-Garcia et al. (2010) followed a batch in a refrigerated truck with the desired set point of 0°C ( $\pm 0.5^{\circ}\text{C}$ ). The lowest temperature recorded was 3°C and highest +8.5°C. This level of temperature variation is unacceptable; however, some temperature fluctuation is expected because most systems require defrosting.

A big concern for temperature control management is the misplacement of products in transport. This is due to the convenience of a few temperature levels in containers and bulk transport (Arduino et al., 2013). One of the possible solutions to the temperature management problem is to assure controllability in all steps in real time. Data should be collected and shared between customer and

supplier through the cold chain, thus making sure there are no temperature deviations at any points. These kinds of technologies are already coming to marked in places like Norway. Some of the technical solutions include Radio Frequency Identification (RFID) and Wireless Sensor Networks (WSN), although this has been adopted with varying results (Badia-Melis et al., 2018). These solutions are, however, not possible in India due to the cost and high technology requirement.

### **2.5 Consequences with bad cold chains**

For meats and seafood, the stage of initial precooling is essential. When frozen, slow freezing results in large ice crystals forming and destroying the cell wall of the product (Leygonie et al., 2012). This process affects the structure of the product and increases runoff liquid when thawed. However, due to the flexible fibrous structure in meats and seafood, it is more resistant to freezing than fruits and vegetables. The structure of fruits and vegetable depend on the rigid cell structure. When thawed, the texture will be highly affected and could reduce quality. The temperature should not go below the freezing point of the food when it is in the chilled temperature level (0-10 °C). This temperature exposure could lead to spoiled products due to freezing damages. In the fish industry, there is a high focus on profitability. Fish is sold in kroners per kg, so all drip loss is loss of money. The fillet holds on the liquid better at lower temperatures, thus keeping the temperature and liquid loss under control is critical for being profitable. As much as 2 percent of a salmon fillet could disappear in 14 days just due to moisture loss (Kaale et al., 2014). One of the biggest, if not the biggest, concern of the cold chain is the health concern; is it safe to eat the food? Vegetative bacteria and microbial activity are highly temperature depended. Thus, we should strive to reduce cooling time.

### **2.6 Environmental impact**

#### **Food waste**

About 40% of the food produced in developing countries are thrown away. The energy and resources put into food production are huge, and then throw edible food away is a waste of resources. Also, the decomposition of the food produces greenhouse gases such as carbon dioxide and methane.

#### **Montreal protocol**

There have been mainly two big protocols highlighting the issues with refrigeration fluids. The first is the Montreal protocol (FN, 2019a). The protocol was an international treaty designed to protect the ozone layer by phasing out production and consumption of CFCs gasses responsible for ozone depletion. Developed countries had a deadline to phase out CFCs until 1996 while developing countries had until 2010. HCFCs and HFCs replaced the CFCs gases because HCFCs are broken down in the lowest part of the atmosphere and pose a much smaller risk to the ozone layer. However, the GWP to some of the HCFCs are in the thousands or tens of thousands and contribute to global warming. For developed countries started the out-phasing of HCFCs in 2004 and the goal is 100%

reduction set to 2020 (iifir, 2017). Developing countries agreed to start reducing HCFCs by 2015 and 100% reduction set to 2030. The phase-out of HFCs are set to be reduced by 80% for the next 30 years.

### **Paris agreement**

The other protocol is the Paris agreement (FN, 2019b). The Paris agreement deals with greenhouse gasses and tries to limit the temperature increase due to global warming. Because some working fluids have high GWP, the introduction and spread of natural working fluids are critical. At the moment the refrigeration sector, including air conditioning, heat pumps, and cryogenics, accounts for 7% of the global greenhouse gas emissions (iifir, 2017). Emissions can be categorized into two groups: direct emissions and indirect emissions. The direct emissions occur during maintenance, operation, and disposal of the system. This could be due to leakages or incorrect disposal. Indirect emissions are, for example, electric generation required to operate the systems, fuel transport, and so on.

## **2.7 Summary of general cold chain**

Over the past decades, the cold chain has seen an increase in interest, due to the high food waste and environmental impact (Shashi et al., 2018). Most industrial countries have a functional cold chain, but room for improvement. Many developing countries have little to no developed infrastructure for the cold chain (NCCD, 2015). Thus, knowledge of how to build a functional cold chain, which is environmental friendly, affordable, and high standard, is an essential part of ensuring food safety for the world. Being successful in finding environmentally friendly solutions could reduce the need for working fluids with high GWP and ODP.





## Cold chains in India

India is one of the biggest producers of food in the world, and at the same time, its population is one of the hungriest (von Grebmer et al., 2017). The main problem is not the lack of food; it is the post-harvest loss. Nearly 40% of all food is lost in production. The food loss results in a value of \$8.3 billion worth of goods being lost every year (Biswas, 2014). Improving the cold chain will benefit India in many ways, including increased food supply and economic growth.

### 3.1 Current status in India

National Centre for Cold-chain Development (NCCD) made a report in 2015 about the status and gap of the cold chain in India. The report shows, among other things, the gap in cold chain infrastructure. Furthermore, how mainly due to government initiatives and subsidy the capacity has increased rapidly over the last decades.

Type of infrastructure	All India requirement	All India created	All India gap
Packing-house	70 080	250	-69 830
Cold storage bulk	34 100 000 MT	31 800 000 MT	-3 270 000 MT
Cold storage hub	936 000 MT		
Reefer vehicles	62 000	9 000	-53 000
Ripening chamber	9 100	800	-8 300

**Table 3.1:** Developed cold chain infrastructure and infrastructure gap in India. Source NCCD (2015)

Table 3.1 shows an overview of the current infrastructure in place and the calculated need. The column to the right shows the gap in the market. The data shows that the most significant gaps are in packing-houses, reefer vehicles, and ripening chambers. There is some gap in the cold storage bulk/hub, but it is relatively small. MT is metric tonnes (1000 kg). However, the infrastructure for cold storage that already exists is only suitable to store potatoes. The number of packing houses created is critical compared to the number required for a functional cold chain. The lack of packing houses makes the cold chain already broken in the first step. The report highlights the lack of

refrigerated transport to be a big issue. The number of refrigerated trucks is negligible compared to more developed countries, for comparison are the percentage around 80-85% of fresh fruit and vegetable is refrigerated during transport in developed countries. The refrigerated trucks present in India today are present mainly for the transport of ice cream and produce at -20 °C. Trucks also require refrigerated source handling points.

There are currently many project involving new cold chains on the way. The Indian government has tried to increase the growth by various government initiatives (Bighane, 2017). There has been set up refrigerated railway carriages in operation in Delhi, Mumbai and Bangalore. Other measures are foreign equity participation of 51% is permitted for cold chain projects, no restriction on import of cold storage equipment and National Horticulture Board may subsidy 25% of the cost of new projects.

## **3.2 Fruit and vegetable**

India is the second largest producer in the world of fruits and vegetables after China. For some fruits, i.e., banana, mango, and papaya, India is the largest (Paulrajan and Jacob, 2009). Producing vast amounts of fruits and vegetables offers opportunities for exporting to other countries and also provide for India's population. During 2017-18 India exported fruit and vegetable goods worth 1 460 million USD (apeda.gov.in, 2019). The main fruit products exported are mangoes, grapes, bananas, and pomegranates. Vegetables include onions, okra, chilies, mushroom, and potatoes. The share of the global market is still only about 1%, even though being the second largest producer. Over recent decades, Indians has seen increasing acceptance for their products due to better supply chain and cold chain.

The supply chain for fruits and vegetables varies with the type of fruit and vegetables, season and the distance to the consumer. In Figure 3.1 is an overview of a simple supply chain to the left, and to the right is the description of the ideal cold chain. To the right is the current status, which is either market green or red. Only green means no need for improvement, both green and red means some form of cold chain is in place but room for improvement, and only red means no cold chain in place. The pictures in the middle are from India, with lines pointing to the corresponding place in the cold chain or supply chain.

### **3.2.1 Domestic supply chain for fruit**

A typical supply chain for banana starts when a farmer seeks a commission agent or a supply company and request a price (NIAEM, 2017). The commission agent has contacts with wholesalers who places orders to the agents. The commission agent informs the farmer of the order, and the farmer has to match demand. From the whole sellers, the fruit goes to either traditional retailers or cart vendors. There are a lot of local fruit and vegetable markets on almost every corner in India.

Banana is a fruit that could be harvested all year in some states in India, thus making it is possible to keep the supply steady. For other commodities that only give one or two harvests through the year, there will be huge spikes of supply that will plummet the price if not stored. The supply chain for mangoes are similar to bananas, but it is more season depended. Therefore some of the mangoes are processed for pulp and concentrate. The commission agent sells the mangoes to

processors that sell concentrate or pulp to secondary processors making juice, jam, ice cream, etc. The processors are selling the product to traders or commissions agents who forwards the product to retailers and end consumers. There is also some export of pulp that is either going through exports firms or from the processors directly.

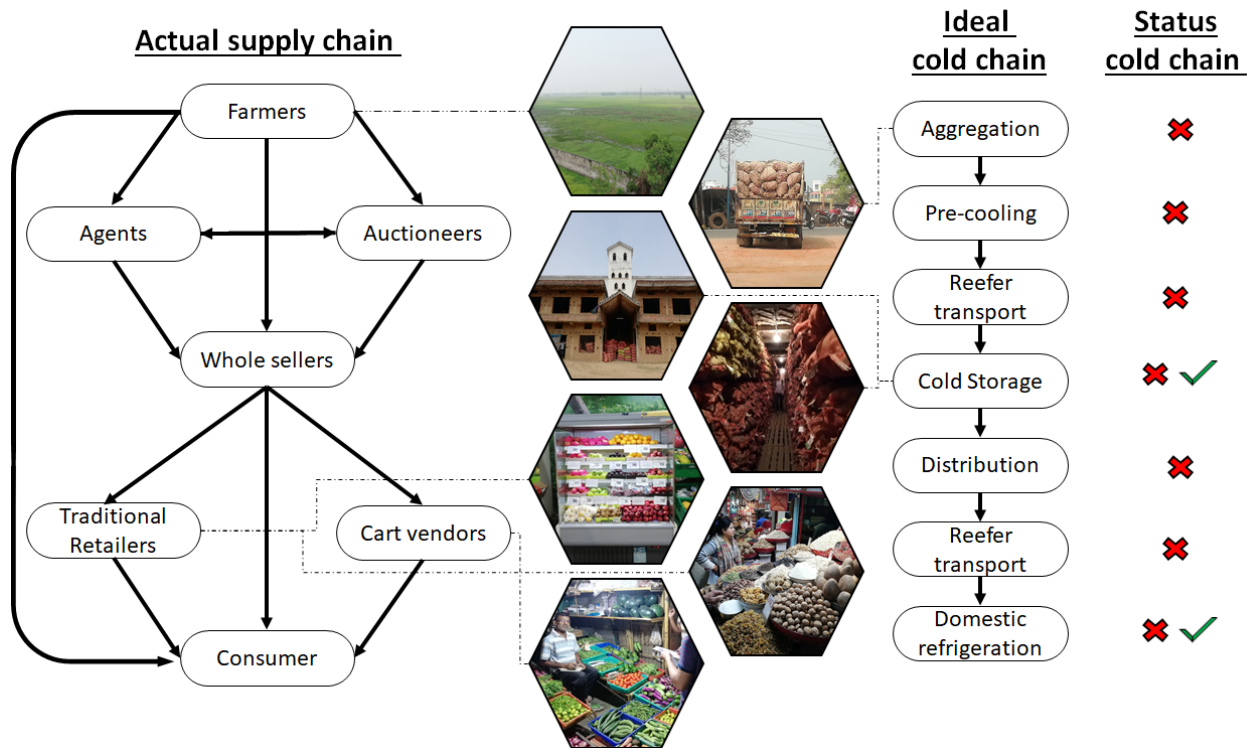


**Figure 3.1:** Supply and cold chain structures for vegetables and fruits with the current status

### 3.2.2 Domestic supply chain for vegetable

The supply chain for vegetables is somewhat similar to the supply chain to fruit. However, it tends to be more local than fruit. This is because most of the vegetables could be grown locally, while some fruit depends on the season and region. Many of the stakeholders are the same as in the fruit supply chain.

There are some cold storages in India, as seen in Figure 3.1 and Table 3.1. These cold storage are mainly for potatoes. Potatoes are an important part of the diet to most Indians, and potatoes are a seasonal vegetable which has to be stored to meet the demand through the year. In Appendix A section A.4 pictures from a visit at a potato storage could be seen.

### **3.3 Inland and marine fisheries**

Food & Agribusiness Strategic Advisory & Research (FASAR, 2015) approximates that 85% of the fish production to be unorganized, scattered and sold on the street. Of this, 70% is marketed fresh and highly exposed to temperature abuse. Most of the remaining 30% is marketed as dried or smoked fish, thus making it less temperature sensitive. Furthermore, India is one of the biggest seafood producers in the world. With a coastline of 8118 km and about 7 million hectares of inland water bodies produce nearly 10 million tonnes of fish annually. An overview of the fish supply chain in India is given in Figure 3.2.

#### **3.3.1 Stakeholders in domestic seafood industries**

The first step in the supply chain is fishermen. The fishermen are going out on the sea to catch fish and bring them to the landing center where the fish is sorted by species. Commission agent stationed at these landing centers inspect the quality and weighs the products. Depending on demand and supply in the area, the two parties agree on a price. The commission agents need to have information on supply and demand to be able to make money. If the fishermen and commission agents agree, the products will be graded, packed, iced, and transported to the market. At the landing centers, fishermen can buy ice to bring out on the boat to start the cooling process already on the boat. The price of ice in India, Kharagpur (March 2019), is about 10 Rupee (1.22 NOK) for 10 kg ice.

Wholesalers receive the fish from commission agents. The size of the wholesaler varies widely and having about thirty retailers they are selling to not unusual. If any form of cooling is used, it is ice. Any unsold fish are stored to the following day. Retailers are the last stakeholder in the supply chain before the consumer. They distribute fish around the city or town. There are mainly three types of retail outlets: traditional retail shop, roadside vendors, and modern retail markets. Usually, retailers buy from the wholesalers early in the morning, and only buys the amount they are going to sell for that and maybe the next day. When the fish market is open, the fish is either kept alive in a water bath or laying on display without any form of cooling. During the night the fish are kept in insulated boxes with ice.

#### **3.3.2 Export seafood**

The export market in India is more professional than the domestic market. In the past, the exporting product was frozen in blocks; this resulted in quality loss and forced the consumer to buy in bulk. Today, seafood gets processed in India, and frozen shrimp is the most valuable product followed by fish. The main markets are the United States, the European Union, and Japan.

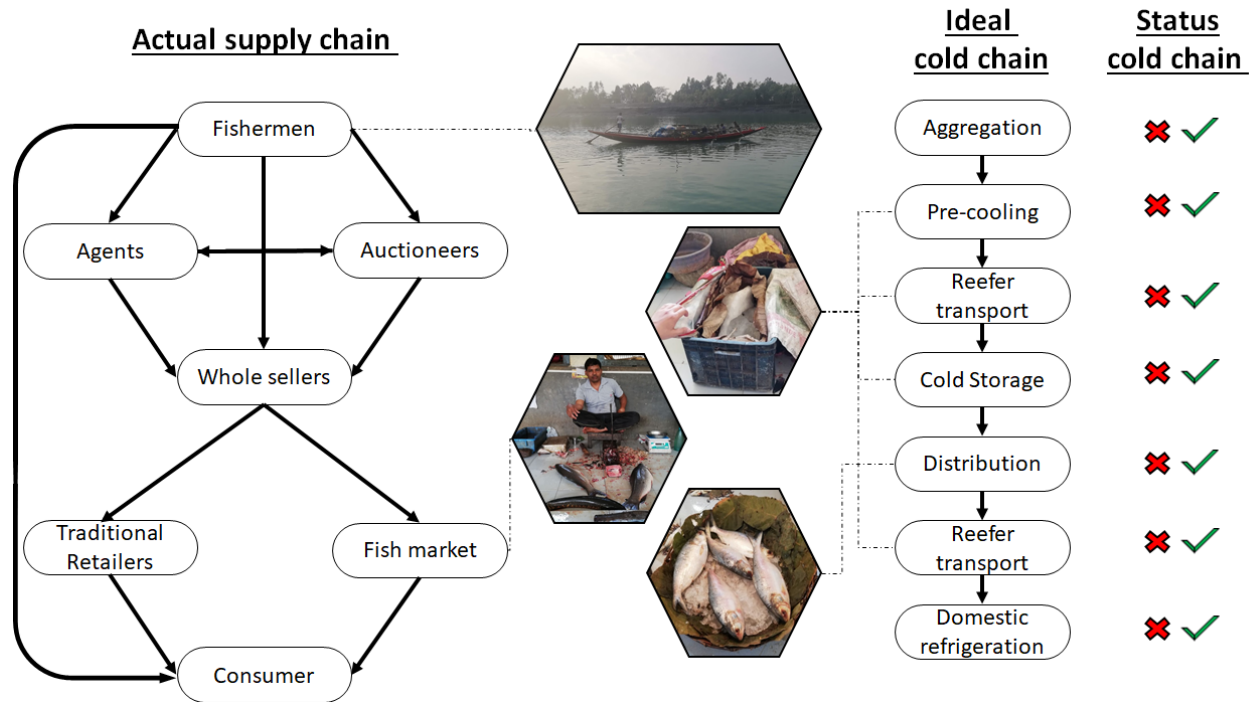


**Figure 3.2:** Supply and cold chain structures for fish with the current status

## 3.4 Diary

India is the largest milk producer in the world with annual production close to 130 million MT and growing 5% per annually. The dairy cold chain also struggles with the same problems as seafood and fruits and vegetable industry. 80% of the milk produced by rural producers is processed in an unorganized way (Subburaj et al., 2015). This makes it challenging to find reliable numbers for total production.

### Diary supply chain

Figure 3.3 shows a typical supply chain with the corresponding cold chain. The supply chain for dairy starts at the farm. There are many small rural villages in India with multiple small farmers. In these small villages, there are organized milk collection points, where the milk is weighed and tested for quality. The next step in the supply chain is the transportation from the collection point to a milk chilling center. A milk chilling center has to be relatively large to be profitable, thus cover many small villages while not exceed transportation time limits. The transportation takes place in nonrefrigerated trucks. The milk is at ambient temperature when it arrives the milk chilling plant and is then chilled down to 4 °C. From the chilling plant trucks transport the chilled milk to process units. These trucks are insulated but do not have refrigeration units. Insulated tanker could maintain the temperature for the milk in some time. The processing unit depends on the milk product. For example, drinking milk has the following process.

*Rawmilk → Chilling → Pasteurization → Standardization → Packing*

After packing the milk is kept in cold stores below 4 °C and further transported in insulated trucks to distributors and agents. Distributors and agents are the link between the processing unit and retailers and consumer.

Ice cream distribution takes place below -20°C and is one of the products that have a functional cold chain the entire way from processing unit to the consumer. Including refrigerated trucks.

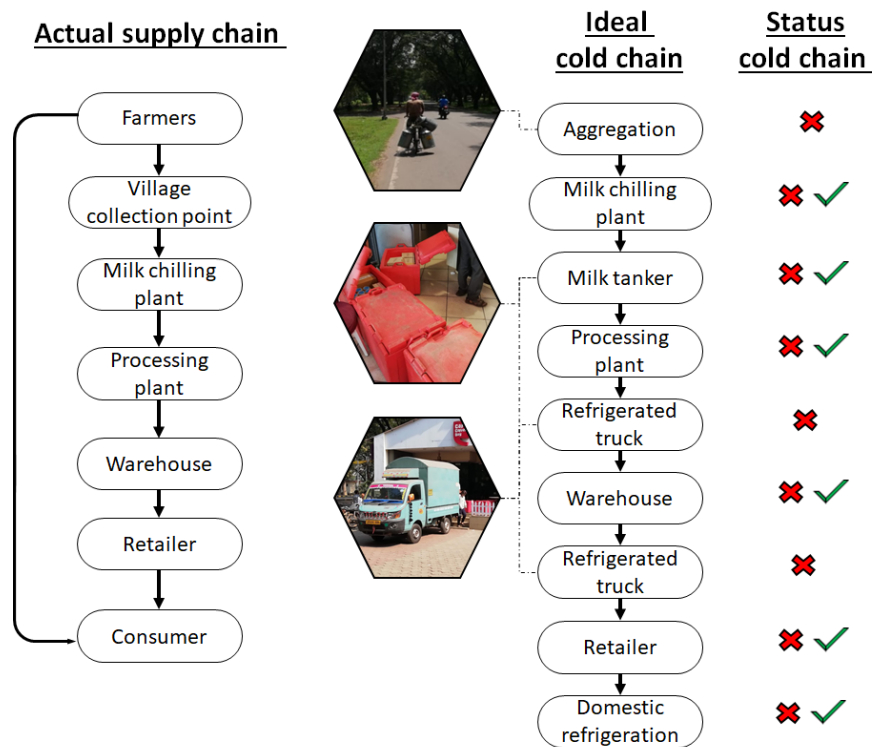


Figure 3.3: Supply and cold chain structures for dairy products with the current status

### 3.5 Poultry

India is the third largest egg producer and fifth largest poultry producer in the world. Due to religious and cultural reasons, there are not much pork and beef consumption. Thus these cold chains will not be discussed. Poultry has had rapid growth over the last three decades. Economic growth has made it possible for more people to afford poultry. The vegetarian share of the population has also decreased. However, the processed meat industry in India is growing slowly compared to the increased demand. Only 2-3% of the poultry meat is processed and branded. There are two main reasons for this. The first reason is the consumer preference for live chicken and skepticism for process meat. The second reason is the lack of infrastructure. Some Indians prefer to have the chicken alive and cut in front of their eyes to keep the freshness, even though it is more unhygienic than processed meat.

### 3.6 Challenges facing the Indian supply and cold chain

There are many issues regarding the Indian supply and cold chain. The different food sectors have various issues which has to be solved. The following sub chapters will explore some of the issues. The issues here are found in the academic literature. To compare what is written in the literature to the actual condition a survey was completed. The results of the survey are discussed in section 3.7

#### Coordination

Having many players in the market consume time and affect the market efficiency. This leads to higher prices and reduced quality. The inefficient way of handling the food results in high losses before the consumer.

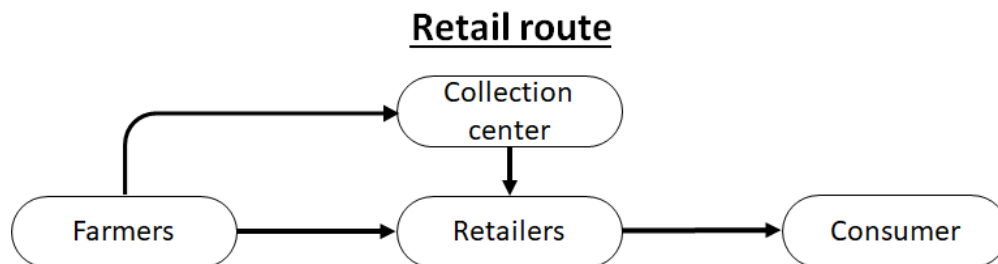


**Figure 3.4:** Example of an efficient supply chain

As mentioned before is the inland fish market in India huge. However, the demand of fish is scatter all over India but the lack of a functional cold chain reduces the availability to meet the demand. The exception is when the consumer is close to the catch area the fish could be in the hands of the consumer the same or next day. One proposed solution to more rural areas is introducing exclusive fish markets. The efficiency of moving seafood would increase, and the increased scale could justify investment in cold storage. The awareness of the cold chain in these areas is a big problem. Education and information on handling the product could increase the lifespan. For example, using clean water to produce ice has been an issue. Contaminated water infects the product and causes loss of value.

#### Financial issues

Arguably the most essential reason for the lack of a high functional supply and cold chain is the economics. The initial investment cost out-weighs the justification of money saved in short term perspective. For sellers at the local market, the investment of a simple refrigeration unit will not make economic sense. The seller at the market only buys the amount that will be sold the same or next day. The remaining fruit and vegetables that go bad due to deterioration is small. One proposed solution to this it for many vendors to buy a cooling unit together.

### **Infrastructure issues**

The infrastructure in India is developing. More people are getting access to electricity and roads are connecting people that previously were too rural. This is a time consuming job and black outs are not uncommon. There are difficult to have a functional cold chain infrastructure if the power and road network are not in place. Products may be damaged during transport if not properly handled (Shukla and Jharkharia, 2013). For example, the loading and unloading is often done by throwing it on a truck and thrown on the ground at arrival.

### **Cold chain issues**

The biggest issue for the cold chain is the lack of cold stores and warehouse facilities. Currently there are some facilities in place, but some of these are already outdated. The focus of keeping the cost down is impacting the quality of the equipment and the cheaper units tends to break down. Thus making the cost and effort useless.

The existing cold stores are build to only handle huge amount of one product, for example potatoes, thus making it inadequate to integrate smaller amount of other products. In Appendix A section A.4 there are some pictures of a big cold store storage for potatoes. Another important prospect is to educate the people operating the machines. Different products need different care. Also education to regular people will help, thus making people more aware of cold chain.

### **Local market**

For fresh produce fruit and vegetable, the need for cooling at the local market is neglected. The argument is that fresh produce only have a holding life of about two weeks and then it is thrown away. Therefor should the products be consumed in this two week window. An interview with National Centre for Cold-chain Development's CEO & Chief Advisor, Pawanexh Kohli, gives a great picture of some mentality in India toward the cold chain.

#### **So when we have enough cold storage, why don't we store the commodities?**

Barring crops that can be stored for the long term, say, onions, potatoes - which are already being stored - why would you store others with short time spans? Take the example of tomatoes. Even if you stored them and transported them to the market after 15 days, they will not survive the trip. You have to move such fresh produce when it is fresh, young and turgid with water. And one should plan to store the proximate to demand. Such items are not amenable to be stored at source but moved closer to demand.

— CEO & Chief Advisor, Pawanexh Kohli, NCCD

With this argument one could argue that India do not have a cold storage gap. The products stored for longer periods, such as potatoes, already have the needed cold storage capacity. How come there are huge losses in the supply chain? Some people believe the losses for products with a short life time are not possible to do anything with.



## 3.7 Survey

A survey was made to understand the current status better. The survey was made to explore the knowledge, awareness, and mindset of regular Indians about the cold chain. The survey reached out to many people of various backgrounds. Students and academics answered the online version of the survey, while vendors were approached at the markets. The local people in West Bengal speak mainly Bengali and some Hindi. With help from another student from IIT Kharagpur and a faculty member, the survey was translated to both Hindi and Bengali. Some of the market vendors showed interested when the survey was given to them in paper form, but it became clear that it would be more efficient to talk to one by one and ask them in person. This gave complete answers and a better understanding of the problems people had relating to the cold chain.

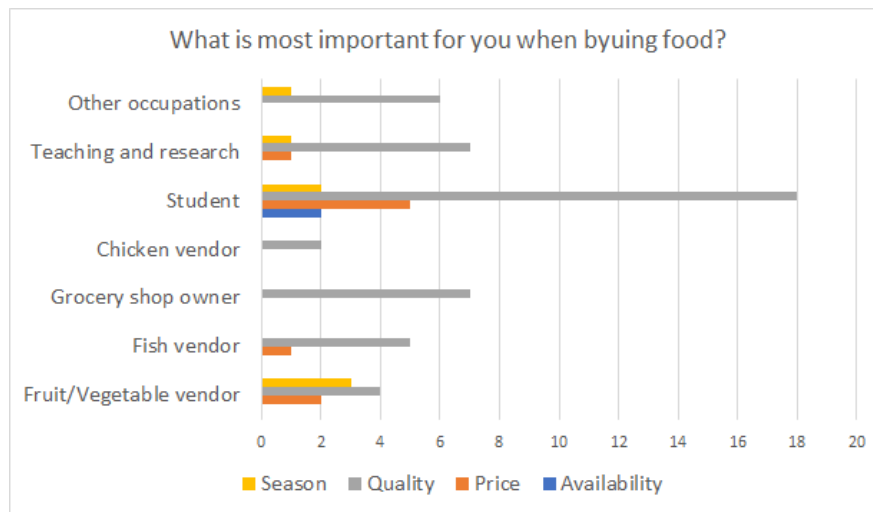


**Figure 3.5:** Survey question 1

The first question is, "What is most important for you when buying food?". The participants had four choices: availability, price, quality, and season. Figure 3.5 shows the occupation of the participants on the y-axis. Most people answered quality, and almost none answered availability. This indicates that people find the food they want. However, some fruit and vegetable vendors are answering season and price as the most important factor, which is influencing the prices and availability.

The next question in the survey was, "Approximately how much of your fruit and vegetables/fish do you throw away due to deterioration or poor quality?". Figure 3.6 shows the number of people on the y-axis, and what percentage they throw away on the x-axis. The figure to the left is for fruit/vegetables and to the right is for fish. Most of the answer is 0-10%. For fruit and vegetable are there some answer in the range 11-20%, and the number of people throwing a higher percentage away is very small.

Figure 3.7 shows only the answers from fruit/vegetable and fish vendors from Figure 3.6. The fish vendors answered they throw away only a small percent of the fruit and vegetables 0-10%. The fruit and vegetable vendors answered a higher percentage of waste. One person throws away that more than 41% of the fruit and vegetables, while the others had more modest numbers. For fish

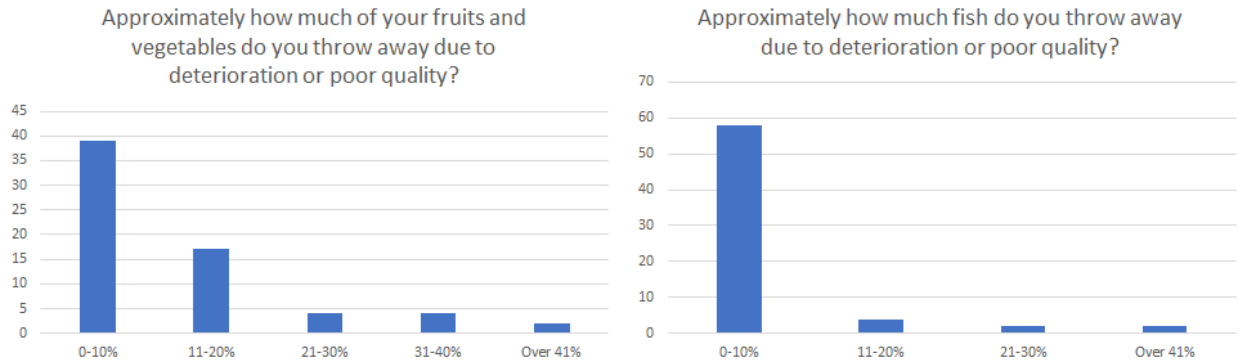


Figure 3.6: Survey question 2

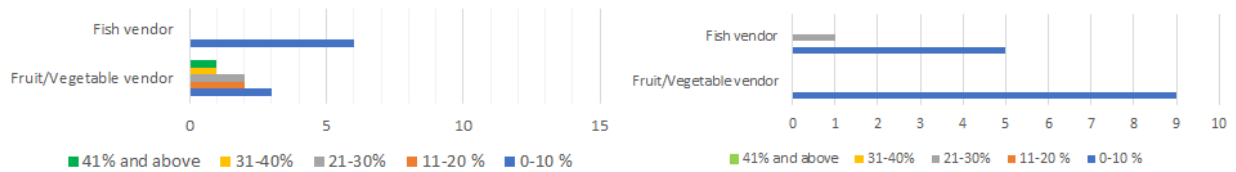


Figure 3.7: Survey question 3

are there only one of the vendors answering that more than 0-10% are thrown away. However, the answers of the vendors indicated that some of the waste of food is happening at the vendors level. Some of them are aware of the problem and reports high losses, while others may understate their losses. The experience during the stay was that the higher losses reported are more accurate.

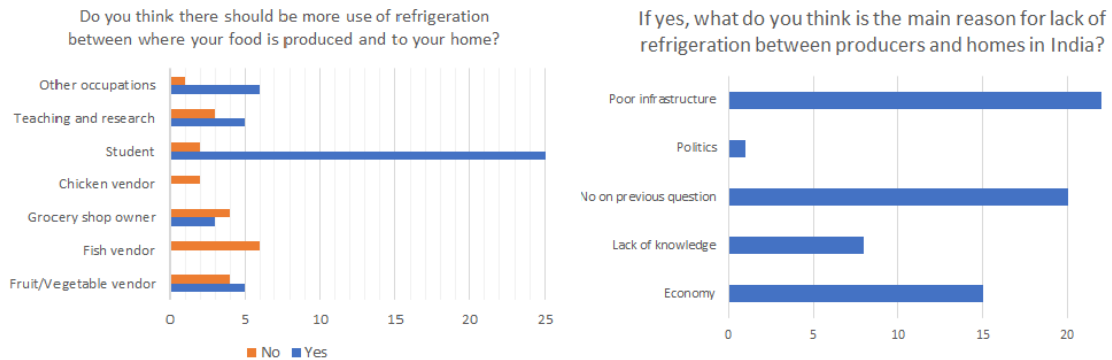


Figure 3.8: Survey question 4

There is a considerable gap in the cold chain from the field to the consumer. The next question was a yes/no question, "Do you think there should be more use of refrigeration between where your food is produced and to your home?", with a follow up question, "If yes, what do you think is the main reason for lack of refrigeration between producers and homes." In Figure 3.8 to the left, the students answers are almost all "yes," which indicates the students are more aware of the benefits of cooling than the other participants. None of the chicken and fish vendors answered yes

to this question, while grocery owners and fruit/vegetable vendors were more 50/50. The follow-up question had four choices: poor infrastructure, politics, lack of knowledge, and economy. Most people stated poor infrastructure and economy as the main reason.

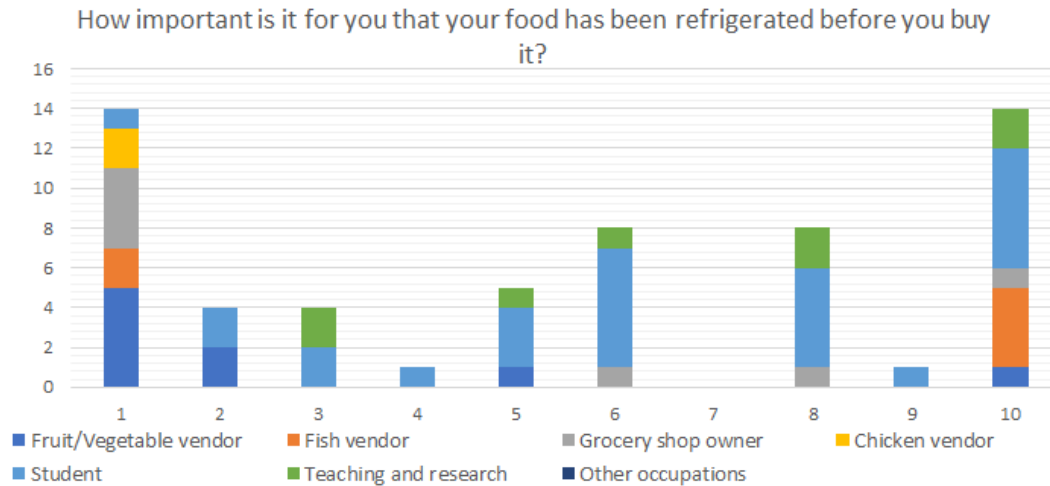


Figure 3.9: Survey question 5

The following question is in somewhat similar to the previous. "How important is it for you that your food has been refrigerated before you buy it?". The participants were asked to give a score from 1 to 10, where one is not important and ten very important. Figure 3.9 shows the number of people giving the same score. Each score also divides into occupations. In the first column, score 1 not important, are the fruit/vegetable, fish, grocery, and chicken vendors most represented. They are handling food every day, and in the current system, it is not important for them that their food is refrigerated. However, there are some fish vendors which the cooling of the product is important. Many students and academics are beware of the importance of cooling products.

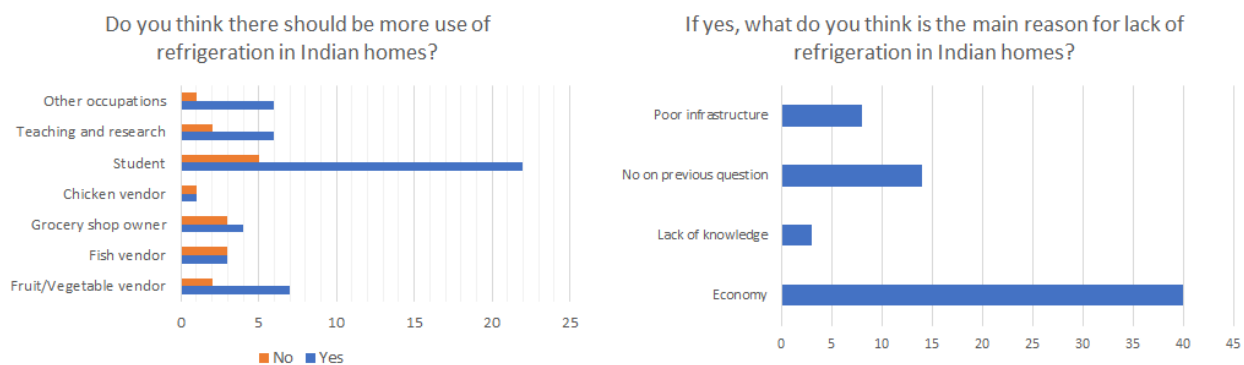
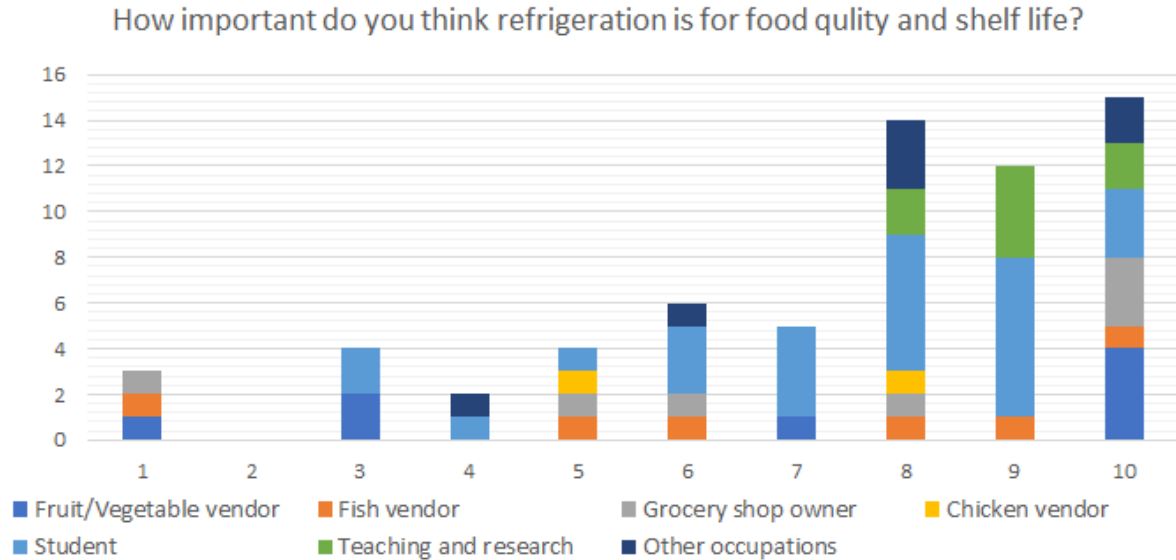


Figure 3.10: Survey question 6

The next question was also a "yes/no" question regarding the cold chain in their homes. "Do you think there should be more use of refrigeration in Indian homes?". With a follow-up question, "If yes, what do you think is the main reason for the lack of refrigeration in Indian homes?". Figure 3.10 to the left shows the occupation to the participants and whether they answered: "yes/no." Most people think more refrigeration should be used in Indians homes. However, the vendors are restrained, and some people do not think it is necessary. The graph to the right shows there is broad agreement it is due to economic reasons.



**Figure 3.11:** Survey question 7

The last question is, "How important do you think refrigeration is for food quality and shelf life?". The participant was asked to give a score from 1 to 10, where one is not important and ten very important. Figure 3.11 shows the number of people giving the same score and their occupation. There are five answers which say it is not important; these participants are fruit/vegetable, fish vendors, and a grocery store owner. However, the rest of the participants are aware of the benefits of cooling the produce.

Comparing Figure 3.11 and 3.9 there is a mismatch between what people think and what is important for them when buying food. Most people say it is important to refrigerate the food for quality and shelf life, while about half of the people do not care if the food they buy has been refrigerated.

### 3.8 Climate in India

The climate in India comprises a wide range of climates across a vast geographic scale. There are three major climatic subtypes, ranging from desert in the west, alpine tundra in north and tropical regions in the south. In general, India has four seasons with some local variation: summer (March-May), rainy monsoon season (June - September), post-monsoon season (October - November)

and winter (December - February). The monsoon season significantly impacts all part of India. Extreme rainfall makes transportation difficult and increases the risk of contagion for food and people. The average solar irradiation gets heavily influenced by the monsoon season. June to August are the months with the best conditions, i.e. tilt of the earth Appendix A, but have the lowest solar irradiation due to the monsoon season. Table 3.2 shows the most important climate indicators for a coastal area (humid, tropical) and one location from the inland area (semi-arid). Respectably Kolkata, West Bengali and Jaipur, Rajasthan. The average temperature through the year is between 20 - 35 C° and the average irradiation is in the range of 2.23 - 6.19 kWh/m<sup>2</sup> per day.

Month	High Temperature °C	Low Temperature °C	Daylight hours hr	Sunshine hours hr	Solar irradiance kWh/m <sup>2</sup>
Kolkata, West Bengal. Coastal climate					
January	26.4	13.3	11	6.6	4.15
February	29.14	16.9	11	7.2	4.86
March	33.5	21.7	12	7.3	5.39
April	35.3	25.1	13	7.8	5.32
May	35.4	26	13	7.3	4.93
June	34.0	26.5	13	4.1	2.93
July	32.3	26.1	13	3	2.23
August	32.1	25.8	13	3.4	2.45
September	32.4	23.9	12	3.9	3.32
October	30.3	19.6	12	5.9	4.17
November	27.0	14.5	11	6.4	5.27
December	26.5	14.0	11	6.6	4.5
Jaipur, Rajasthan. Inland climate					
January	22.4	8.4	11	8	5.45
February	25.0	10.8	11	9	6.40
March	31.0	16.0	12	8	6.59
April	37.1	21.8	13	9	6.01
May	40.3	25.9	13	9	6.34
June	39.3	27.4	14	7	4.74
July	34.1	25.8	14	5	4.07
August	32.4	24.7	13	5	3.68
September	33.8	23.2	12	8	6.10
October	33.6	19.4	12	9	6.19
November	29.0	13.8	11	9	5.73
December	24.5	9.2	10	8	5.44

**Table 3.2:** Monthly climate indicators for Kolkata and Jaipur

### **3.9 Summary cold chain in India**

Most of the problems facing India's cold chain will not be fixed overnight, and an iterative process over time will improve the supply and cold chain. The process has already started with the export market and high-value product in India. Over time the improved process will be implemented for more and more products. People are aware of the benefits of the cold chain, but the survey showed that they were not concerned that their food was a part of the cold chain.

People need some form of refrigeration to reduce food waste. An unorthodox solution is a solar-based adsorption ice maker, which could be a good solution for rural farmers and fishermen with limited access to electricity. The system can be off-grid because it uses solar heat as driving force. India has great solar energy resources.

## Adsorption systems

Sorption systems have been a known technology for a long time without extensive research being conducted. Sorption system is an umbrella term for adsorption and absorption system. Absorption system uses two working fluids to operate, while adsorption use one working fluid and one working solid. However, the shift for green energy and ecological problems with HCFCs and CFCs working fluids has increased the interest in studying unconventional refrigeration systems (Wang and Oliveira, 2006). Sorption refrigerators could use waste heat or even solar power to produce cold.

### 4.1 Why adsorption systems?

The International Institute of Refrigeration in Paris has reported that approximately 15% of all the electricity produced in the whole world is utilized for refrigeration and air-conditioning processes (Goyal et al., 2016). As described in chapter 3 are there three main problems with refrigeration unit systems in India.

1. Power: the electric grid is not built out sufficient, and blackouts are common
2. Economic: startup cost and operation cost
3. Reliability: usability and robust

Adsorption systems are noiseless, non-corrosive, and works without a compressor. For the compression process, the system uses thermal compression instead of a traditional compressor. Furthermore, no electricity is needed. The system could be placed in places where the electrical infrastructure is not built out, i.e., the system will be off grid. The driving force in the system is solar irradiation.

India, because of its geographical location, has big potential for utilizing solar energy to meet the cold demand. On average, India has radiation of  $200MW/km^2$  and capturing some of it could meet the energy need of today and tomorrow (indiaenergyportal.org, 2018). For an off-grid system using solar energy is India an ideal place. The sunlight is free, and the operation cost will be minimal. The only operation cost will be water.

The system is easy in use with only four main valve and four components. The system will have one cycle over one day using the solar heat to compress the working fluid and produce ice during the day, which works as thermal energy storage.

### Competing refrigeration systems

There are several ways to produce cold. The most common is a vapor compressor system, as seen in Figure 5.2. One common environmental way is solar panels with a traditional refrigeration system. Due to the nature of the electromagnetic wavelength specter reaching the ground, only a small portion of the energy is transformed into electrical energy. This is a good solution when the sun is shining. However, a large area is needed to be covered with solar panels to provide enough energy, and this system will require a form of energy storage system to meet demand throughout the day. An absorption system could solve most of the same problem as the proposed adsorption system. However, it would be a more complex system with more parts.

## 4.2 Adsorption technology

### Adsorption phenomena

There are mainly three different adsorption phenomena: physical adsorption, chemical adsorption, and composite adsorption. Physical adsorption is due to weak van der Waal forces between adsorbent (solid) and adsorbate (refrigerant). Chemical adsorption is due to the strong chemical bond between adsorbent and adsorbate, which is form by a chemical reaction. The energy required for one mole chemical adsorption is much higher than one mole physical adsorption. Thus physical and composite adsorption is the most promising phenomena to use for cold production (Younes et al., 2017a). Examples of working pairs for adsorption is: activated carbon/methanol, activated carbon/ammonia, zeolite/water, and silica gel/water.

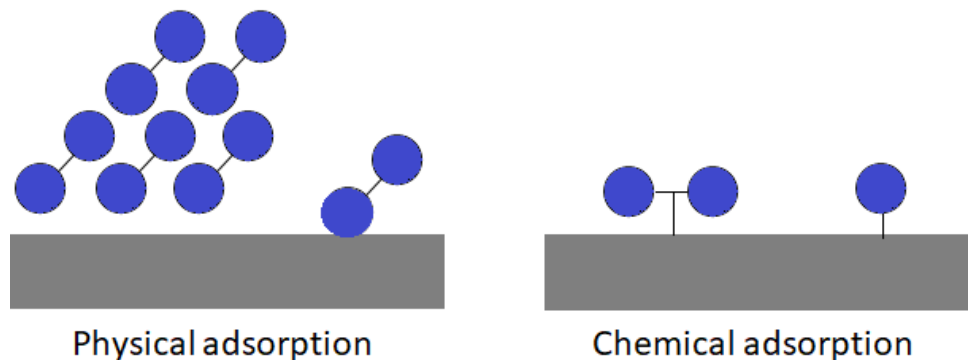


**Figure 4.1:** Physical vs chemical adsorption

### Adsorption systems

Adsorption system could have different design depending on the need and heat source. There are mainly two groups of systems: intermittent and continuous operation. For an intermittent system will cold only be produced parts of the day, and some form of thermal energy storage must be in place. While for a continuous system, the system has more beds. A bed is a bulk of adsorbent which is exposed to temperature and pressure differences. The operation of the system is described



in detail in chapter 6. However, more beds are needed because they will work in shifts. One will be desorbing while the other is adsorbing. This system requires extra components and are more advanced than the system proposed. Continuous systems are a good solution if the heat source is constant through day and night.

Adsorption systems have some desirable properties. Firstly, it has no moving parts. Refrigerant is flowing around in the system driven by the thermal compression. Therefore it is almost maintenance free. The system is also relatively small and easy to move, thus making it suitable for mobile applications. Recent application of nanotechnology in the development of adsorbent material may have been a big step forward towards making this technology competitive with available technologies in the market (Choudhury et al., 2013).

### 4.3 Possible adsorption working pairs

The right working pair is essential for making the best possible adsorption system. Each working pair has an optimal temperature working range, giving them different application such as air conditioning, water chilling, or ice making. Thus, the best working pair depends on the purpose of the system. The working pairs can also be categorized in high and low-pressure systems, i.e., above atmospheric pressure or below and above. Systems working below atmospheric pressure must be build different than systems operating above atmospheric pressure. Moreover, exposed to an influx of air which will influence the performance of the system. Some of the requirement for a perfect refrigerant are.

- High latent heat of vaporization per volume unit or mass unit
- Thermal stable
- Environmental friendly, non-flammable and non-toxic
- Saturation pressure between 1 and 5 atm in the temperatures working range

Unfortunately, no refrigerant fulfills all of the criteria.

#### **Silica gel/water**

Water is an ideal working fluid with no environmental harm and no toxicity. However, this working pair could not be used for evaporation below 0°C because of the risk of water freezing in the system. Silica gel/water is suited for applications like water cooling and air conditioning (Wang et al., 2009). The same problem arises for other working pairs using water as adsorbate.

#### **Activated carbon/methanol**

Activated carbon and methanol is one of the most researched working pair for adsorption system. Activated carbons can adsorb high quantities of methanol and low adsorption heat, which is in the range 1800 - 2000 kJ/kg (Srivastava and Eames, 1998). However, methanol is flammable and toxic alcohol, therefore should be handled with care. The thermodynamic properties of methanol show that a system will operate sub-atmospheric, see Figure 4.2. This may cause an influx of air to the system and reducing ice production. Methanol decomposes at 120 °C, and research shows that aluminum alloys were found to have a stronger catalytic effect on the decomposition reaction than

copper, which has to be considered when designed. However, methanol is a natural working fluid, environmentally friendly, and could be used for application below 0°C.

Table 4.1 shows experimental data for methanol as working fluid and different types of activated carbon. The constant ( $X_0, D, n$ ) are fitted to Dubinin-Astakhov equation, discussed in detail in section 5.4.  $X_0$  shows how much the AC can maximally absorb of a working fluid, and Maxsorb III has the highest adsorption uptake. The temperature shows the temperature range the experiment where done.

Methanol					
Activated carbon type	Temperature [°C]	$X_0$ [kg/kg]	$D$ [ $K^{-n}$ ]	$n$ [–]	Source
LH	20 – 110	0.860	$2.574 \times 10^{-4}$	1.32	(Younes et al., 2017b)
ACF (A-35)	10 – 120	0.425	$5.02 \times 10^{-7}$	2.15	(Younes et al., 2017b)
Maxsorb III	20 – 60	1.24	$4.02 \times 10^{-6}$	2.0	(El-Sharkawy et al., 2009)

**Table 4.1:** Experimental data for activated carbon with methanol as working fluid

### Activated carbon/ethanol

Ethanol is also an alcohol and studied as a possible working fluid. Ethanol has some of the same thermodynamic characteristics as methanol. The adsorption heat is lower for ethanol than for methanol, and in the range of 1000 - 900 kJ/kg (Srivastava and Eames, 1998). It is a natural fluid, environmentally friendly and unlike methanol non-toxic. Ethanol is flammable and works below atmospheric pressure, according to Figure 4.2.

Ethanol					
Activated carbon type	Temperature [°C]	$X_0$ [kg/kg]	$D$ [ $K^{-n}$ ]	$n$ [–]	Source
ACF (A-20)	10 – 60	0.797	$1.72 \times 10^{-6}$	2	(Younes et al., 2017b)
Maxsorb III	20 – 60	1.23	$1.15 \times 10^{-5}$	1.75	(El-Sharkawy et al., 2008)

**Table 4.2:** Experimental data for Ethanol

### Activated carbon/R134a

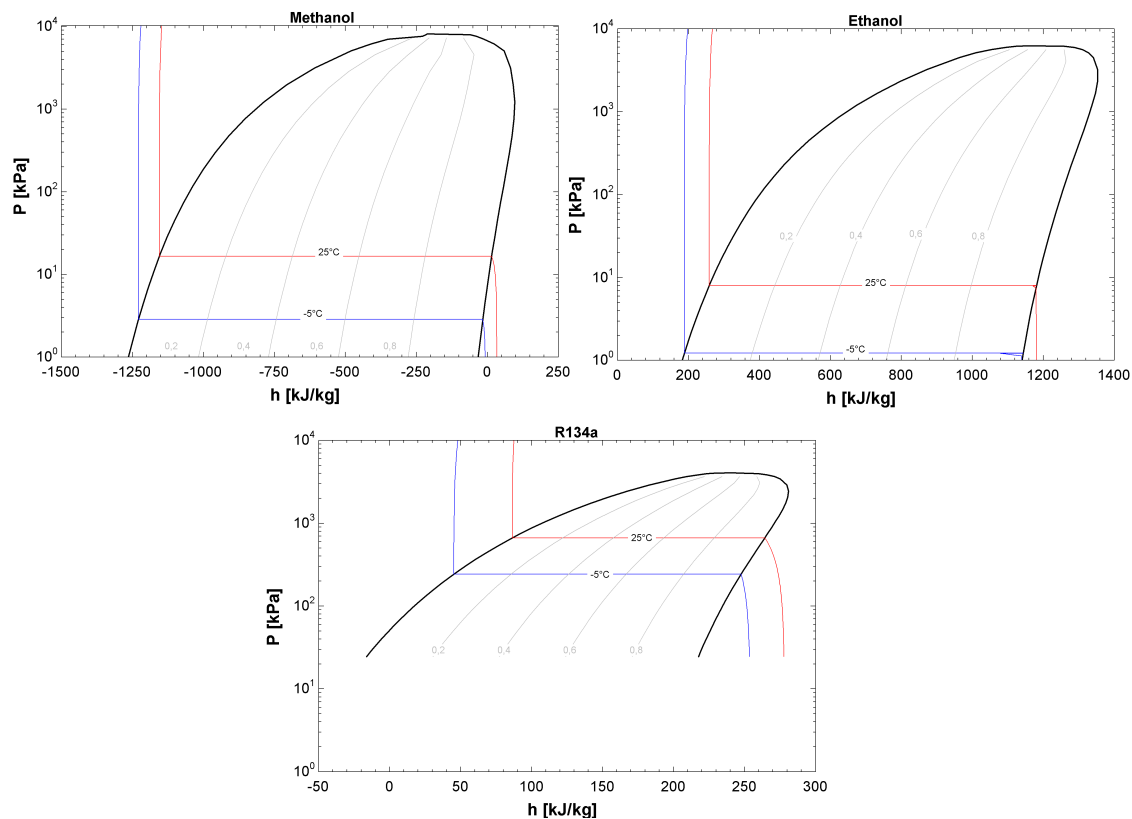
R134a is a hydrofluorocarbon (HFC) gas with insignificant ozone depletion potential. However, it has a global warming potential of 1 430. R134a is non-flammable and non-toxic. Moreover, seen in Figure 4.2 will work above atmospheric pressure.

Figure 4.2 compare the pressure levels to methanol, ethanol, and R134a. From the figure methanol and ethanol operates below atmospheric pressure, while R134a operates above, with an evaporation temperature of –5°C and condensation temperature of 30 °C. The latent heat of each working fluid could be found at –5°C. Working fluids with high latent heat could produce more

R134a					
Activated carbon type	Temperature [°C]	$X_0$ [kg/kg]	$D$ [ $K^{-n}$ ]	$n$ [-]	Source
GAC	25 – 65	1.68	$2.50 \times 10^{-6}$	1.83	(Askalany et al., 2012b)
ACF	30 – 80	1.256	$6.51 \times 10^{-5}$	1.4	(Askalany et al., 2012a)
Maxsorb III	5 – 70	1.945	$2.93 \times 10^{-4}$	1.17	(Saha et al., 2009a)

**Table 4.3:** Experimental data for R134a

cold per kg refrigerant, thus require less adsorbent and adsorbate. Methanol has a latent heat of about 1100 kJ/kg, ethanol 950 kJ/kg and R134a 200 kJ/kg, at  $-5^\circ\text{C}$ .



**Figure 4.2:** Pressure-enthalpy plots of Methanol, ethanol and R134a. Working temperature  $-5^\circ\text{C}$  and  $30^\circ\text{C}$

### Activated carbon/Ammonia

Ammonia is a natural fluid and also environmentally friendly. However, it is also toxic and corrosive, so safety precautions must be in place. Ammonia has the advantage of high latent heat, making the amount of working fluid less. For a refrigeration adsorption system, the heat source temperature needed is about  $170^\circ\text{C}$ . Making it unsuitable for small system design.

Adsorbent-adsorbate pair	Heat source temperature
Silica gel- water	60 – 85°C
Activated carbon-R134a	60 – 80°C
Activated carbon-methanol	80 – 100°C
Activated carbon-ethanol	80 – 100°C
Activated carbon-ammonia	~ 170°C

**Table 4.4:** Possible working pairs and temperature range. Source (Choudhury et al., 2013)

### Activated carbon/Other adsorbents

Methane as adsorbate is possible, but the maximum uptake of methane on Maxsorb III is only 0,3 kg/kg (Thu et al., 2014), which is much lower than methanol, ethanol, and R134a. Other hydrocarbons is also possible.

Research has been conducted on other working fluids such as R507a, R450A, R290, and R600a (John et al., 2017). These working fluids have high uptake, but are more suitable for many cycles per day.

## 4.4 Activated carbon

The requirement of a suitable adsorbent is high adsorption and desorption capacity. Thus a large amount of refrigerant will be in circulation each cycle. The adsorbent should also have low specific heat and good thermal conductivity. It is vital that the adsorbent is environmentally friendly, non-toxic, and non-corrosive (Wang et al., 2009). Activated carbon is characterized by its high adsorption capacity, large surface area, high surface reactivity, and pore size. Thus fulfills the requirement for a suitable adsorbent except for good thermal conductivity. This is an issue which has to be taken into account when designing the bed.

Activated carbon is formed by thermal decomposition of carbonaceous material and is activated with steam or carbon dioxide at high temperatures (Do, 1998). There are many types of activated carbon, and the type is mainly determined by the carbon, which could be made of materials such as wood, peat, coal, fossil oil, bone, coconut shell, and nut stone, but also influenced by the production process.

To get a better understanding of activated carbon Figure 4.3 shows a schematic representation of the pore structure, which will differ with the type. The net structure of activated carbon pores is composed of irregular channels, and the pore sizes can be classified by diameter size: macro-, meso- and micropores. It is important that the diameter of the atoms for the working fluid is smaller than the pores. Otherwise, would the atoms block adsorption area in the pores. It is the large surface area inside of the pores that makes it possible to adsorb large amounts of the adsorbate.

### Activated carbon fibre

Activated carbon fiber is generally used in the production of fabric, such as cloth, tissue, etc. Compared with granular activated carbon has carbon fiber better mass transfer performance (Saha et al.,

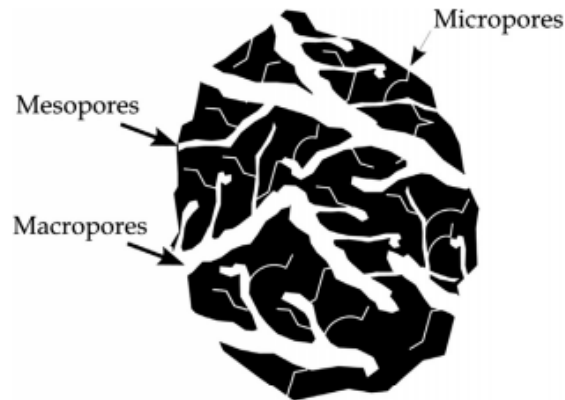


**Figure 4.3:** Schematic representation of adsorbent pore structure (Hassan et al., 2015)

2007). The specific surface area of activated carbon fibers is larger than that of activated carbon, the pores of activated carbon fiber are more uniform than that of activated carbon, and the heat transfer performance of activated carbon fibers is also larger than that of activated carbon. The disadvantages of activated carbon fibers are the anisotropic thermal conductivity, and the higher contact thermal resistance between the fiber and the adsorber wall, when compared with granular activated carbon (Wang et al., 2009).

### Activated carbon

The difference between activated carbon and other types of adsorbent is the surface feature. The whole surface of activated carbon is covered by an oxide matrix and by some inorganic materials, and therefore, it is non-polar or has a weak polarity (Wang et al., 2009). The adsorption heat of activated carbon pairs is lower than that of other types of physical adsorbent pairs. The best activated carbon on the market today is Maxsorb III.

### Maxsorb III

Maxsorb III has many intrinsic characteristics that make it superior over other activated carbons. For example, Maxsorb III has a large surface area and fast inter-particle adsorption kinetics (El-Sharkawy et al., 2008; Saha et al., 2008). Maxsorb III mainly consist of micropores with different width, and the adsorbent adsorbs on sites with high energy i.e., narrow pores. When the high energy areas are filled up, the adsorbent will gradually fill up larger pores. Here is the affinity weaker and less energy is required. Later the adsorbate will adsorb onto sites of lower energy (Saha et al., 2009b). Currently is Maxsorb III the adsorbent with the highest performing properties, as seen in Table 4.1. The rapid development in nanotechnology will uncover new material structures, that will increase the efficiency of adsorption systems even further.

From Table 4.5, the thermal conductivity is low compared to other materials. However, El-Sharkawy et al. (2016) studied the influence of using Maxsorb III in combination with expanded graphite and binder. Experimental results show that the adsorption equilibrium capacity of ethanol onto consolidated composite(70% Maxsorb III, 20% expanded graphite, 10% binder) is 0.89 kg/kg

Maxsorb III			
Parameter	Unit	Value	Source
$C_p$	$[J/kg]$	$200 + 2T + \frac{3605410}{T^2}$	(Uddin et al., 2017)
$d_p$	$[\mu m]$	105	(Uddin et al., 2017)
$k$	$[W/mK]$	0.066	(El-Sharkawy et al., 2016)
$\rho$	$[kg/m^3]$	281	(El-Sharkawy et al., 2016)

**Table 4.5:** Maxsorb properties

which is about 74% of the maximum adsorption uptake of Maxsorb III/ethanol pair. The thermal conductivity rose from  $\sim 0.066W/mK$  to  $\sim 0.24W/mK$ , and even higher conductivity values for higher percents of additives, which resulted in lower values of uptake.

## 4.5 Previous adsorption solar based ice making system

One of the main problems with adsorption technologies has been the need for high- temperature waste heat. Therefore has some research focused on finding the lower limits for desorption. In a paper by Saha et al. (2006), three different systems have been tested: silica gel - water, activated carbon - ethanol and activated carbon - R134a. The results showed that waste heat down to  $60^\circ C$  could be utilized.

Reviews have been done to compare theoretical COP of different working pairs (Goyal et al., 2016; Choudhury et al., 2013), and an overview from earlier simulations is given in Appendix A section A.3. For the solar based ice makers, most focus is given to activated carbon and methanol. The main difference in the designs is flat plate, flat plate with tubes, or compound parabolic concentrator. The compound parabolic concentrator is most relevant for activated carbon and ammonia because of the high temperature Table 4.4. Therefore, is it interesting to explore the performance with different adsorbate with the best adsorbent.

## Theory

### 5.1 Cold production - Heat pump theory

To understand adsorption systems, knowledge of a regular heat pumping, i.e., refrigeration, is helpful. The purpose of refrigeration systems is to take heat from one place, to lower the temperature in this area, and give off the heat to the surroundings. Heat flows from warm areas to cold areas to make all areas the same temperature; this is thermodynamics second law. Therefore, we must insulate the refrigeration area to reduce the heat flow from the ambient to the refrigerated space.

Evaporation and condensation are the phenomena that occur when we have a working fluid exposed to an ambient temperature higher or lower than the phase shift temperature. For water, the phase shift temperature between liquid and gas is  $100\text{ }^{\circ}\text{C}$  at 1 atm. The temperature of the fluid is not going to change, even though the ambient temperature is higher than  $100\text{ }^{\circ}\text{C}$  before all the fluid has evaporated (boiled), thus becoming water vapor. After the phase shift, the water vapor temperature could increase. The same principle applies to water vapor exposed to temperatures lower than  $100\text{ }^{\circ}\text{C}$ . It is important to notice that these phenomena are temperature and pressure dependent. As some know, boiling water at the top of Mount Everest gives a water temperature of only  $71\text{ }^{\circ}\text{C}$ . This is because of the lower pressure, which is about 0.34 bar. The opposite also applies, higher pressure gives a higher boiling point. Evaporation absorbs heat, while condensation releases heat, seen in the Figure 5.1.

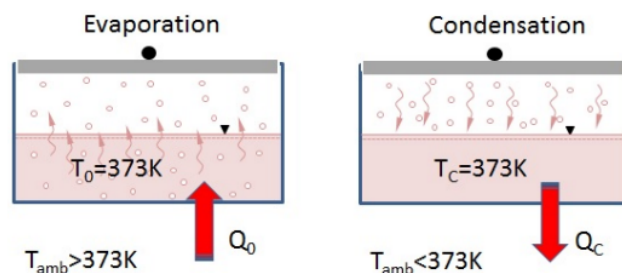


**Figure 5.1:** Heat flow evaporation and condensation. Source:(Eikevik, 2018)

Knowing how fluids could absorb and release heat at different temperature with different pressure levels, a refrigeration system seems possible. However, there is a need for components that could change the pressure. Compressors utilize mechanical work to increase pressure, while an expansion valve reduces it. Figure 5.2 illustrates a simple refrigeration system. The four main components for a functional refrigeration system are present: condenser, expansion valve, evaporator, and compressor. These four components are the minimum required for a closed evaporative process. A closed process is keeping the working fluid within the system.

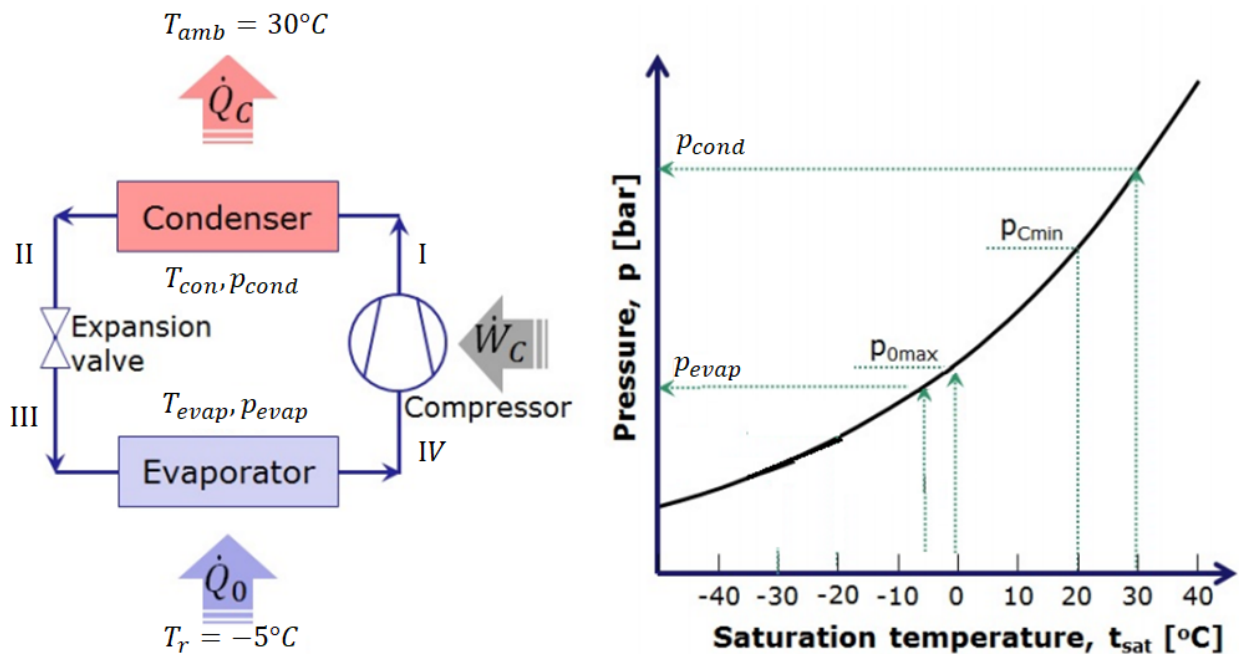


**Figure 5.2:** Heat pump system with high and low temperature. Source: (Eikevik, 2018)

As we can see from Figure 5.2 there is an ambient temperature of  $+20^\circ\text{C}$  and an evaporation temperature in the refrigerated area of  $-5^\circ\text{C}$ . For a specific working fluid, these temperatures will give an evaporation and condensation pressures, noted as  $p_{c,min}$  and  $p_{0,max}$  in the right of Figure 5.2. To achieve heat transfer, there must be a temperature difference; the temperature in evaporator has to be lower than  $5^\circ\text{C}$  and the temperature in condenser higher than  $+20^\circ\text{C}$ . In Figure 5.2 the temperature difference is set to 10 and  $5^\circ\text{C}$ , giving the conditions  $p_{evap}$  and  $T_{evap}$  in the evaporator and  $p_{cond}$  and  $T_{cond}$  in the condenser.

Understanding the heat flow a  $p - h$  diagram Figure 5.3 is used together with the schematic in Figure 5.2. There are marked four points in the schematic, and they could be found in the  $p - h$  diagram.

Point I is after the compressor and before the condenser. The compressor step requires a lot of energy, and in the compression step the temperature increase. In the condenser is heat released from the working fluid to the ambient.  $Q_{amb}$  is the total amount of heat given to the surroundings. When the working fluid is fully condensed, point II in Figure 5.3 is reached.

The next step in the process is an expansion valve. The purpose of an expansion valve is to reduce the pressure. In Figure 5.3, the process between II and III has a constant enthalpy value, i.e.



$h_{II} = h_{III}$ . As the pressure decrease, so do the temperature of the working fluid. A part of the working fluid will after throttling be in gas phase and not useful in the evaporator.

In the evaporator, point III to IV, heat is taken up  $Q_{evap}$ . The working fluid goes from liquid phase to gas phase. Moreover, when all the working fluid is evaporated, the working fluid can go in the compressor to be compressed for a new cycle.

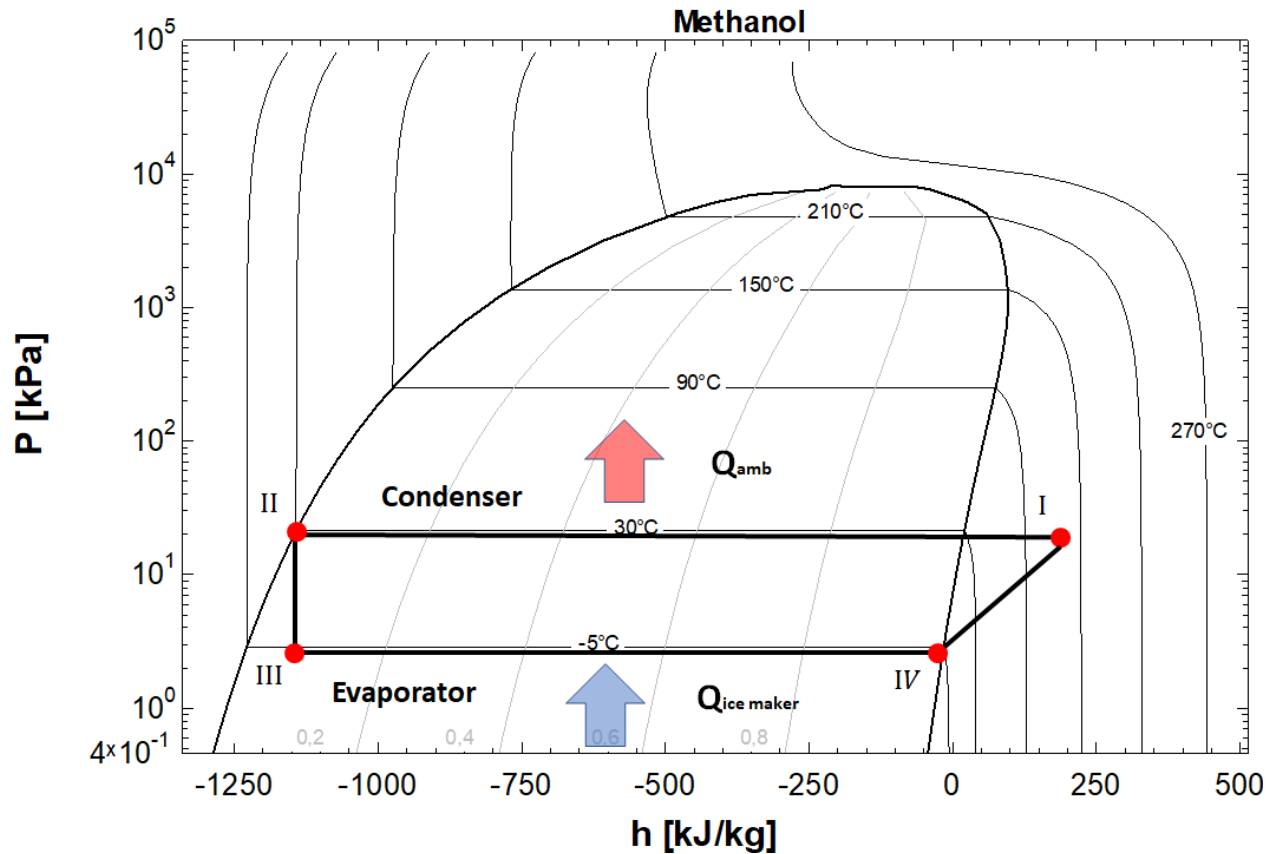


**Figure 5.3:** Pressure-enthalpy diagram for a methanol refrigeration cycle

## 5.2 Ice production

The amount of cold produced is equal to the amount of heat the evaporator takes up. The freezing process starts when sensible heat is removed to lower the temperature of the water (Fellows, 2017). Figure 5.4 illustrates the time-temperature freezing of pure water. In the pre-freezing time interval, sensible heat is removed from the water. Pure water freezes at  $0^{\circ}\text{C}$  but could be subcooled before the initial crystallization. Thus, the evaporation temperature has to be set below  $0^{\circ}\text{C}$ . In the base case of the system the evaporation temperature is set to be  $-5^{\circ}\text{C}$ .  $-5^{\circ}\text{C}$  gives the system some driving force. If the temperature is set lower, the freezing time of the ice would decrease but reduce the efficiency of the system. However, in Figure 5.4 there is a dip in temperature before it rises to  $0^{\circ}\text{C}$ , this is when ice crystals start to form there is some latent heat of crystallization released. The phenomenon of crystals forming from liquid is known as nucleation. In the freezing time period, the crystals grow, and there share liquid will decrease. When all the water is frozen, the temperature could further be reduced to evaporator temperature.

The most common types of ice are block ice, tube ice, and flake ice (FAO, 2019). The amount of water used to produce ice is just over one ton per ton ice. Due to some water may be required for cooling or heating and defrosting if necessary. If fresh water is used, the water has the same requirements as drinking water.

- Block ice: could be from 10–150 kg, where 150 kg is the limit of convenience to handle. Water filled in metal cans produce the ice when lowered into refrigerated brine. Dimensions and temperatures determine production time. This way of production is costly and labor intensive.
- Flake ice: A drum is refrigerated by the working fluid and water is sprayed on forming a 2-3 mm thick ice layer. Scrapes rotate in the drum and remove the ice.
- Tube ice: Water is frozen in 50 mm diameter tubes. The ice loosens during defrosting and chopped in pieces.
- Plate ice: Water is frozen on a vertical plate and released by running warm water on the other face of the plate.

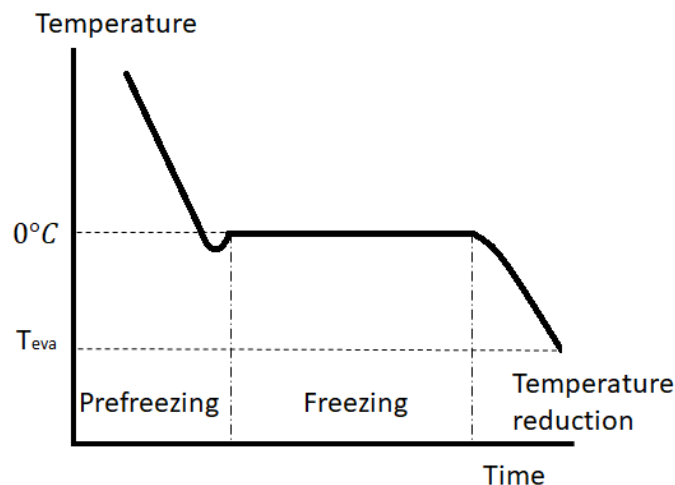


**Figure 5.4:** Temperature-time plot of freezing process of water

## 5.3 Solar irradiation as heat source

The average solar irradiation outside the atmosphere is  $\sim 1360 \text{ W/m}^2$ , but due to the atmosphere, the amount will be reduced when it reaches the earth. Air mass is the amount of atmosphere irradiation must pass through before hitting the earth. Outside of the atmosphere, the air mass is 0 and defined to be 1 when the sun is direct normal to the surface at the equator.

At the equator, the sun will be direct normal at noon. However, this is not the case at other latitudes. To optimize the solar irradiation, the solar collector should have an angle accounting for the position of the sun and latitude of the solar collector. If the collector does not follow the sun crossing the sky, will it result in lower irradiation, thus lower temperature in the bed. In developed countries, this job will be done by a simple electric system. However, in India labor is cheap, and the solar collectors could be moved physically by hand. Solar irradiation will vary through the day depending on the elevation angle, zenith angle and the azimuth angle which is defined in Figure 5.5.

The mathematical relation of solar irradiation is given in Equation 5.1, where  $\beta$  is the elevation angle of the solar collector.

$$I = I_{abs}A[\cos(\theta_{el})\sin(\beta)\cos(\theta_A - \theta_Z) + \sin(\theta_{el})\cos(\beta)] \quad (5.1)$$

The optimal tilt angle dependent on the geographical latitude and the time of the year due to the tilt of the Earth on its axis of rotation. The maximum declination variation is  $+23.45^\circ$  on June 21, and minimum declination is  $-23.45^\circ$  on December 22. The variation through the year is given by Equation 5.2, where  $d$  is the first day of the year January as  $d = 1$ . The latitude of Kolkata and Jaipur is  $22.6^\circ$  and  $26.9^\circ$ . Giving the average tilt of angle from the horizontal the same. The optimal tilt angle for every other week of the year is shown in Appendix A section A.1

$$\delta = -23.45^\circ \cos\left[\frac{360}{365}(d + 10)\right] \quad (5.2)$$

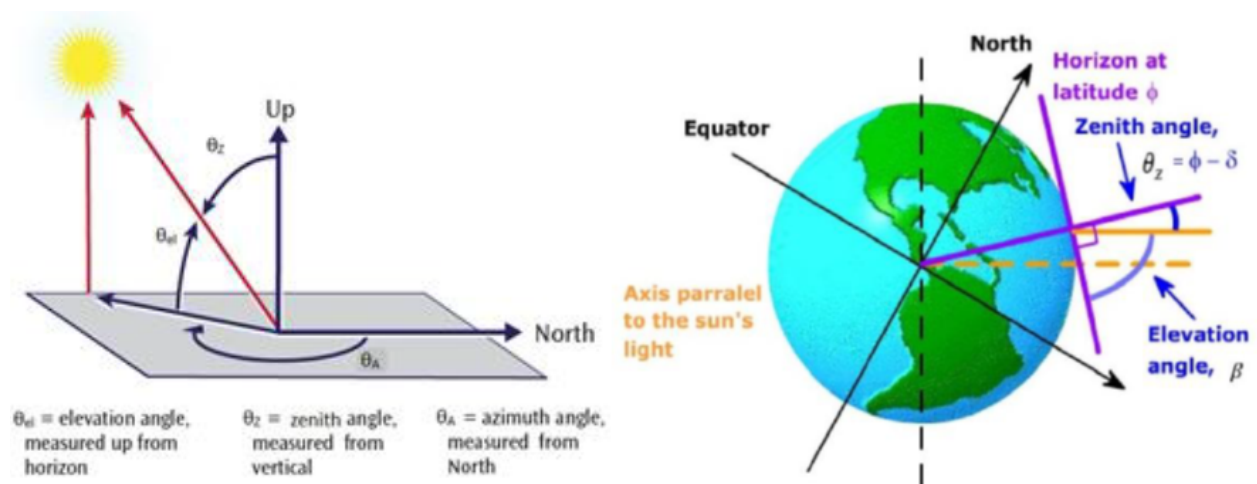


**Figure 5.5:** Solar angles and tilt of the earth

## 5.4 Adsorption

One of the most common equations to use for calculating adsorption/desorption is the Dubinin-Astakhov state equation. The absorbed mass of working fluid,  $x$  (kg working fluid/ kg AC), is related to the bed temperature, system pressure, and characteristics to the adsorbent and adsorbate.

$$x(T, P) = \omega_0 \rho_m(T) \exp \left[ - \left( \frac{R}{\epsilon E_0} \right)^n \left( T \ln \left( \frac{P_s(T)}{P} \right) \right)^n \right] \quad (5.3)$$

Fortunately, could Equation 5.3 be simplified.  $X_0$  is the maximal adsorbent uptake of the adsorbate, which is related by  $\omega_0$  the limiting micropore volume of the adsorbent and  $\rho_m(T)$  the density of adsorbent. For simplicity is the density assumed to be constant.

$$X_0 = \omega_0 \rho_m(T) \quad (5.4)$$

The second part of the expression that could be simplified is introducing  $D$ , a characteristic constant for the working pair. It is made up of the gas constant  $R$ , affinity coefficient  $\epsilon$ ,  $n$  is the characteristic parameter, and the characteristic adsorption energy  $E_0$  of the working pair.

$$D = \left( \frac{R}{\epsilon E_0} \right)^n \quad (5.5)$$

The simplified Dubinin-Astakhov state equation Eq. 5.6 has been verified experimentally and values for  $D$ ,  $X_0$  and  $n$  are found in the literature. The equation is temperature and pressure depended.  $P_s(T)$  is the saturated pressure according to the adsorbent temperature.

$$x(T, P) = X_0 \exp \left[ - D \left( T \ln \left( \frac{P_s(T)}{P} \right) \right)^n \right] \quad (5.6)$$

The experimental data for some working pairs were found in Chapter 3. In Table 5.1 are the values for Maxsorb III and different working fluids gathered.  $q_{st}$  is the isosteric heat of adsorption/desorption. That is the energy required to separate the working fluid from the activated carbon. The isosteric heat of adsorption/desorption consists of the latent heat of the working fluid and an additional term which is related to the van der Waals forces between the adsorbent and adsorbate.

Parameter	$X_0$ [kg/kg]	$q_{st}$ [kJ/kg]	$n$ [-]	$D$ [K <sup>-n</sup> ]	Source
Methanol	1, 24	1900	2	$4, 022 \times 10^{-6}$	(El-Sharkawy et al., 2009)
Ethanol	1, 2	1026	1, 8	$9, 265 \times 10^{-6}$	(El-Sharkawy et al., 2014)
R134a	1, 945	210	1, 17	$2, 930 \times 10^{-4}$	(Saha et al., 2009b)

**Table 5.1:** Experimental data for Maxsorb III

## 5.5 Heat loss

Eq. 5.7 gives the heat loss, where is  $U_L$  the overall heat transfer coefficient and temperature difference of the bed and ambient.

$$Q_{loss} = U_L(T_{bed} - T_{amb}) \quad (5.7)$$

In the design of the solar collector, three parts are influencing the overall heat transfer coefficient. The top of the absorber has a glazing cover and an air gap represented by  $U_{top}$ . The heat coefficient on the back and sides will depend on the insulation material, and thickness and are represented by  $U_{back}$  and  $U_{sides}$ . The overall heat transfer coefficient is given by Eq. (5.8)

$$U_L = U_{top} + U_{back} + U_{sides} \quad (5.8)$$

The following equations are according to Duffie and Beckman (2013) accurate within  $\sim 0.3W/m^2$  °C from ambient to 200°C.  $N$  is the number of glass covers,  $\beta$  is the collector tilt given in degrees, and  $h_w$  wind heat transfer coefficient. The glass plate reflects some of the irradiation which is represented as the emittance of glass  $\epsilon_g$  and emittance plate  $\epsilon_p$ .  $\sigma$  is the Stefan Boltzman constant.

$$U_{top} = \left( \frac{N}{\frac{C}{T_{bed}} \left[ \frac{(T_{bed} - T_{amb})}{(N+f)} \right]^c + \frac{1}{h_w}} \right)^{-1} + \frac{\sigma(T_{bed} + T_{amb})(T_{bed}^2 + T_{amb}^2)}{\frac{1}{\epsilon_p + 0.00591Nh_w} + \frac{2N+f-1+0.133\epsilon_p}{\epsilon_g} - N} \quad (5.9)$$

- $f = (1 + 0.089h_w - 0.1166h_w\epsilon_p)(1 + 0.07866N)$
- $C = 520(1 - 0.000051\beta^2)$  for  $0^\circ < \beta < 70^\circ$
- $e = 0.430(1 - 100/T_{bed})$

### Heat loss with insulation

The energy loss through the back side of the collector could be represented by two series resistors. Resistance in the insulation and resistance in convection and radiation to the environment. The calculations with insulation are the resistance to the convection and radiation is set to zero. Giving the approximation in Eq. (5.10), where  $k$  is the thermal conductivity of the insulation and  $L$  is the thickness of the insulation. The value of thermal conductivity is set to  $\sim 0.045W/m^\circ C$  in the literature (Duffie and Beckman, 2013) and the thickness in the range 5 – 10 cm.

$$U_{back} = \frac{k}{L} \quad (5.10)$$

Finding the heat loss through the edges is difficult. The losses is estimated by assuming one-dimensional sideways heat flow around the perimeter of the collector system. Where  $(UA)_{edge}$  edge loss coefficient area and  $A_c$  collector area. The heat loss through the sides are going to be small compared to the top and back side losses.

$$U_{sides} = \frac{(UA)_{edge}}{A_c} \quad (5.11)$$

### Heat loss without insulation

During the cooling of the system, the heat transfer coefficient will differ from heating. The back cover insulation will be removed and  $U_{back}$  will increase and represented by  $U_{back.wi}$  where  $wi$  means without insulation.  $U_{sides}$  will be smaller than the back losses.

$$U_L = U_{top} + U_{back.wi} \quad (5.12)$$

The temperature of the backside of the bed will be higher than the ambient and natural convection will occur. However, the temperature will not be uniformly distributed through the bed during the cooling process. The transient heat transfer is given by Equation 5.13, where  $T_{new}$  is the new temperature,  $T_{amb}$  is the ambient temperature and  $T_{old}$  is the old temperature. The following theory and equations are taken from TEP4265.

$$\theta = \frac{T_{new} - T_{amb}}{T_{old} - T_{amb}} \quad (5.13)$$

$\theta$  is the dimensionless temperature given in Equation 5.14, which is depended on the Fourier and Biot number. For Biot numbers between  $0.1 < Bi < 100$  the following equation shows the temperature distribution through the body.  $\cos(\mu_n \frac{x}{L})$  represents the exact point of the calculated temperature.

$$\theta = \sum_{n=1}^{n \rightarrow \infty} \frac{2 \sin \mu_n}{\mu_n + \sin \mu_n \cos \mu_n} \cos(\mu_n \frac{x}{L}) \exp(-\mu_n^2 F_o) \quad (5.14)$$

$Bi$  is the Biot number where  $b$  is the external heat transfer coefficient,  $L$  is the length through which conduction occurs, and  $k$  is the thermal conductivity of the body.

$$Bi = \frac{b L}{k} \quad (5.15)$$

$F_o$  is the Fourier number, where  $a$  is thermal diffusivity and  $t$  is time. The thermal diffusivity is defined as  $a = k/c_p \rho$ , where  $c_p$  specific heat and  $\rho$  is the density of Maxsorb III.

$$F_o = \frac{a t}{L^2} \quad (5.16)$$

$\mu_n$  is the roots of parametric equation given below.

$$\frac{1}{\tan \mu_n} = \frac{\mu_n}{Bi} \quad (5.17)$$

## System operation

### 6.1 System overview

The system has mainly four main components, excluding valves. These are shown in Figure 6.1 and indicated: 1 Bed, 4 Condenser, 5 Receiver, and 7 Evaporator. While component number 2, 3, 6, and 8 are valves. Each component will be described in section 6.4.

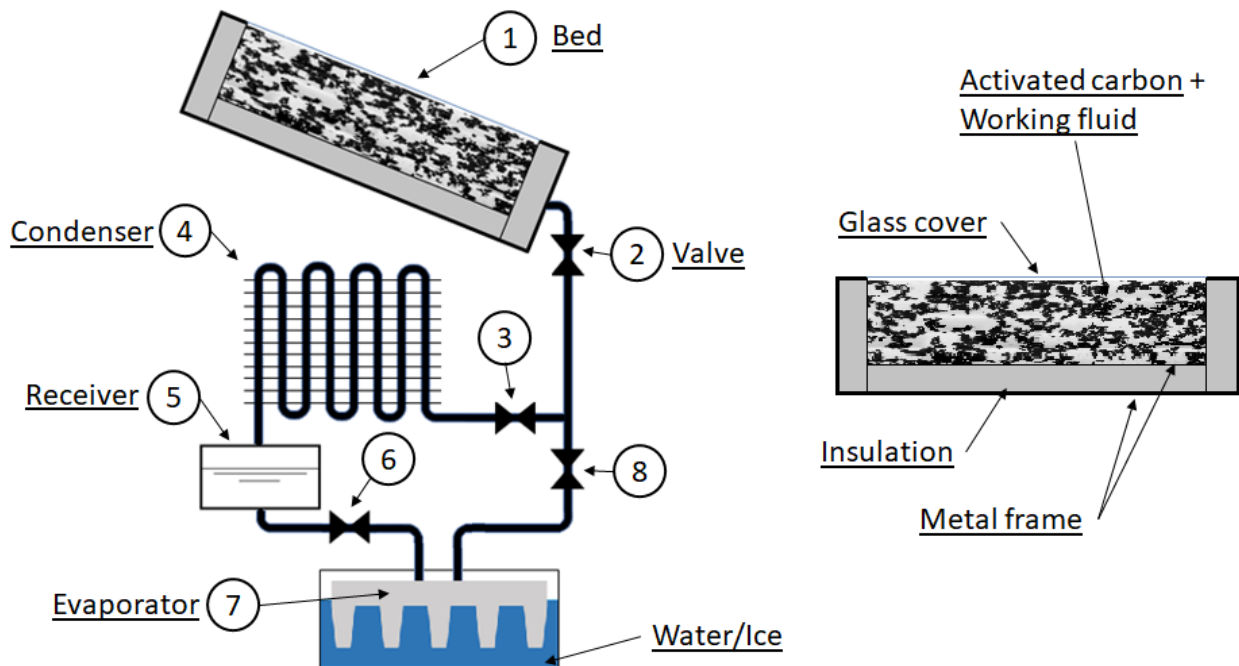


**Figure 6.1:** Components of the system

## 6.2 Thermodynamic description

The system in focus is not familiar to many, so to get a better understanding of the operation of the system, the following chapters go in detail how the thermal compression, adsorption and desorption process work. Since there is only one bed in the system, the system is operating intermittent, i.e. it is not producing continuous cold. In this system, one cycle lasts one day. The temperature rises during the day and falls at night.

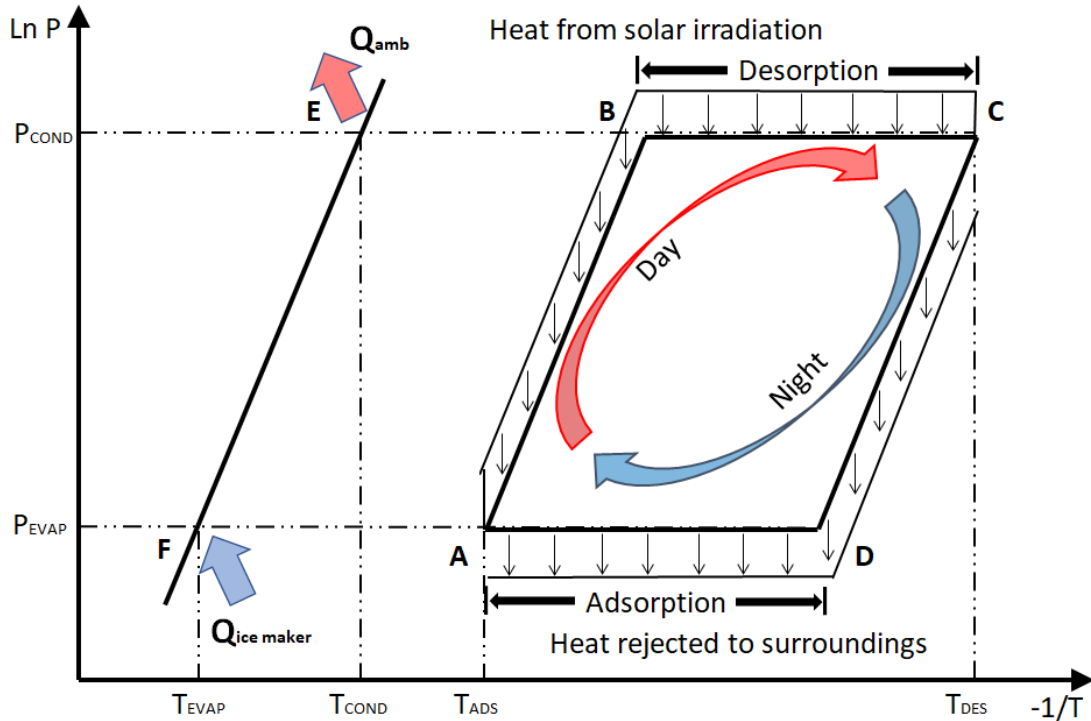


Figure 6.2: Pressure-temperature diagram for a cycle through one day

### Isosteric heating: Stage 1 (A → B)

The first step is during the day. Valve (2) is closed, as seen in Figure 6.3. At the start of the process, the bed is at the lowest temperature, see Figure 6.2. Solar irradiation is heating the bed, causing the vapor in the bed to expand, thus increasing the pressure. The temperature is rising from  $T_{ads}$  to  $T_B$  and the pressure is increasing from  $p_{evap}$  to  $p_{cond}$ . This pressure increase makes a pressure difference in the system, which is driving the system. The valve to the bed is closed until the pressure reaches  $p_{cond}$ . The volume in the bed is not changing, therefore making it an isovolumetric process. This process is called thermal compression. The pressure levels are decided by the condensing temperature and evaporator temperature, which will be further discussed in section 6.3. When the pressure in the bed reaches the desired pressure level valve (2) could be partly opened, and stage 2 of the will start.



**Isobaric desorption: Stage 2 (B → C)**

The second step is heating the bed from  $T_B$  to  $T_{des}$  or  $T_C$ . Valve (2) let out working fluid at the same rate as desorbed from the bed, see Figure 6.3, this will ensure the right pressure level in the system. The working fluid flows through valve (3), since valve (8) is closed. After valve (3) the working fluid goes through the condenser (4) giving off heat to the surroundings and condensing, then collected in the receiver (5). As the temperature is rising from state point B working fluid will be desorbed from the activated carbon. The bed will desorb until the maximum temperature in the bed is reached, which is given as  $T_{des}$  in Figure 6.2.

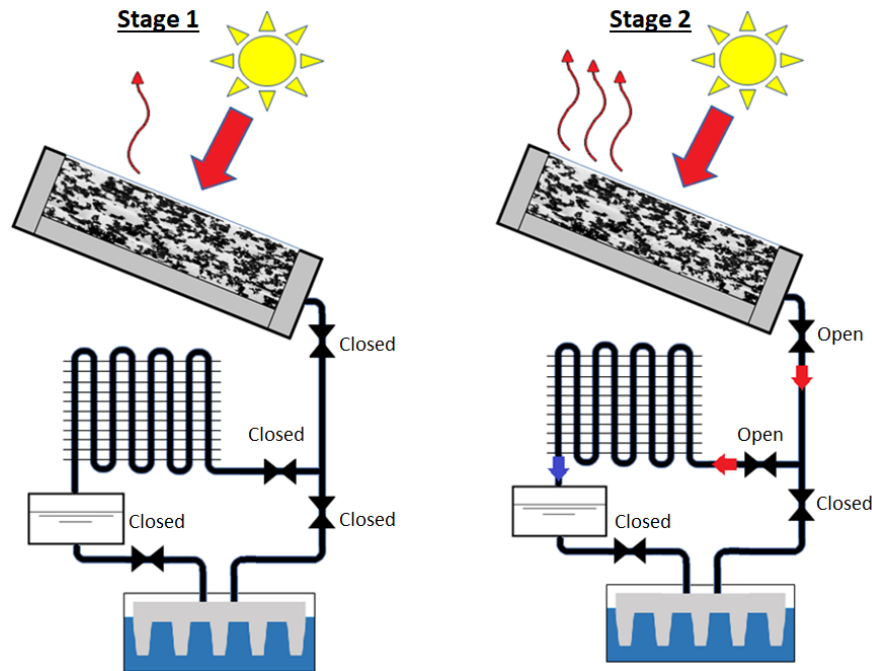


**Figure 6.3:** Stage 1 and 2 of the system cycle

**Isosteric cooling: Stage 3 (C → D)**

The third step is cooling and depressurization and is similar to the first step. To increase the heat transfer from the bed, the insulation on the backside of the bed is removed. All the valves are closed, as shown in Figure 6.4. Heat is transferred from the bed to the surrounding, thus reducing the temperature in the bed. As the temperature is decreasing the pressure decrease as well, seen in Figure 6.2. The bed cools from  $T_{des}$  ( $p_{cond}$ ) to  $T_D$  ( $p_{evap}$ ). The pressure levels will be further discussed in section 6.3. Because all the valves are closed, there is no mass flowing in and out of the bed, so this is also an isovolumetric process. The working fluid is in the receiver (5) at high pressure ( $p_{cond}$ ).

**Isobaric adsorption: Stage 4 (D → A)**

The fourth, and final, step of the bed cycle is further cooling and adsorption of working fluid. Valve 2, 6, and 8 gets partly opened as seen in Figure 6.2. Working fluid from the receiver (5) are throttled from high pressure ( $p_{cond}$ ) to low pressure ( $p_{evap}$ ), point E and F in Figure 6.2. The throttling process will reduce the temperature of the working fluid so that ice could be produced. The working fluid goes from a mixture of liquid and gas after valve (6) to only gas after the evaporator (7). When the temperature of the bed decreases from point D → A, the bed could adsorb working fluid. After the working fluid has evaporated in the evaporator (7), the gas flow in the bed through valve (8) and (2), and the absorbent will adsorb the refrigerant because of its chemical affinity at this temperature. This process continues until the lowest possible temperature is reached  $T_{ads}$ . The evaporating temperature decides the pressure, and this is close to an isobaric process. The process is back to step one and can start a new cycle.

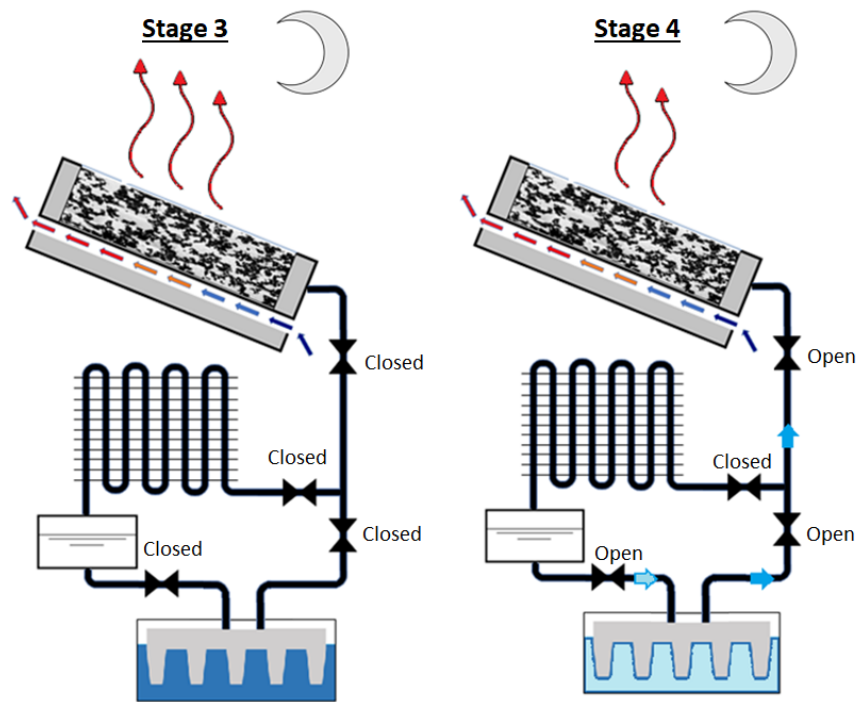


**Figure 6.4:** Stage 3 and 4 of the system cycle

## 6.3 Pressure levels and temperature variation

### Pressure levels

There are two main pressure levels in the system, marked  $p_{evap}$  and  $p_{cond}$  in Figure 6.2. The pressure levels are decided by the saturation pressure at given by temperatures  $T_{evap}$  and  $T_{cond}$ .

For  $p_{cond}$ , it is the condenser temperature deciding the saturation pressure. When the working fluid desorbs from the bed in stage 2, the working fluid is flowing through the condenser (4). The condenser temperature has to be set higher than the ambient temperature, which varies day by day. For example, the ambient temperature is  $25^{\circ}C$ , that means the temperature in the condenser must be  $30^{\circ}C$ , if we chose  $\Delta T = 5^{\circ}C$ . The saturation pressure is a function of temperature, and by knowing the condenser temperature, the corresponding pressure level could be found. The pressure levels of the different working fluids are given in Table 6.1.

The same logic applies for  $p_{evap}$ , but the evaporator temperature  $T_{evap}$  is deciding the saturation pressure. The purpose of the system is to make ice. Thus the temperature has to be below  $0^{\circ}C$ . However, if the temperature is too low the efficiency of the system will decrease. Furthermore, if the temperature is set too close to  $0^{\circ}C$  there will not be any driving force in the evaporator. A selection of temperatures and their corresponding pressure is shown in Table 6.2.

It is worth noting the pressure levels for methanol and ethanol are below atmospheric pressure, while R134a is above, the saturation temperatures given in Table 6.2.

Working fluid pressure ( $kPa$ )			
Temperature	Methanol	Ethanol	R134a
$20^{\circ}C$	12,71	6,049	572,1
$25^{\circ}C$	16,57	8,057	665,8
$30^{\circ}C$	21,39	10,63	770,6
$35^{\circ}C$	27,36	13,90	887,5

**Table 6.1:** Relevant condensing temperatures and their corresponding saturated pressures. Data from EES

Working fluid pressure ( $kPa$ )			
Temperature	Methanol	Ethanol	R134a
$-5^{\circ}C$	2,860	1,233	243,5
$-4^{\circ}C$	3,054	1,321	252,9
$-3^{\circ}C$	3,259	1,415	262,5

**Table 6.2:** Relevant evaporator temperatures and their corresponding saturated pressures. Data from EES

### Influence of pressure levels

The two temperatures setting the two pressure levels influences the operation of the system greatly. Dubinin-Astatakhov state equation is a function of temperature and pressure, as seen in Section 5.4. To understand how the temperature and pressure are influencing the operation, it is easier to introduce a  $x - T$  diagram.

The y-axis in Figure 6.5 is representing the uptake of working fluid in kg per kg of activated carbon, while the x-axis is the temperature of the bed. The lines are representing the state of Dubinin-Astatakhov equation with constant pressure and increasing temperature. As the temperature is increasing the activated carbon is less able to hold on the working fluid, i.e. the activated carbon desorbs. Looking at the black line (2.86 kPa), which has a saturation temperature of  $-5^{\circ}\text{C}$ , the activated carbon is fully adsorbed at  $\sim 270\text{K}$  while fully desorbed at  $\sim 340\text{K}$ . Then looking at a constant temperature, for example,  $\sim 340\text{K}$ , the activated carbon uptake is increasing with the increasing pressure. For 2.86 kPa is the x value  $\sim 0$  kg/kg, for 9.65 kPa  $\sim 0.1$  kg/kg, for 21.39 kPa  $\sim 0.4$  kg/kg, and for 43.65 kPa  $\sim 0.9$  kg/kg. Thus, increasing pressure will make the activated carbon able to hold on the working fluid better.

As discussed in section 6.3, will the condensing pressure level increase if the condensing temperature increase. In Figure 6.5 this could be seen on the blue ( $15^{\circ}\text{C}$ ), red ( $30^{\circ}\text{C}$ ) and green line ( $45^{\circ}\text{C}$ ). From an operational perspective, will the distance from state point A to B, see Figure 6.2, increase with the increased pressure difference. Furthermore, the energy required to increase the pressure is increasing. Thus minimal pressure difference is optimal.

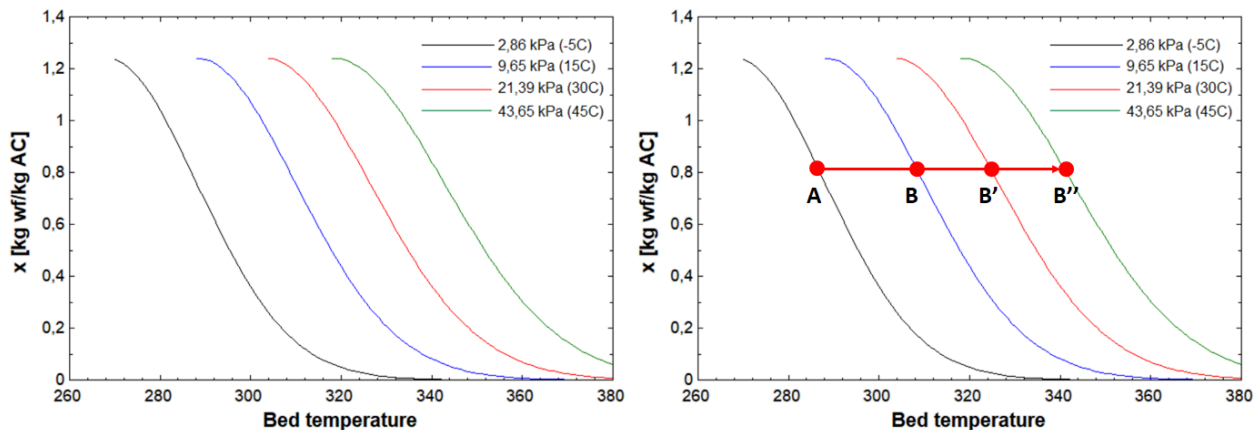


**Figure 6.5:** Adsorbent uptake - bed temperature diagram with varying condensing temperature

### Influence of maximum temperature

The maximum temperature  $T_{des}$  can be influenced by the design of the system, which is influenced by the solar irradiation collector or heat losses. Figure 6.6 shows the effect of increasing the maximum temperature of the bed. Here is the evaporation temperature set to  $-5^{\circ}\text{C}$  with a corresponding pressure of 2,86kPa and the condensation temperature  $30^{\circ}\text{C}$  giving a pressure of 21,39kPa. The state points in Figure 6.6 are the same as in Figure 6.2. The maximum temperature in the bed is given in state C, while the adsorption temperature is state A. For a maximal temperature of

$\sim 340K$  gives a relatively small  $\Delta x$ , but increasing the maximal temperature will increase the  $\Delta x$ . However, the increase in  $\Delta x$  is not linear with the temperature for higher temperatures. This will be studied closely in the section 8.1.4.

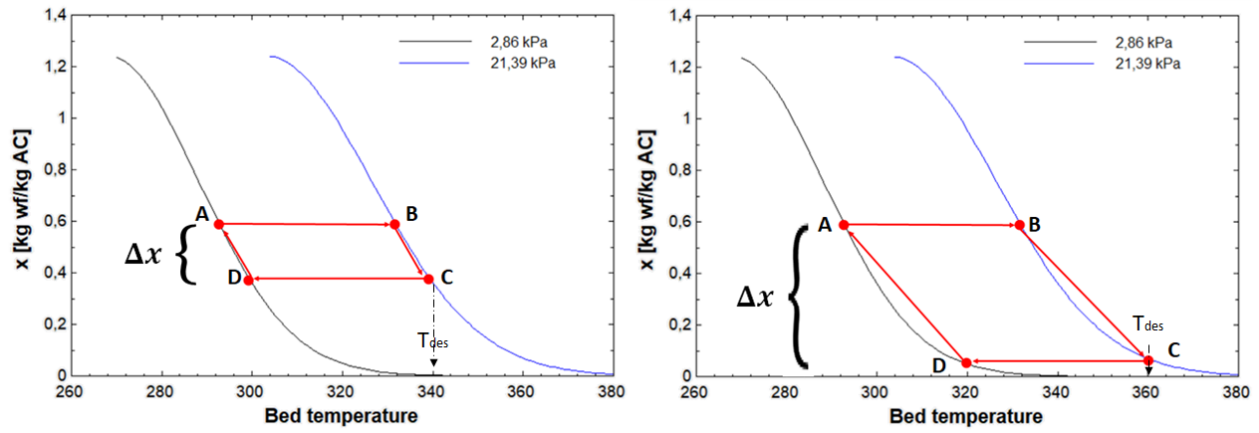


**Figure 6.6:** Influence of increasing desorption/maximal bed temperature

### Influence of adsorption temperature

The adsorption state point is represented as  $A$  in Figure 6.7. The adsorption temperature is decided by the lowest temperature the bed reach. It is depended on the ambient temperature and the design. The figure shows that decreased adsorption temperature increases the  $\Delta x$ , thus lower adsorption temperatures increase the COP and amount of working fluid adsorbed and desorbed.

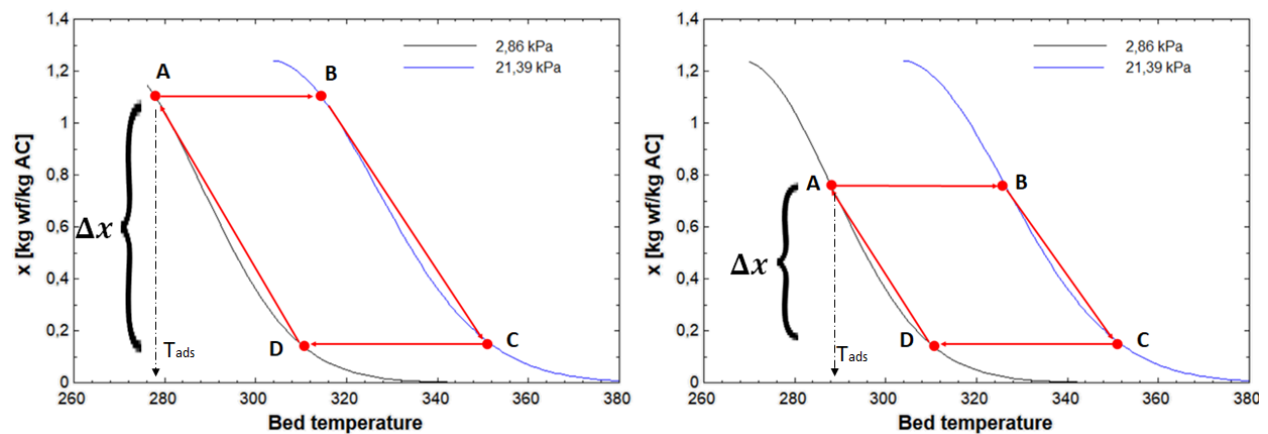


**Figure 6.7:** Influence of decrease the adsorption/minimal bed temperature

## 6.4 Components of the system

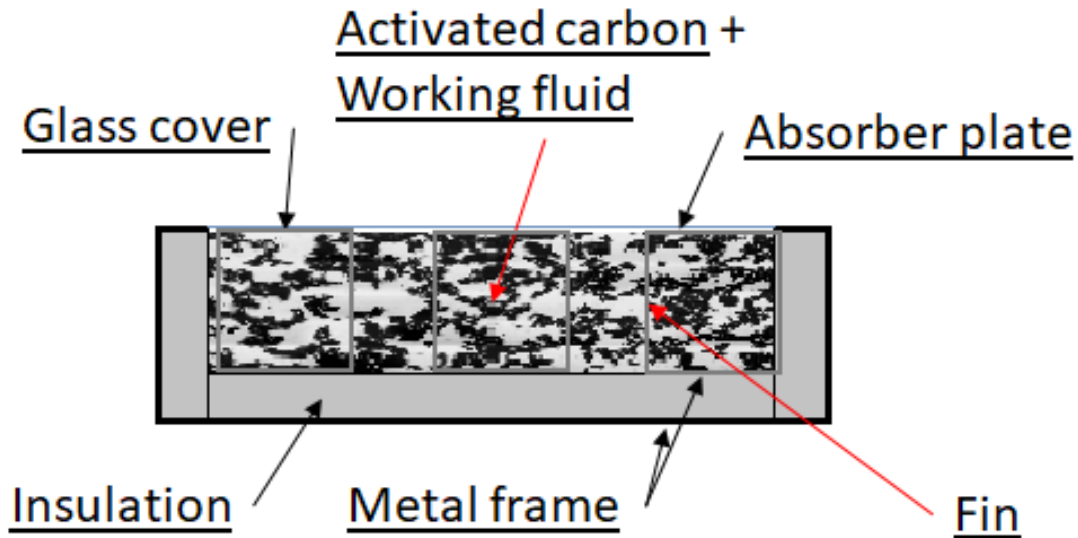


**Figure 6.8:** Components on the bed

The system aims to produce 10 kg of ice every day. In the first basic design, the size of the solar collector is decided to be  $1m^2$ . This size makes it relatively small, and calculation could be simplified. Later the size may be redesigned to satisfy the 10 kg demand.

The design of the system is based on earlier designs, such as Wang and Oliveira (2006), Passos et al. (1989), Hamrahi et al. (2018), and Alghoul et al. (2007).

### 6.4.1 Collector

The collector is the central part of the system. This component is the most important to have optimized and consists of four main parts: adsorbent bed, insulation, glass cover, and absorber plate. There are three important heat transfer processes, which are:

- Rapidly increasing the temperature in the bed during heating
- Isolation to achieve highest possible temperatures
- Rapidly decrease the temperature in the bed during cooling

#### Adsorbent bed

The adsorbent bed is where the adsorbent is. There are different types and designs; however mainly two designs are possible for this system: rectangular and tubular adsorbent bed. In the rectangular design, the adsorbent is spread uniformly in a rectangular geometry divided by fins which distribute the heat equally. In the tubular design will the adsorbent be distributed in cylinders. These tubes are typically made of metals with high thermal conductivity properties. A tubular design has the advantage of simple construction and capacity to withstand pressure difference. However, the

rectangular design could easier distribute the heat, and there is room for more activated carbon in one single bed.



**Figure 6.9:** Possible tubular and rectangular adsorption bed

### Absorber plate

The adsorber plate should be made from metal with high thermal conductivity. Copper is a possibility if the bed temperatures below  $120^{\circ}\text{C}$ . At temperature above  $120^{\circ}\text{C}$  copper and methanol will decompose to formaldehyde and dimethyl ether (Alghoul et al., 2007). Aluminum is lighter, cheaper and has no chemical reaction with methanol below  $150^{\circ}\text{C}$ , but may be exposed to corrosion if impurities are present. Stainless steel has lower thermal conductivity than the previously mentioned materials but is still a design option.

The thickness of the absorber plate should be thin, so heat from the solar irradiation transfers to the activated carbon. The plate should be coated with a material with high absorptivity and low emissivity. The amount of heat the collector can accumulate is highly depended on the absorptivity of the solar collector.

### Glazing cover

The glazing-cover let through solar radiation and reduces the heat loss to the atmosphere. There are multiple different glazing cover design. Single-glass, double-glass, and TIM cover are the most used.

### Insulation

The insulation is placed at the sides and bottom of the collector to reduce the heat loss. Form literature is the thickness varying between  $5 - 10\text{cm}$ .

## 6.4.2 Condenser

The working fluid dissipates heat from the vapor and condenses in the condenser. It is important to either place the condenser in a slope or vertical, so the working fluid flows into the receiver. In warm climates, is it important to place the condenser in the shadow and avoid having it heated by the sun. To increase the heat transfer materials with high thermal conductivity should be chosen. Alternatively, a design with fins or increased heat transfer area could be added. If the air temperatures are very hot during the day water could be sprayed on the condenser or the condenser could be put in an open water tank.

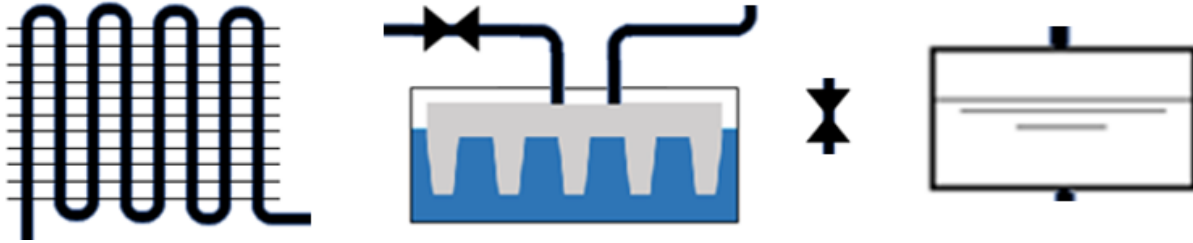


**Figure 6.10:** Condenser, evaporator, valve and reservoir

### 6.4.3 Evaporator and water tank

The evaporator removes heat from the water to make ice. It should be designed so it is easy to remove the ice. In Figure 6.10 a trapezoidal shape is used. The working material must have high thermal conductivity, and the water tank has to be insulated to reduce heat loss to the surroundings. It is important to design the water tank in the right size. If it is too small, cold will go to waste, and if it is too big, the water will only be chilled, not frozen.

### 6.4.4 Reservoir and valves

The reservoir is a tank to store the working fluid after the condensation. If the working fluid is throttled down right after condensation, there is no place to go after evaporation. Thus it is stored to the adsorption process. Some of the valves only need to be able to let working fluid one way, while the valve to the bed needs to let working fluid flow both ways.



## 6.5 Economics

The price of the system is critical. There are two factors in play; initial investment and operating costs. The investment cost for the adsorption system is going to be higher than a small scale electric ice maker. However, it is the operation cost the adsorption system has advantages.

In Table 6.3 are an overview of some key numbers for a commercially available system. The initial cost of the system is 610 NOK, and the operation cost for electricity per year is 655 NOK with numbers from June 2019. The system is made in China, and the quality is debatable. This is a problem that concerns buyers, the life expectancy of the system. For simplicity is the life expectancy of this system set to 5 years.

Small commercial ice maker	
Iceplus home instant mini small 220V portable ice maker	
Capacity	15 kg/ 24 hour
Price	610 NOK
Power usage	100 W
Energy price	6 Rupee per kWh
Energy cost per day	14.4 Rupee ~ 1.8 NOK
Energy cost per year	655 NOK
Working fluid	R134a

**Table 6.3:** Cost of an electric small scale ice maker

The prices in Table 6.4 is from alibaba.com. The evaporator is a simple block ice maker, and the condenser is a standard air cooler. The price of the two components is in the high end. There are two possible designs for the bed: flat plate and tubular. The prices for these components are picked from solar water heaters, which has similar designs as this system. The piping inside the bed and double covers are included in this number. The price of the most available commercial activated carbon is about 110 kg per kg, and cheaper if bought in bulk. Unfortunately, do not the producer of Maxsorb III display the price per kg. Since Maxsorb III is the cutting edge technology regarding activated carbon, the price is at least 10 to 100 times of ash granular. However, this price will reduce with scale and production improvements over time.

Cost of adsorptions system components		
Component	Type	Price NOK
Evaporator	Block ice	240
Condenser	Air cooler	400
Bed	Flat plate	2400
Bed	Tubular	3500
Activated carbon	Ash granular per kg	110
Activated carbon	Maxsorb III per kg	-

**Table 6.4:** Approximately cost of components in the system

Figure 6.11 shows the cost over a commercial ice maker and the two proposed system designs. Time frame is ten years, which is set to the expected life span of the adsorption system. The expected life span of the commercial system is five years, and then a new similar system is bought. The operation cost every year for the commercial system is the cost of electricity, while the adsorption system does not have any operation cost. In the calculation is the price of ash granular used and 20 kg adsorbate. The cost of tubular design is more expensive (6340 NOK) than the cost of flat plate design (5240 NOK). The cost for the commercial system and flat plate design are even after about six years, for the tubular design it is almost eight years. However, if more expensive activated carbon is used, the cost is not eared back in 10 years.

If the production cost of the system is reduced, and the cost of Maxsorb III is low, the system can compete with commercial systems regarding cost.

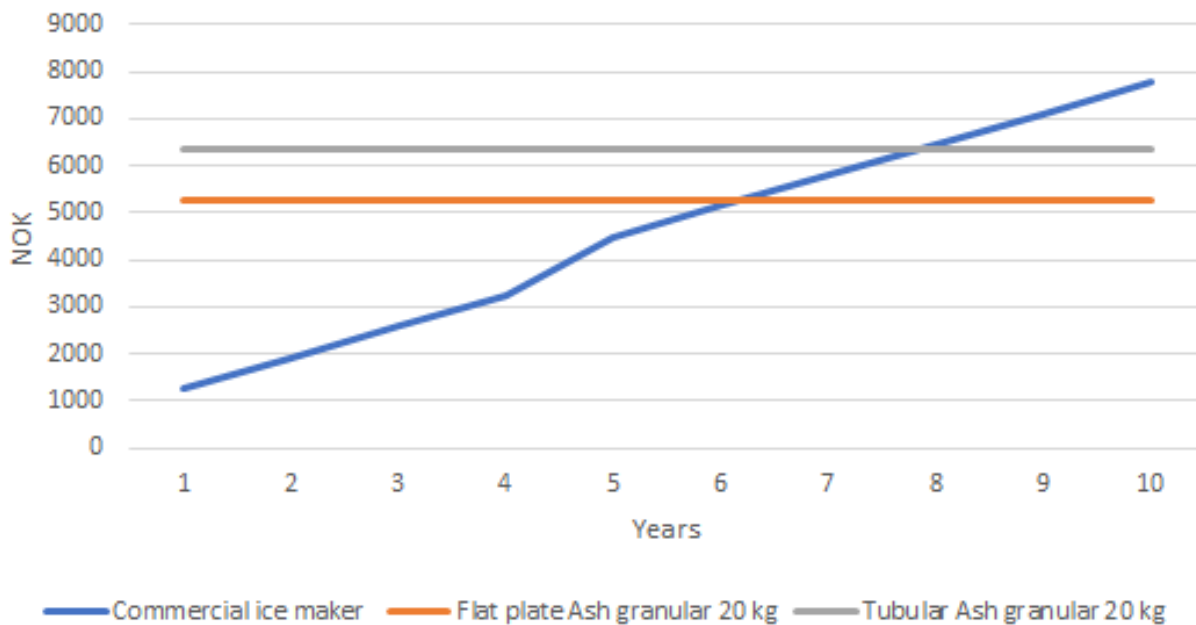


**Figure 6.11:** Operational cost of commercial and adsorption system over 10 year

# Modeling

The modeling is done in three main parts. First, a simple 6-point analysis to compare the three working fluid. Then the thermal profile in the bed is explored to map possible thickness of the bed. Finally, the operation through a day with the variation of solar radiation and ambient temperature is modeled. All of the calculations are done in Engineering Equation Solver (EES) and the code are in Appendix B.

## 7.1 6-point analysis

For the 6-point model, the state points (A, B, C, D, E, F) seen in Figure 6.2 is used. The temperature and pressure are set to investigate the operation of the system. There are only two pressure levels, as is discussed earlier, which are decided by the evaporator temperature and condenser temperature, and further decide state point E, F. While state points (A, C) are decided by the maximum and minimum temperature the system reach. State point B is given by the relation in Equation 7.1.

$$\frac{T_B}{T_{cond}} = \frac{T_A}{T_{evap}} \quad (7.1)$$

Equation 7.1 is valid while  $T/T_{sat}$  is constant along an isostere, see Figure 6.2. The same also applies for state point D.

$$\frac{T_D}{T_{evap}} = \frac{T_C}{T_{cond}} \quad (7.2)$$

Dubin-in-Astakhov state equation depends on temperature and pressure, see chapter 5.4, and with the state point temperatures in Equation 7.1 and Equation 7.2, all the point could be decided.

### Isosteric heating (Stage 1 A → B)

For the isosteric heating stage, the energy input goes to increasing the temperature and pressure in the bed. The energy input in the system is given by Equation 7.3, where  $Q_{AB}$  is the energy input

required to achieve  $p_{con}$  and  $T_B$ .  $C_p$  represent the specific heat,  $m$  is the mass for each component in the bed, and  $x_{max}$  is the maximum uptake of working fluid. The subscripts are  $w$  for side walls,  $AC$  for activated carbon, and  $wf$  for working fluid.

$$Q_{AB} = \int_{T_A}^{T_B} (C_{p,w}m_w + C_{p,AC}m_{AC} + C_{p,wf}m_{AC}x_{max})dT \quad (7.3)$$

### Isobaric desorption (Stage 2 B → C)

In the desorption stage there is an extra term of the heat balance equation, see Equation 7.4. This term represents the heat of desorption  $q_{st}$ , that is the heat required to evaporate the working fluid and separate it from the activated carbon.

$$Q_{BC} = \int_{T_B}^{T_C} (C_{p,w}m_w + C_{p,AC}m_{AC} + C_{p,wf}m_{AC}x_{min})dT + \int_{x_{max}}^{x_{min}} (m_{AC}q_{st})dx \quad (7.4)$$

### Isosteric cooling (Stage 3 C → D)

After the maximum temperature is reached, the cooling process of the system starts. The net heat will be negative, that is out of the bed, and the pressure and temperature decrease. This step is similar to step 1.  $x_{min}$  is the minimum amount of working fluid in the bed.

$$Q_{CD} = \int_{T_C}^{T_D} (C_{p,w}m_w + C_{p,AC}m_{AC} + C_{p,wf}m_{AC}x_{min})dT \quad (7.5)$$

### Isobaric adsorption (Stage 4 D → A)

Stage 4 is the adsorption process. The bed is giving off heat to the surroundings, and the temperature is decreasing. The bed is adsorbing working fluid until the minimum temperature is reached  $T_A$ .

$$Q_{DA} = \int_{T_D}^{T_A} (C_{p,w}m_w + C_{p,AC}m_{AC} + C_{p,wf}m_{AC}x_{min})dT + \int_{x_{min}}^{x_{max}} (m_{AC}q_{st})dx \quad (7.6)$$

### Working fluid

The working fluid from one cycle is the amount the bed can adsorb and desorb in kg/kg multiplied with the amount of activated carbon.

$$m_{wf} = (x_{max} - x_{min})m_{AC} \quad (7.7)$$

**Heat requirement**

The total heat required to operate the system is given by Equation 7.3 and 7.4.

$$Q_{input} = Q_{AB} + Q_{BC} \quad (7.8)$$

**Cold production**

The cold production depends on the amount of working fluid, throttling losses, latent heat of vaporization.

$$Q_{cold} = m_{wf} y' h_{evap} \quad (7.9)$$

Equation 7.10 defines the ice production. It is chosen to include the mass of evaporator since the box containing the activated carbon also is included in the calculations.

$$m_{ice} = \frac{Q_{cold}}{(h_{ice} + c_{p.water}(T_{iw} - 0) + c_{p.ice}(0 - T_{ice}) + m_{evap}c_{p.wall}(T_{iw} - T_{ice}))} \quad (7.10)$$

**COP**

Equation 7.11 defines the COP for the 6-point analysis. It is important to notice how the COP is defined to understand why the COP for this simulation is so high. The energy input is only the minimum, i.e. no heat losses, etc.

$$COP = \frac{Q_{cold}}{Q_{input}} \quad (7.11)$$

## 7.2 Temperature distribution through the bed

Section 5.5 introduced the Fourier and Biot number as a reminder is the two equations given again below.

$$Bi = \frac{b L}{k} \quad Fo = \frac{a t}{L^2} \quad (7.12)$$

### Plane design

For Biot numbers between  $0.1 < Bi < 100$  the following equations shows the temperature distribution through the body. The  $\cos(\mu_n \frac{x}{L})$  term represents the exact point in the bed from 0 to L the calculated temperature.

$$\theta = \sum_{n=1}^{n \rightarrow \infty} \frac{2 \sin \mu_n}{\mu_n + \sin \mu_n \cos \mu_n} \cos\left(\mu_n \frac{x}{L}\right) \exp(-\mu_n^2 Fo) \quad (7.13)$$

Setting  $x = 0$  the temperature profile for the center is found, setting  $x = L$  gives the temperature profile of the surface of the plate, and setting  $x = \frac{1}{2}L$  gives the temperature profile in the middle of the plate. The average temperature of the plate is essential to understand the heat load of the system. Equation 7.14 gives the average temperature profile.

$$\bar{\theta} = \sum_{n=1}^{n \rightarrow \infty} \frac{2 \sin^2 \mu_n}{\mu_n^2 + \mu_n \sin \mu_n \cos \mu_n} \exp(-\mu_n^2 Fo) \quad (7.14)$$

### Tubular design

For the tubular design are following equations valid. The  $J()$  is the Bessel function.

$$\theta = \sum_{n=1}^{n \rightarrow \infty} \frac{2 J_1(\mu_n)}{\mu_n [J_0^2(\mu_n) + J_1^2(\mu_n)]} J_0\left(\mu_n \frac{x}{r}\right) \exp(-\mu_n^2 Fo) \quad (7.15)$$

$$\bar{\theta} = \sum_{n=1}^{n \rightarrow \infty} \frac{4 Bi^2}{\mu_n^2 (\mu_n^2 + Bi^2)} \exp(-\mu_n^2 Fo) \quad (7.16)$$

$\mu_n$  is the roots of parametric equation 5.17, and can be rewritten as 7.17. For the modeling three terms are used ( $n = 3$ ), more terms have minimal impact.  $\mu_n$  values are iterated.  $\mu_1$  is in the range 0 to 2,  $\mu_2$  is in the range 3 to 5, and  $\mu_3$  is in the range 6 to 8.

$$y_n = \frac{\mu_n}{Bi} \quad y_n = \frac{1}{\tan \mu_n} \quad (7.17)$$

The average dimensionless temperature is calculated by Equation 5.13.

$$\theta = \frac{T_t - T_{amb}}{T_{t=0} - T_{amb}} \quad (7.18)$$

## 7.3 Simulation through the day

The simulation through the day are somewhat similar to the 6-point analysis. The left side of the all the stages  $A \rightarrow B \rightarrow C \rightarrow D \rightarrow A$  is replaced with  $I(t) - Q_{loss}(t)$ , where  $I$  is the solar irradiation and  $Q_{loss}$  is the heat loss of the bed. Based on solar irradiation data, ambient temperature and the bed temperature,  $I$  and  $Q_{loss}$  could be calculated.  $I(t)$  and  $Q_{loss}(t)$  will decide the temperature and pressure, following Figure 7.1. With this simulation the behavior of the system could be followed over a 24 hour period.

### Mass flow

Following the desorption and adsorption through the day, the mass flow rate can be decided and the size of the tube approximated.

$$\dot{m}_{wf}(t) = (x(t) - x(t - \Delta t))m_{AC} \quad (7.19)$$

### Solar irradiation

The solar irradiation is modeled with a sinus curve given by Equation 7.20.

$$I(t) = I_{max} \sin\left(\frac{\pi(t - t_{sunrise})}{(t_{sunset} - t_{sunrise})}\right) \quad (7.20)$$

### Ambient temperature

The ambient temperature is modeled with a sinus curve given by Equation 7.21.

$$T_{amb}(t) = \frac{T_{max} + T_{min}}{2} + \frac{T_{max} - T_{min}}{2} \sin\left(\frac{\pi(t - t_{sunrise})}{(t_{sunset} - t_{sunrise})}\right) \quad (7.21)$$

### COP

The COP for the simulation through the day are slightly different than for the COP in 6-point analysis. The heat input is all the solar irradiation through the day, also know as solar coefficient of performance.

$$SCOP = \frac{Q_{cold}}{\int_{Sunrise}^{Sunset} I(t) Adt} \quad (7.22)$$

### Modelling assumption

The follwing assumption is utilized in the simulation:

- The bed porosity is constant
- Uniform particle size of Maxsorb III
- The vapor of the working fluid behave as an ideal gas
- The temperature of the working fluid and activated carbon is at the same temperature

- The values for Maxsorb III given in Table 4.5
- Thermodynamic values for the working fluid from EES

**Model structure**

Figure 7.1 shows the model structure for the simulation through one day. The heat loss is calculated with the temperature from the previous time step, and the solar irradiation conditions are known.

The first logic-step is comparing the heat loss to the heat input. If the heat input is bigger than the heat loss, the bed heats up. Then the pressure in the bed is deciding the next step. Are the pressure in the bed lower than the condenser pressure, the heat input will go to increasing the temperature and pressure in the bed. If the bed pressure is higher than the condensation pressure, all the heat goes to increasing the temperature in the bed.

At a certain temperature level will the heat loss surpass the heat input. First, the pressure and temperature will decrease until the pressure in the bed falls below the evaporator pressure. Then only the temperature will decrease, and the ice production starts.

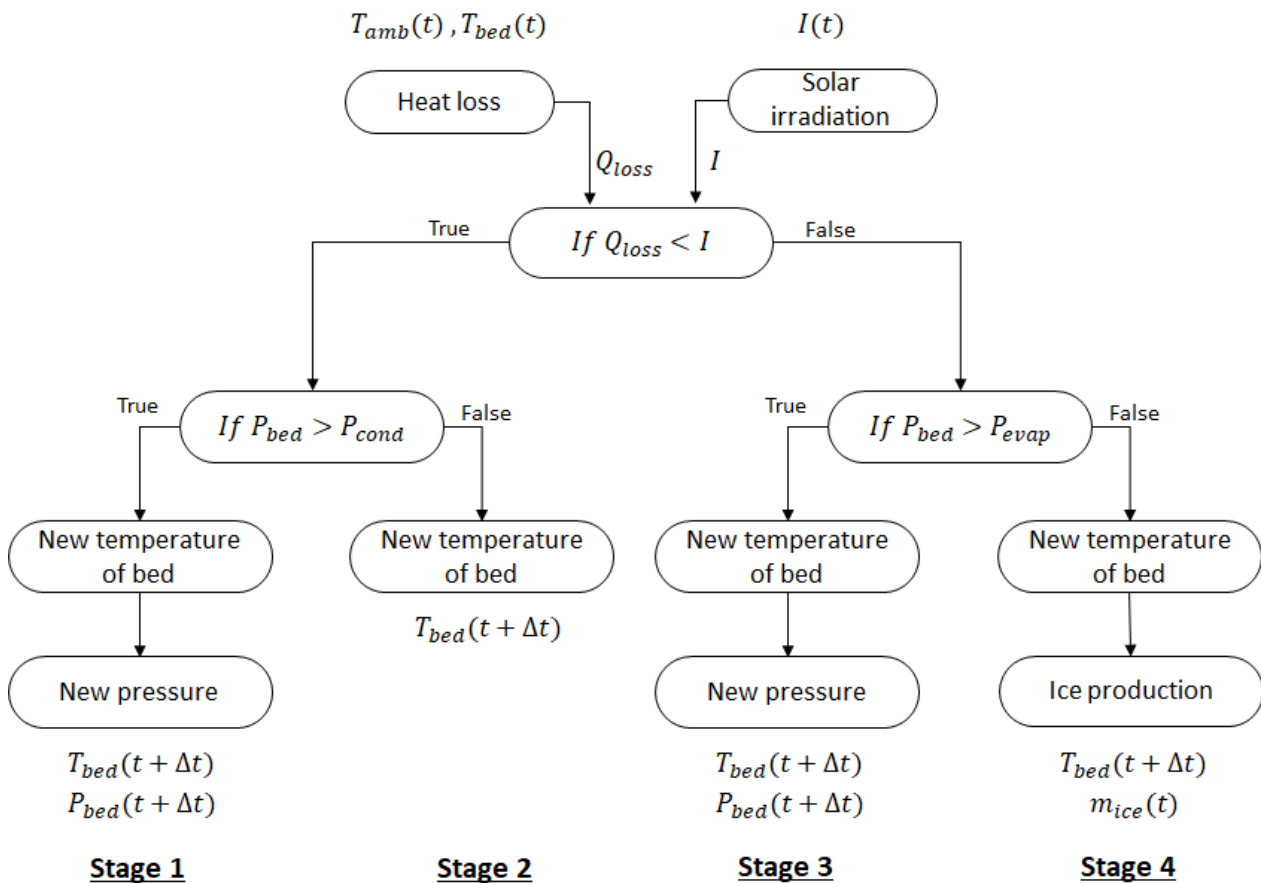


**Figure 7.1:** Simulation structure for the operation through one day



## Results and discussion

The results and discussion part have three main parts. Part one focus on the thermodynamic analysis of the system without considering the setup and heat losses. The second part considers the transient temperature profile in the bed. Moreover, the third part considers the actual system operation. All parts are necessary to find the working temperature range and dimension of the system.

### 8.1 Thermodynamic analysis

The first model is a simple 6-point model taking account of all the important state points. The cycle is described earlier in Figure 6.2. The code and parameters for the analysis are found in Appendix B section B.1.

#### 8.1.1 Validation of the code

Wang et al. (2000) made a theoretical model of an adsorption ice maker. This system uses the same cycle in the ice production process. However, it is using water to heat the bed of activated carbon powered by a solar water heater. The article describes the working of the system and a theoretical model, as well as experiments on a developed prototype. The theoretical model is using an activated carbon type named coconut shell. Coconut shell gives different values to the Dubinin-Astakhov equation compared to Maxsorb III. The author of the article also used a slightly different version of Dubinin-Astakhov. The results focus mainly on the main parameters: desorption -, adsorption -, evaporator -, and condenser - temperature. However, the results in Table 8.1 shows that the results are in close agreement with the result of Wang et al. (2000). For the following result in this chapter, the values of coconut shell are switched with values of Maxsorb III, while the parameters of design of the system are the same as before.

Inlet water temperature	$T_{iw} = 15^{\circ}C$		$T_{iw} = 10^{\circ}C$		$T_{iw} = 10^{\circ}C$	
Evaporation temperature	$T_{eva} = -10^{\circ}C$		$T_{eva} = -10^{\circ}C$		$T_{eva} = -10^{\circ}C$	
Generation temperature	$T_{max} = 93,6^{\circ}C$		$T_{max} = 86,6^{\circ}C$		$T_{max} = 84,9^{\circ}C$	
Adsorption temperature	$T_{ads} = 23,7^{\circ}C$		$T_{ads} = 19,6^{\circ}C$		$T_{ads} = 19,5^{\circ}C$	
Condenser temperature	$T_{con} = 25^{\circ}C$		$T_{con} = 20^{\circ}C$		$T_{con} = 15^{\circ}C$	
Study	Wang	Present	Wang	Present	Wang	Present
COP	0,44	0,43	0,48	0,48	0,51	0,52
Ice in kg	6,3	6,4	7,9	7,9	8,7	8,7

**Table 8.1:** Wang et al. (2000) values of COP and kg ice produce

### 8.1.2 Effect of main factors

It is interesting to look at the effect of varying the main factors of the system. To do this, the other values of the system must be constant. In Table 8.2 shows the temperature parameters used in the simulation. The working pair of methanol and Maxsorb III will be used to look at the trends.

Ambient temperature	Evaporation temperature	Generation temperature	Adsorption temperature
$30^{\circ}C$	$-5^{\circ}C$	$100^{\circ}C$	$30^{\circ}C$

**Table 8.2:** Parameters used in simulation

#### Adsorption temperature

The adsorption temperature is the lowest temperature the bed reaches during the night. In Figure 8.1, the effect of increasing adsorption temperature is shown. The lines are isotherms with different condensing temperatures. The figure to the left shows the COP is slightly decreasing with the increase of adsorption temperature, and around 305 K the COP rapidly decreases. To understand the decrease in the COP, it is easier to have a look at Figure 6.7. The  $\Delta x$  in the system is decreasing as the adsorption temperature is increasing. Holding the other parameters constant, that is desorption and evaporation temperature, the COP will approach zero.

Figure 8.1 to the right shows the amount of ice produced. The amount highly depends on the adsorption temperature. However, to reach temperatures in the range of 270 - 290 K extra equipment is required. Since the system only depends on cooling from the surroundings during the night. It is unlikely to reach temperatures this low without extra equipment, i.e. some form of extra heat exchangers.

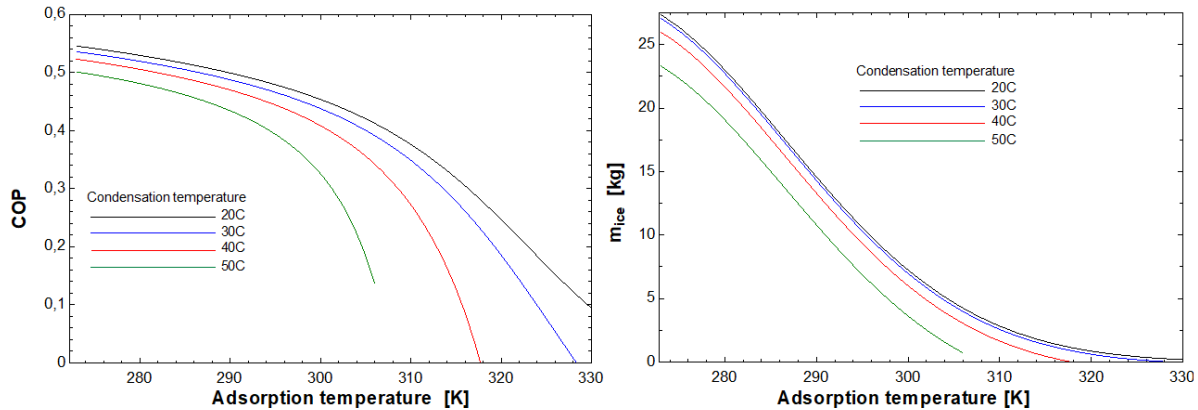


Figure 8.1: Effect of increasing ambient/condenser temperature.

### Desorption temperature

Figure 8.2 shows the influence of increasing the maximum bed temperature. The graph to the left shows the effect on COP and the graph on the right shows the effect on ice amount produced. The lines are isotherms, which represent the evaporative temperature levels. The trend is clear: higher maximum bed temperature gives more ice produced. However, at about 380K the amount stagnates, and there is only a minimal amount of ice produced extra per extra temperature increase. Looking back to Figure 6.6 the temperature in focus yields no more working fluid to desorb. The extra heat added to increase the temperature are not contributing to working fluid desorbed. Intuitively will the amount of ice increase with higher evaporator temperature, i.e. closer to  $0^{\circ}C$ . However,  $\Delta T$  influence the freezing time, and is  $\Delta T$  reduced too much may the driving force in the system be too low to produce ice.

The same trends are in the graph to the left. The COP increase as the temperature in the bed increases, until about 380 K, then the COP stagnates and slightly start to decrease. This is because of the lack of extra ice produced, there is no working fluid left to desorb. The decrease in COP comes of the increased temperature of the bed without more output of ice, thus more heat input without extra cooling output.

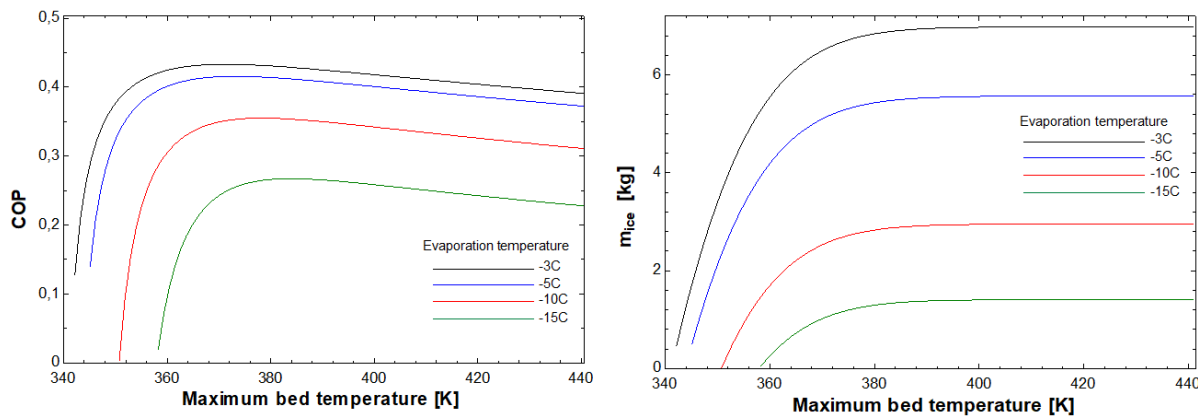


Figure 8.2: Effect of increasing bed temperature/desorption temperature

### 8.1.3 Comparing working pairs with Maxsorb III as adsorbent

The following chapter will compare different working fluids with Maxsorb III as adsorbent. Dubinin-Astakhov state equation is fitted experimentally for each working fluid to describe the influence of temperature and pressure. The x-axis shows the bed temperature, and the y-axis is the amount of working fluid the adsorbent adsorbs with the given temperature and pressure in Figure 8.3, 8.4 and 8.5. The evaporation temperature is  $-5\text{ }^{\circ}\text{C}$  and condensation temperature is  $30\text{ }^{\circ}\text{C}$ . The values used in the calculation is found in the literature and given in Table 5.1.

The light blue box is representing the temperature range expected for the adsorption temperature. Here  $273 - 300\text{ K}$ , where the lower temperature is too optimistic. The light red box is representing the expecting temperature of desorption, which is in the range of  $340 - 380\text{ K}$ . This range is set due to the lower end of temperature to drive similar system is  $60\text{ }^{\circ}\text{C}$ . The higher end is set due to expected temperatures and the chemical decomposition of methanol at  $120\text{ }^{\circ}\text{C}$ .

#### Methanol

The isobars in Figure 8.3 is the working system pressure levels. The shape of the two curves are the same, but the high-pressure curve is shifted to the right. The curve is relatively flat in the beginning, then the gradient starts to decrease more and more until the gradient slowly starts to increase as the temperature is increasing, and the curve converges to zero. The curves of methanol are relatively steep, i.e., have a high negative gradient, compared to other working fluids. That makes the temperature interval, from the adsorbent fully adsorbed to complete desorbed, relatively short. This property is desired for adsorption-based ice making system because the small temperature difference in adsorption/desorption phase requires less energy. However, the amount of  $\Delta x$  and  $X_0$  is also essential. If the working fluid is only able to take up  $0,1\text{ kg/kg}$ , the fact it could desorb and adsorb in a small temperature range does not weigh up for the small amount of possible working fluid that can be utilized in the cooling process.

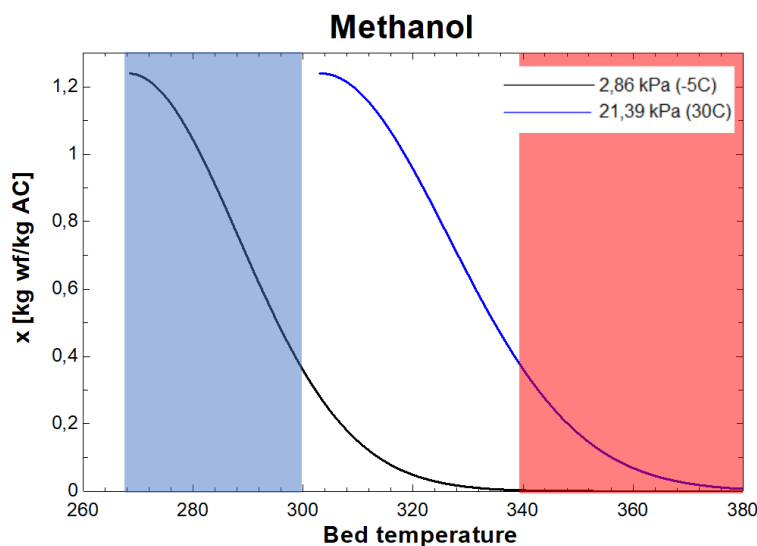


**Figure 8.3:** Blue field - possible adsorption temperatures, Red field - possible desorption temperatures.

In Figure 8.3 there is one big concern using methanol as working fluid. That is to reach low enough temperatures during adsorption to utilize the whole amount of methanol the Maxsorb has potential to adsorb. The extreme points of the blue box, at 273 K the  $x$  value is at 1,24 kg/kg while at 300 K the  $x$  value is only at 0,4 kg/kg. One solution to this problem is to increase the evaporation temperature as close to 0 °C as possible, thus shifting the curve to the right.

The curve of high pressure looks promising, and the adsorbent is almost completely desorbed at 380 K. This suggests that the system can work at higher condensation temperatures, i.e. higher ambient temperatures during the day.

## Ethanol

The curves of ethanol and methanol are somewhat similar. The first thing to notice is the shape of the curves. The  $X_0$  value for ethanol is slightly lower than for methanol. The curve is relatively flat in the beginning, and a lower gradient than methanol, which results in the desorption and adsorption temperature interval is longer than for methanol. In other words, to desorb and adsorb the same amount of working fluid as methanol, must the ethanol be exposed to higher or lower temperatures. Ethanol does not have the same thermal decomposition problem as methanol. Thus the workaround for this is to increase the desorption temperature, which depends on the solar irradiation. The adsorption uptake at 300 K is 0,5 kg/kg compared to methanol's 0,4 kg/kg.

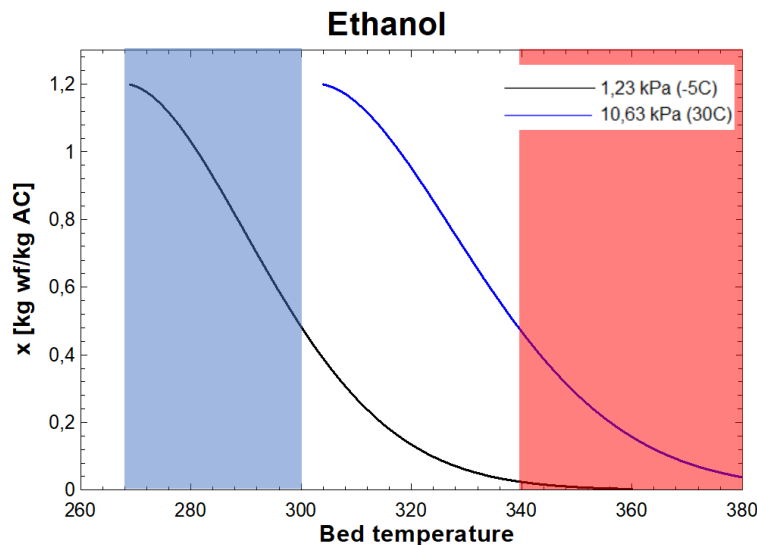


**Figure 8.4:** Blue field - possible adsorption temperatures, Red field - possible desorption temperatures.

## R134a

The curves for R134a is completely different than the curves of methanol and ethanol. Firstly, R134a has a much higher value for  $X_0 \sim 1,945$  kg/kg, thus will Maxsorb III be able to adsorb much more R134a. However, the shape of the R134a curves is decreasing much more slowly than for ethanol and methanol. Therefore will the temperature interval of adsorption and desorption the

same amount as methanol and ethanol be much bigger. Unfortunately is the solution not as simple as increasing the temperature of desorption. Around 375 K, the curves in Figure 8.5 stops, due to the working fluid is approaching two-phase area. This yields only a  $\Delta x$  potential of maximum 0,6 kg/kg for R134a systems. One possible solution to weigh up for this is to increase the thickness of the bed. However, as section 8.2 will show, other problems will occur when the thickness of the bed increases.

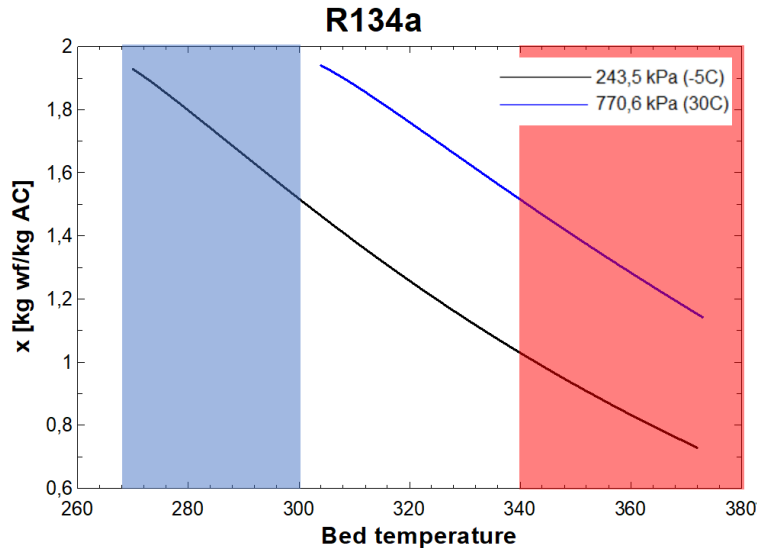


**Figure 8.5:** Blue field - possible adsorption temperatures, Red field - possible desorption temperatures.

### 8.1.4 Simple 6 point comparison

In the following subchapter compares the performance of the three working fluids. Which is helpful to dimension the system to produce 10 kg of ice. The size of the solar collector is decided to be  $1m^2$ , and 20 kg of Maxsorb III is used as a starting point. With the density of Maxsorb III, the thickness turns out to be 7.1 cm. The following results will help to decide if the thickness need to increase or decrease to meet the demand of 10 kg ice. The parameters in Table 8.3 were used together with the temperature parameters in Table 8.2.

#### Increasing the desorption temperature

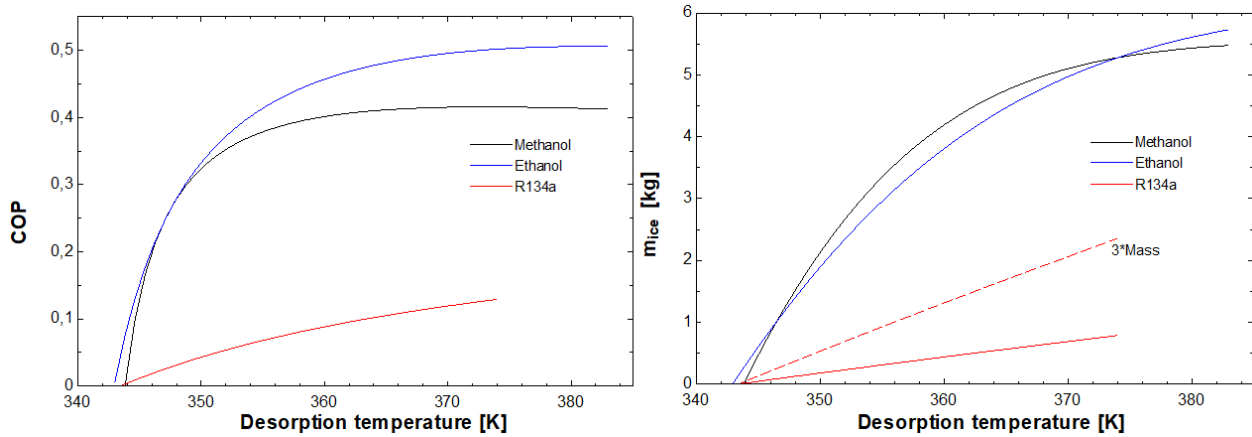
Figure 8.6 shows the variation of COP and ice production with increasing desorption temperature. The values of R134a stand out right away. The COP and ice produced are much lower compared to methanol and ethanol. The small amount of produced ice may be ignored to some degree because the thickness of the bed could increase. However, increasing the amount of Maxsorb three times produces only 2.5 kg. The curve to R134a is relatively flat compared to the two other working fluids.

The curves for methanol and ethanol are similar. Ethanol starts to produce ice at slightly lower temperatures than the other two working fluids. The COP rises sharply in the interval 345 - 355 K

Parameter	Description	Value
Solar collector/bed		
$C_{p,wall}$	Specific heat of the wall	0.48 [kJ/kgK]
$C_{p,AC}$	Specific heat of Maxsorb	0.92 [kJ/kgK]
$\rho$	Density of Maxsorb	281 [kg/m <sup>3</sup> ]
$m_{AC}$	Mass of activated carbon	20 [kg]
$m_{wall}$	Mass of wall	5 [kg]
Working fluid		
$C_{p,methanol}$	Specific heat	2.53 [kJ/kgK]
$C_{p,ethanol}$	Specific heat	2.57 [kJ/kgK]
$C_{p,R134a}$	Specific heat	0.88 [kJ/kgK]
Evaporator		
$m_{evap}$	Mass of evaporator	4 [kg]
$C_{p,water}$	Specific heat	4.18 [kJ/kgK]
$C_{p,ice}$	Specific heat	1.92 [kJ/kgK]
$\Delta h_{water}$	Latent heat of fusion	334 [kJ/kgK]

**Table 8.3:** Parameters used in simulation

and then start to converge. Methanol is converging toward a COP of 0.4, while ethanol is converging toward 0.5. The difference in COP is mainly due to the difference in isosteric heat. Methanol's isosteric heat value is higher than ethanol's, which will influence the COP. The amount of ice produced seems to be relatively similar for ethanol and methanol. It is worth noting that ethanol starts to produce ice first, then methanol overtakes ethanol for a short while, and finally, ethanol produces most ice. This behavior is due to the curves of Figure 8.3 and 8.4. Methanol has a steeper curve and produces more ice per extra temperature increase in the interval 345 - 360 K, but is overtaken by ethanol in the temperature interval above 360 K.

**Figure 8.6:** Working fluid with increasing desorption temperature

### Increasing the adsorption temperature

There are the same tendencies in lowering the adsorption temperature as increasing the desorption temperature. The highest adsorption temperature the system can produce ice is about 328 K. The COP value and ice production for R134a are modest compared to methanol and ethanol. Ethanol has the best COP values for the whole temperature interval. However, methanol is the working fluid producing the most ice below  $\sim 305$  K. At low temperatures, methanol utilizes the steep curve, i.e. the short temperature interval between desorption and adsorption. The desorption temperature here is constant 373 K, as given in Table 8.3, and ethanol is less desorbed than methanol at this temperature. This gives methanol an advantage and therefore produces more ice than ethanol.

It is worth noting the scale on ice produced in Figure 8.6 and 8.7. The scale to Figure 8.7 is much bigger than the scale to Figure 8.6. This indicates the system will perform better with lowering the adsorption temperature one degree, compared to increase the desorption temperature one degree. Figure 8.6 also suggest that ethanol system should operate at a higher desorption temperature than methanol systems, due to more ice produced and no risk of thermal decomposition in this temperature range.

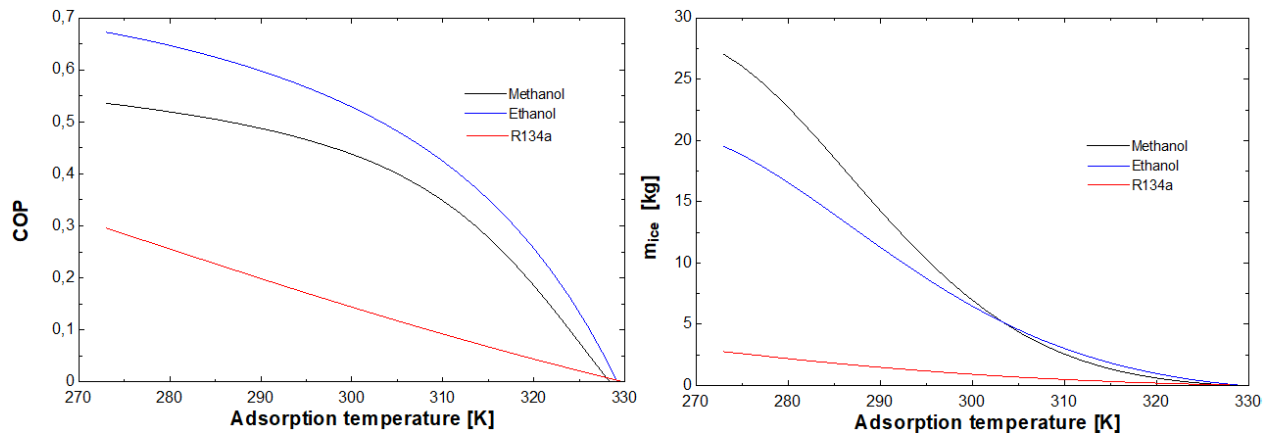


**Figure 8.7:** Working fluid with increasing adsorption temperature

Figure 8.8 shows the working fluids performance when the adsorption temperature and the desorption temperature is both varying. If the night temperature is low, the temperature during the day may also be low, and the bed may not be able to reach high desorption temperatures. The same applies if the temperature is high during the day and night time.

Figure 8.8 to the top left shows adsorption temperature of 10°C, methanol and ethanol are producing above 10 kg of ice with desorption temperatures above 70 °C. For an adsorption temperature of 20°C to the top right, only methanol is able to produce 10 kg ice with a desorption temperature of 90 °C and above. While for adsorption temperatures above 20 °C the system is not able to produce 10 kg ice. R134a is not close to producing 10 kg in any of the cases studied. For 30 °C and 40 °C as adsorption temperature, the system depends on reach the highest desorption temperature to produce any ice.



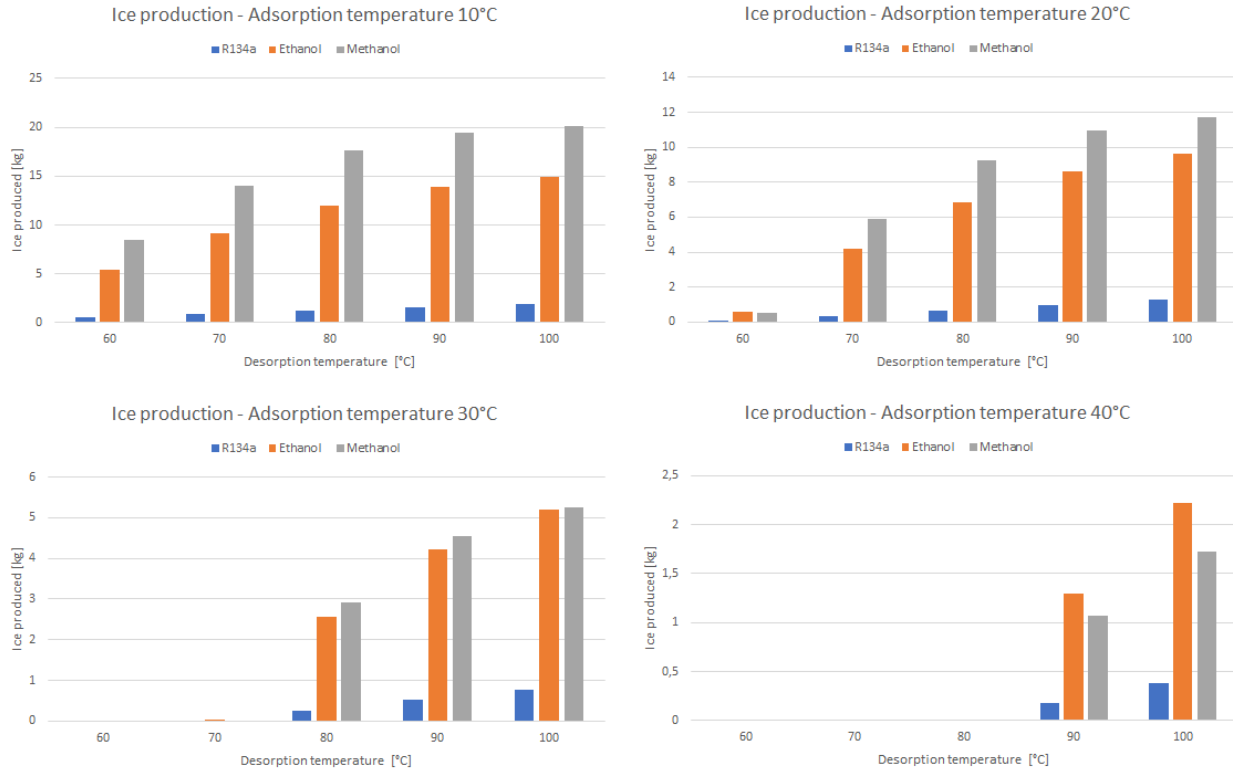


Figure 8.8: Working fluid with increasing adsorption and desorption temperature

### 8.1.5 Summary of thermodynamic analysis

The thermodynamic analysis result shows there is great potential using methanol and ethanol in an adsorption based ice maker, however that is not the case for using R134a with Maxsorb III. R134a is not close to producing 10 kg of ice per day, which is the goal of the system; therefore, will the following calculations only consider methanol and ethanol. Looking at methanol and ethanol is methanol producing more ice at lower adsorption temperatures, but are overtaken by ethanol for the higher adsorption temperatures. The two working fluids have the same performance when the adsorption temperature is  $\sim 28$  °C. So for adsorption temperatures below 28 °C is methanol the best-working fluid, while for temperatures above 28 °C is ethanol the best-working fluid. Ethanol generally has a higher COP than methanol, but this is mainly due to the high isosteric heat of methanol.

## 8.2 Transient analysis - cooling time

One of the most important aspects of the system is to heat up and cool down quickly. As described in section 5.5, the characteristics of Maxsorb III decides the temperature profile in the bed, i.e. how long it takes for the whole bed to cool down. There are mainly four parameters that in some degree could be varied:  $k$  conductivity,  $\alpha$  external heat transfer coefficient,  $\rho$  density, and  $L$  thickness of the bed.

It is important to realize that the following chapter does not take into account the adsorption heat. Only the cooling process of the bed, i.e. Stage 3 (C  $\rightarrow$  D) in Figure 6.2.

### 8.2.1 Flat plate design

There are mainly two possible designs for the adsorbent bed: flat plate bed and tubes. Figure 8.9 shows to the left the temperature variation in time for four different points of the plate. While the figure to the right is showing where on the plate they are. The red line is the edge of the bed, the part exposed to the ambient air when the insulation is removed. The blue line in representing the middle of the plate, i.e.  $0.5L$ . The black line is the part which is the farthest from the ambient air. The top cover will be insulating this part during cooling, so it is assumed there are no heat losses here. The green line is the average temperature through the whole plate.

Intuitively will the edge of the bed cooled down first. The outer part of the plate is rapidly cooled down and only uses a couple of minutes. The further in the plate, the longer time it takes. For the midpoint, with the given conditions, it takes 20 minutes to cool down. Moreover, the center point uses over 30 minutes to cool down. The graph to the midpoint and center point has a flat part for the first part of the cooling. This is because it takes some time for the temperature difference to go through the material, thus will not be affected right away. The average temperature has a smoother graph than the others.

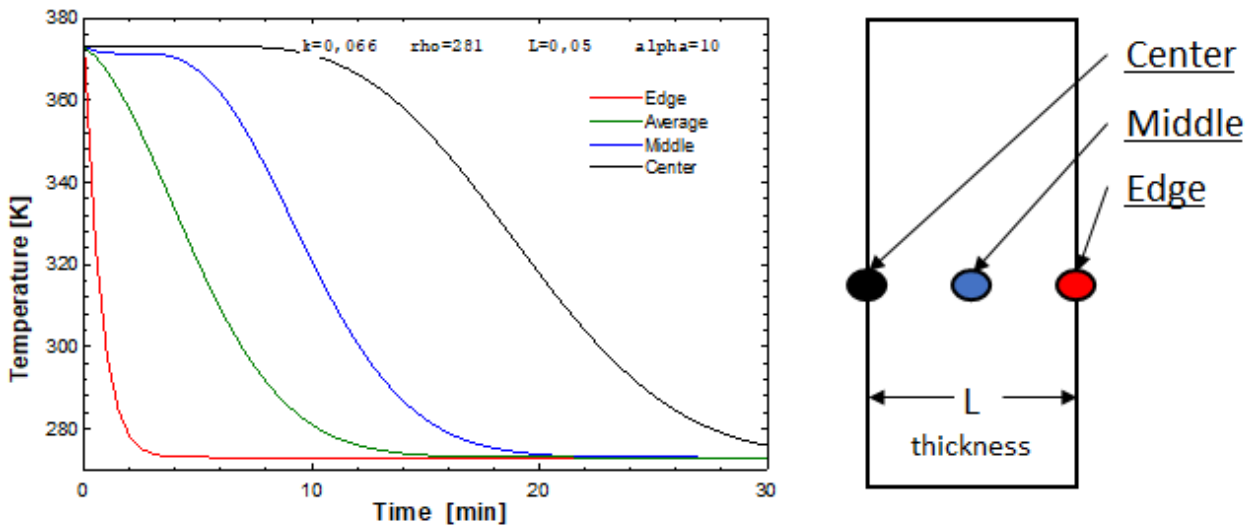


**Figure 8.9:** Temperature profile of four points on a flat plate

## Conductivity

The conductivity is very low for Maxsorb III with a value of 0.066 W/mK. However, there are possible to add additives to increase the thermal conductivity though this will influence the uptake of working fluid. Pure Maxsorb III  $k = 0.066$  is used in Figure 8.9. In Figure 8.10 there are added additives to the conductivity value. In the graph to the left  $k = 0.10$  and in the graph to the right  $k = 0.20$ . The graphs show the cooling time is highly depended on the conductivity. Using pure Maxsorb III, the center part of the bed will not be cooled down before 30 min. This is reduced to 25 min for  $k = 0.10$  and 20 min for  $k = 0.20$ . The cool down time influences the center point and midpoint the most. The average and edge temperature are not effected.

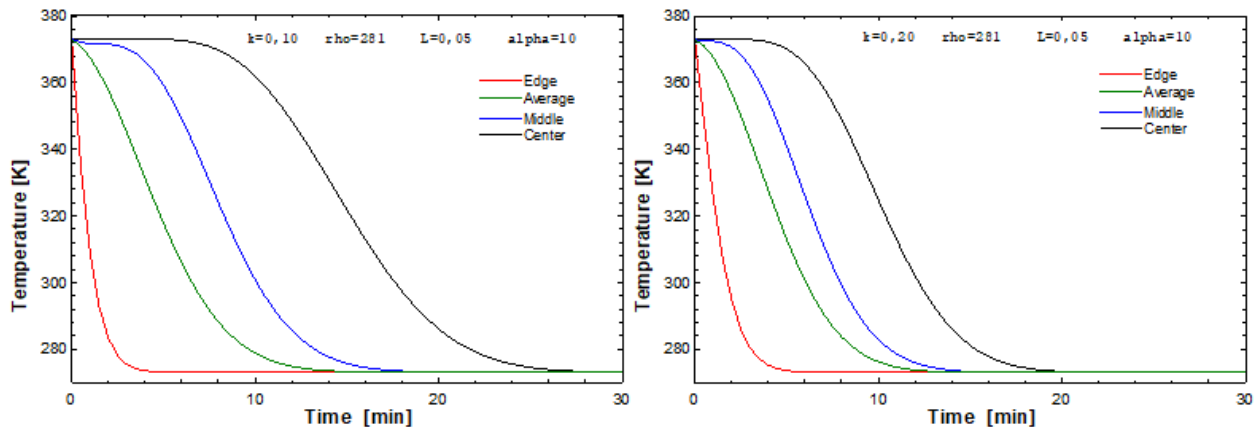


**Figure 8.10:** Change in transient temperature profile with varying conductivity

## External heat transfer coefficient

The external heat transfer coefficient could vary between 1-10 W/Km<sup>2</sup> for natural air convection on a plate. From Figure 8.11 the increase of  $\alpha = 1$  to  $\alpha = 5$  reduces all the points cool down time with about 15 minutes.

## Density

The density could, to some degree, be regulated in production. In Figure 8.12 the density to the left is  $\rho = 300\text{kg/m}^3$  and the density to the right is  $\rho = 500\text{kg/m}^3$ . The cool down time reduces if the density reduces.

## Thickness of bed

The thickness of the bed is the most natural part, from a designer perspective, to optimize. In subsection 8.1.4 the solar area of the bed is decided to be 1 m<sup>2</sup> with 20 kg adsorbent and with the lower end of density  $\sim 281\text{kg/m}^3$  that gives a thickness of 7.12 cm. However, this did not satisfy the expected 10 kg production of ice every day with high ambient temperatures. Therefore it is

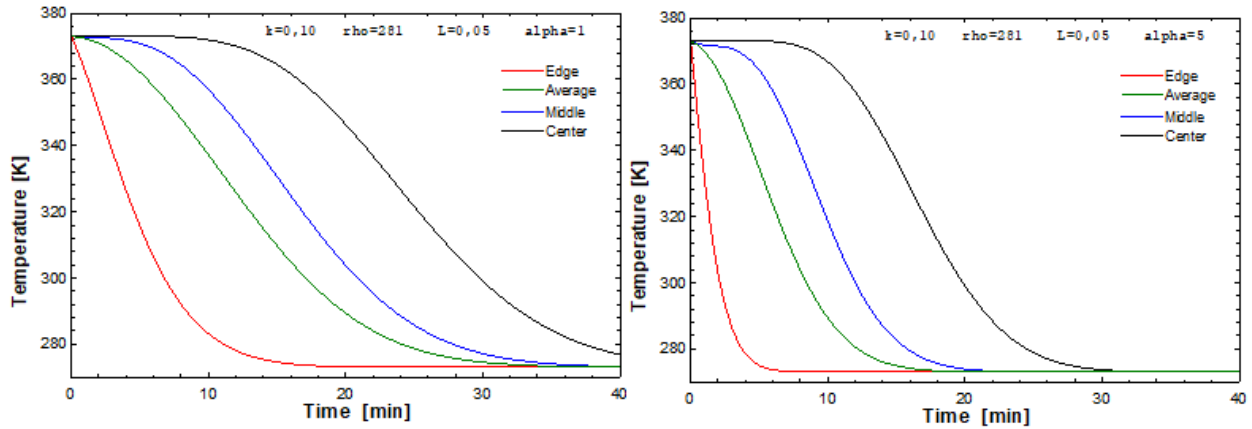


**Figure 8.11:** Change in transient temperature profile with varying external heat transfer coefficient

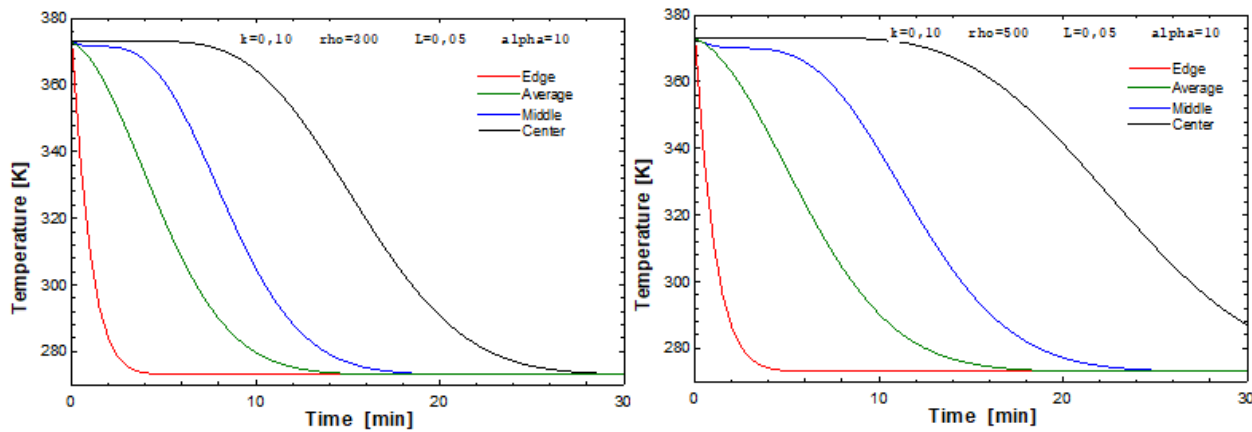


**Figure 8.12:** Change in transient temperature profile with varying density

important to find the limit for maximum bed thickness, which will decide whether the bed should be thicker or the solar area increased.

In Figure 8.13 the following values are used  $k = 0.066$ ,  $\rho = 281$  and  $\alpha = 5$ . This is the lower end values for conductivity, density, and external heat transfer. The graph to the left has a thickness of only 2.5 cm and a short cool down time. The graph to the right has a thickness of 5 cm and the cool down time almost double for all points except the edge.

Increasing the thickness to 7.5 cm in Figure 8.14 the cool down time for the center is 1 hour. The midpoint uses about 35 minutes to cool down, and the average temperature of the bed is about 25 minutes. For the thickness of 10 cm, the center part of the bed cools down after about 90 minutes.

Taken the heat of adsorption into account, it is important that the heat from the inner parts of the plate could transfer the heat out to the edge, i.e. the ambient air. Thus, making a definite limit of thickness is difficult, since the cool down time for the bed is through the whole night. To have some tolerance, the thickness of the bed is acceptable up to 7.5 cm without any additives in the Maxsorb III.

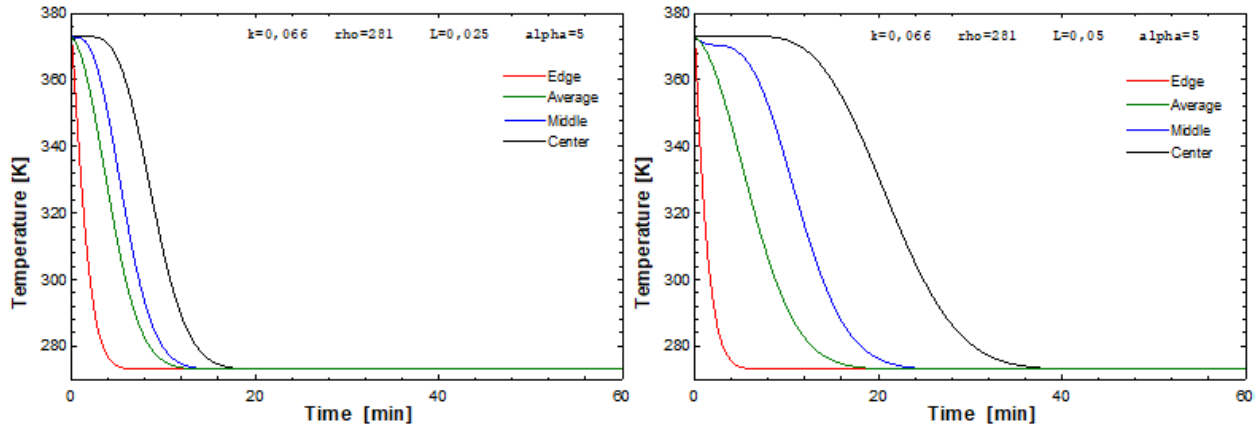


Figure 8.13: Change in transient temperature profile with bed thickness of 2.5 and 5 cm

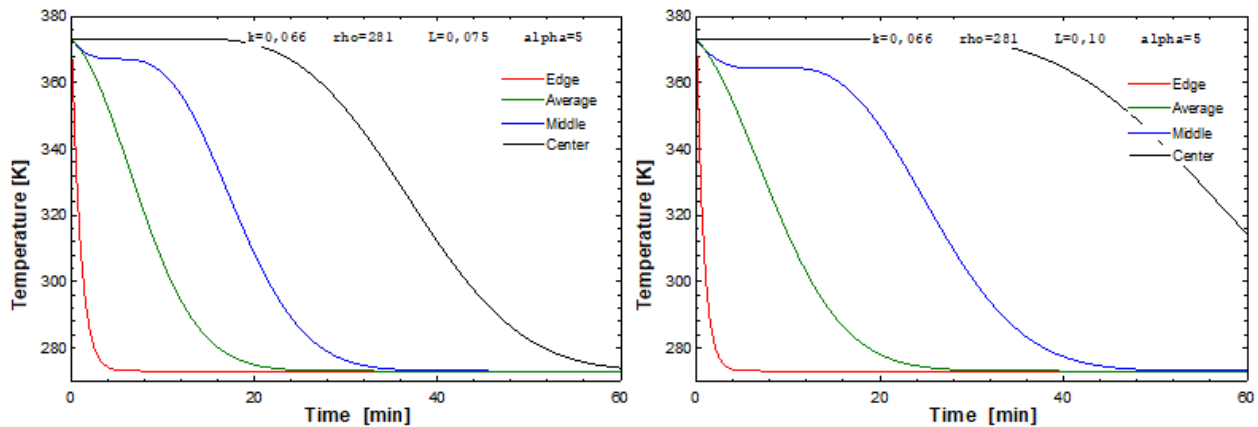


Figure 8.14: Change in transient temperature profile with bed thickness of 7.5 and 10 cm

## 8.2.2 Cylinder design

Another possible design for the bed is using tubes filled with Maxsorb III. Figure 8.15 shows a cross-section of a tube. There is an outer tube and an inner tube. The adsorbent is in the area between. This design has some advantages. First, the cylinder design has shorter cooling time than a flat plate bed due to heat can be released from all around the cylinder, not only one side. Secondly, the removed center of the tube makes the adsorbate flow easily in and out of the adsorbent. However, there are some downsides. The amount of adsorbent per area is less, and the solar irradiation will directly heat only one side during heating.

Table 8.4 are using  $1m^2$  ( $1 \times 1$ ) as a basis and the outer radius is based on the number of tubes that will fit in this design. The volume column is calculated with the inner radius equal zero. The total volume is decreasing as the number of tubes are increasing. The column to the right is discussed bellow the table.

Figure 8.16 simulate the time it takes for the cylinder design to cool down  $100^\circ C$  with a radius of 10 cm to the left and 6,25 cm to the right. For the 10 cm design it takes about 90 minutes for the inner part to cool down, the midpoint takes about 60 minutes, and the average temperature takes

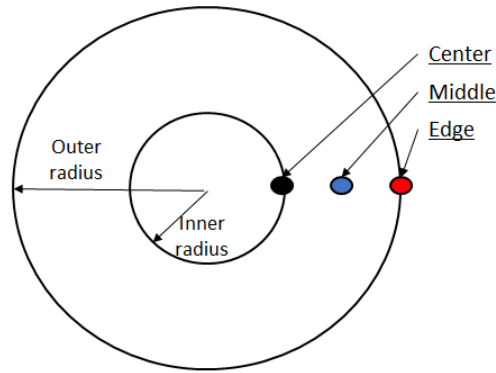


Figure 8.15: Cross section of adsorbent tube

Outer radius [m]	Number of tubes	Volume [m <sup>3</sup> ]	Inner radius [m]
0,1000	5	0,1570	0,0328
0,0833	6	0,1308	0,0219
0,0714	7	0,1121	0,0146
0,0625	8	0,0981	0,0093
0,0556	9	0,0872	0,0054
0,0500	10	0,0785	0,0024

Table 8.4: Dimensions of possible tube bed design

about 25 minutes. The 6,25 cm design cools down faster. The inner point cools down in about 50 min, and the average temperature cools down in about 20 minutes. The cylinder design will reduce the cool down time per volume, but the correct dimensions the inner part has to be removed.

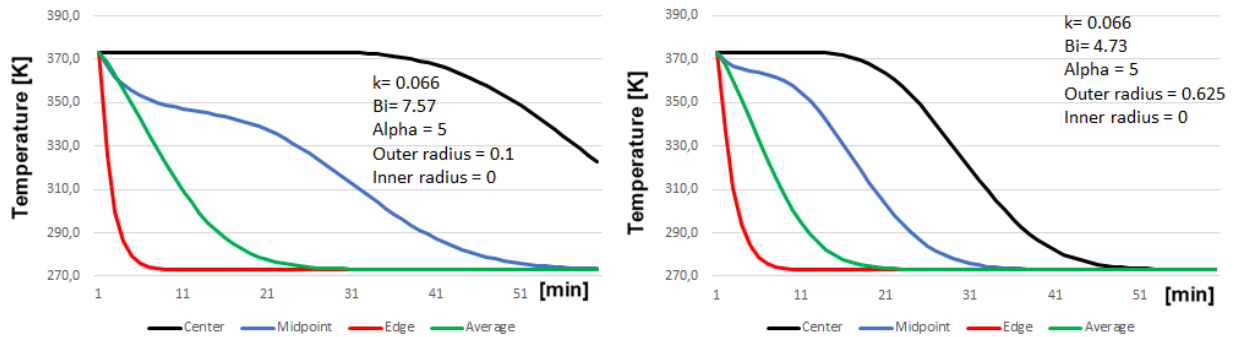
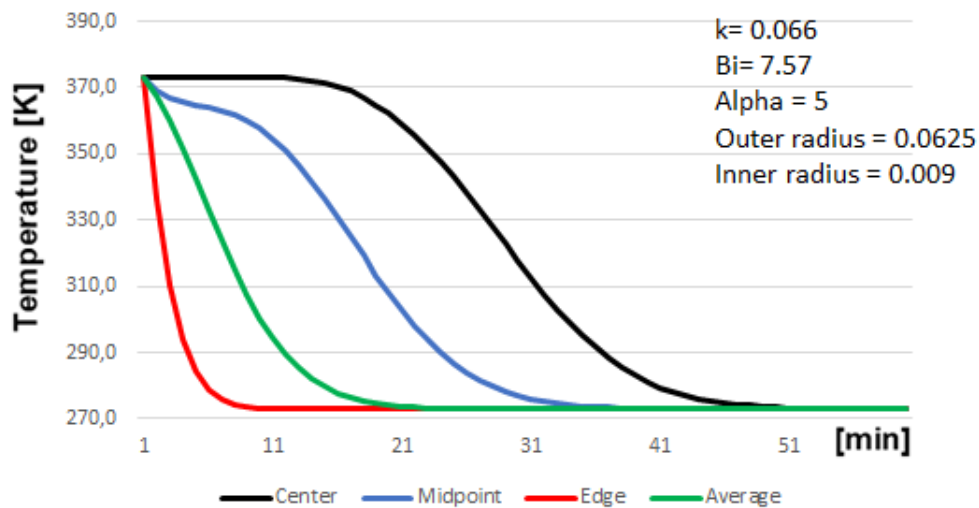


Figure 8.16: Change in transient temperature profile with tubular radius increase

Assuming there is 20 kg of adsorbent in the bed and a density of 281 kg/m<sup>3</sup> gives a required volume of 0.0712 m<sup>3</sup>. The column to the right in Table 8.4 gives the inner radius for the required volume of the cylinder with the given outer radius in the column to the left. Figure 8.17 shows the temperature profile of a cylinder design with an outer radius of 6.25 cm and an inner radius of 0.9 cm. The calculations show that only the center and midpoint is reduced, while the average

temperature is not that much reduced compared to Figure 8.16. However, this design compares to the flat plate design in term of the volumetric size. Figure 8.17 and Figure 8.14 with 7.5 cm thickness has about the same mass of Maxsorb III  $\sim 20$  kg in  $1m^2$  solar area. The cool down time for the tube design about 15 minutes shorter for the center point and about 5 minutes shorter for the average temperature.



**Figure 8.17:** Cylinder design - Transient temperature profile of 20 kg Maxsorb III

### 8.2.3 Summary of transient analysis

The transient analysis shows how the density, conductivity, and external heat transfer of Maxsorb III is influencing the design of the system by limiting the thickness of the bed. However, for the time period in focus, the thickness up to 7.5 cm is acceptable. The two different design, flat plate and tubular, have different advantages and disadvantages. The flat plate has a simpler geometry, thus more uniform heat distribution, and more volume per areal. The cylinder design has a shorter cool-down time. The calculations show that the average temperature cool-down time of tube design is about 5 min shorter than the flat plate design for the same amount of mass. The small benefit of faster cool-down time does not influence the operation of the system significant since the system cools the whole night. Therefore are the simple geometry, flat plate, chosen for the system to keep cost down.

### 8.3 Simulation through a day

There are many factors which are going to influence the operation of the system through one day. Some are more important than others, among heat loss and solar irradiation.

#### 8.3.1 Solar irradiation - heating

The solar irradiation depends on the geographical location, time of the year, and local variations. In Figure 8.18 is the solar irradiation the black line and heat losses the blue line. The red and blue area under the black graph combined is the energy input, i.e. solar irradiation. Some of the energy gets lost to heat losses through the collector, marked as the blue areal. Furthermore, the useful energy for heating the bed and desorbing the adsorbent is only the red areal. The figure shows how the irradiation varies through the day, in this graph is  $t = 0 \sim 06:00$  in the morning and  $t = 12 \sim 18:00$ , which gives a maximal heat input around  $t = 6 \sim 12:00$ . The heat loss graph is gradually increasing as the temperature difference between the bed and ambient are increasing, see Figure 8.20. At about  $t = 11$  the heat loss and solar irradiation are equal, i.e. the temperature in the bed does not increase further. That is due to the decrease in solar irradiation and increase in heat losses.

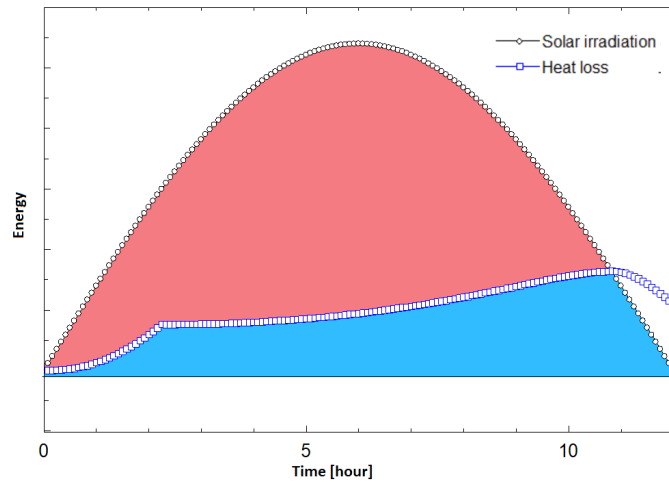


**Figure 8.18:** Solar irradiation and heat loss

#### 8.3.2 Heat losses

In section 5.5 heat losses through the top are described. The most important parameters are the number of glass covers  $N$ , and the wind heat transfer coefficient  $h_w$ . The influence of the angle of the bed has little impact on the top heat loss. Figure 8.19 shows the heat loss increases with an increased temperature difference. The ambient temperature is 300 K, while the temperature of the bed increases with the x-axis. The y-axis shows the heat loss. The dotted lines are using two glassed while the solid line is using one glass cover. The different colors represent the wind heat transfer coefficient. It is important to use two glasses and try to protect the cover for direct wind.



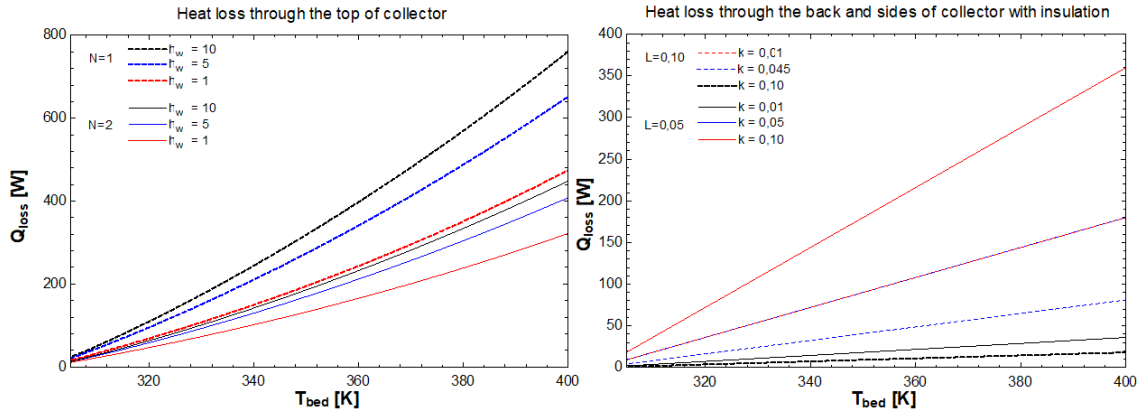


**Figure 8.19:** Heat loss through the top and the back/sides of the collector

The insulation on the sides and back sides will also have some heat losses. Insulation has different thermal conductivity, and the thickness could be decided. From section 5.5 is the thermal conductivity in the literature  $\sim 0.045W/mK$ . Figure 8.19 shows the heat loss with an increased temperature difference of the bed to the ambient temperature. The dotted line uses a thickness of 10 cm, and the solid line uses 5 cm. The different colors represent different values of conductivity. The dashed red line and full blue line is overlapping. The difference between a thickness of 5 and 10 cm is significant, and 10 cm insulation should be used.

### 8.3.3 Time frame

As described in chapter 6 are there four main stages for the system through the day. Figure 8.20 shows when the stages are happening throughout the day. The x-axis is the time, and the y-axis is the temperature. The blue line is representing the ambient temperature, which is increasing during the day and decreasing during the night. The orange line is representing the bed temperature. The sunrise is 06:00 and the sunset is 18:00.

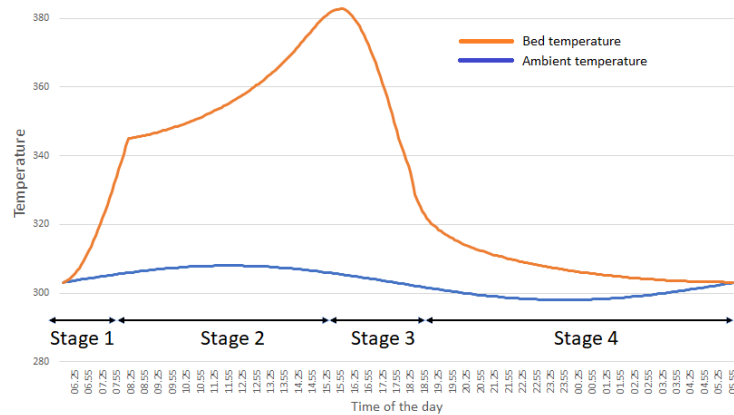


**Figure 8.20:** Bed and ambient temperature through a day

Stage 1 is the first two and a half hour until the pressure is the right level. The bed is filled with working fluid, and the temperature rise is quite rapid. Then stage 2 starts, which is desorption. The desorption process requires a lot more energy. It starts at about 08:30 and the highest temperature the bed reach is 16:30. This is before the sun is going down, also seen in Figure 8.18. Due to the methanols high heat of desorption, the temperature rise is much slower than in stage 1, even though the heat input is higher. Stage 3 start when the heat input is equal to the heat loss, and the depressurization starts. Stage 3 lasts about two hours until 18:30. There is still solar irradiation until 18:00, which is slowing down the cooling process. The last stage is the adsorption process. This process will either go on to the bed reaches the same temperature as the ambient temperature or the sunrise, which starts a new cycle.

The ice is produced during stage 4. The rate of ice produced depends on the rate of the adsorption process. Figure 8.21 shows the ice production starts at about 18:30 and keeps on as long as the adsorption process. The figure shows that the highest production of ice is at the start of the adsorption. This is due to the bed is cooling down fast in the begging due to the temperature difference of the bed and ambient.

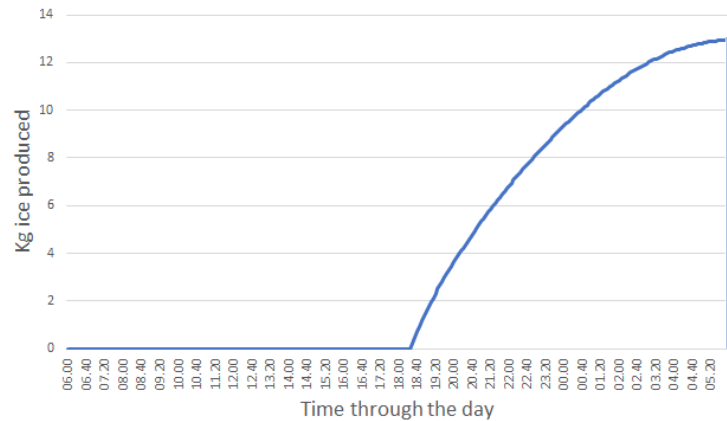


**Figure 8.21:** Ice production through the day

### 8.3.4 Varying solar irradiating

In Table 3.2 the average solar irradiation through the year in kWh/day is shown. Moreover, Figure 8.22 shows the influence different solar irradiance levels has on the system. The different stages can be recognized at all the solar irradiance levels. However, the time it takes to complete stage 1 for lower solar irradiance levels is longer than for the higher levels. Also, the maximum temperature is highly impacted by the heat input. The step between stage 2 and 3 is almost at the same time for all the levels. Further is the cooling process similar for all the levels.

The highest heat input in Figure 8.22 gives the highest desorption temperature, further gives the highest amount of methanol desorbed, which yield a higher amount of ice. In Figure 8.23, the higher the heat input is the higher ice production. Counter-intuitively is it the bed that is experiencing the highest temperatures that starts to produce ice first. This is due to activated carbon

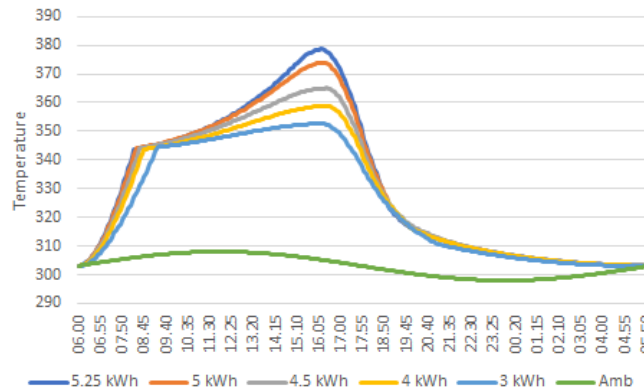


**Figure 8.22:** Solar irradiation effect on bed temperature

adsorbs methanol easier when it fully desorbed, i.e. at higher temperatures. Therefore the ice production process could start earlier.

In Table 3.2, the lowest average month heat input in Kolkata is  $2.23 \text{ kWh/m}^2$  per day in July.  $2.23 \text{ kWh/m}^2$  is not sufficient to produce 10 kg of ice, as seen in Figure 8.23. There are two possible solutions to this. The first solution is to increase the solar collector area. This could be as simple as some tinplate sheets to concentrate the solar irradiation on the adsorbent bed. Another solution could be some form of woodstove that uses the flue gas to heat the back side of the bed. The heat required from the woodstove would be 2 kWh to reach about 10 kg of ice produced.

If the ice is used as cooling elements in a freezer, the harvesting season for most products, except apples and some tomatoes, are outside of the monsoon season. It is during the monsoon season the solar irradiance is reduced.

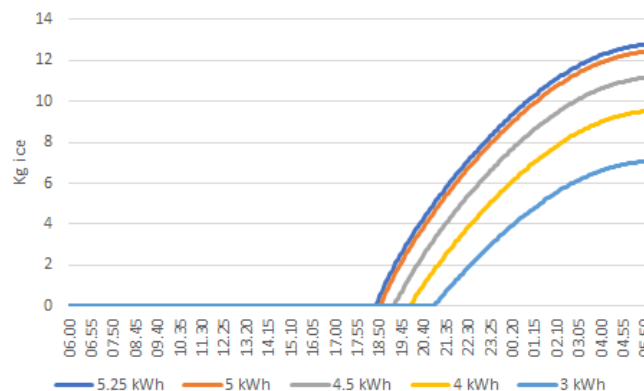


**Figure 8.23:** Solar irradiation effect on ice production

### 8.3.5 Varying ambient temperature

In Figure 8.24 is the condenser temperature varied. The condenser temperature is a non-zero center amplitude, and the ambient temperature amplitude is  $5^\circ\text{C}$ . The solar irradiance is constant and

characteristic from Figure 8.22 is recognized.

The temperature on the start of the day influences the amount of working fluid adsorbed in the bed, which will influence the temperature profile throughout the day. In stage 1 are the temperature profiles almost identical for all temperature levels. The only difference is that the lower temper has a slightly lower gradient since there is more working fluid to heat up. The condenser temperature greatly impacts the temperature in the bed in stage 2. The lower condenser temperatures have a higher amount of working fluid, thus will the temperature in bed in stage 2 have a lighter increase. That is every degree increased will desorb more working fluid for lower condenser temperature, see Figure 6.6.

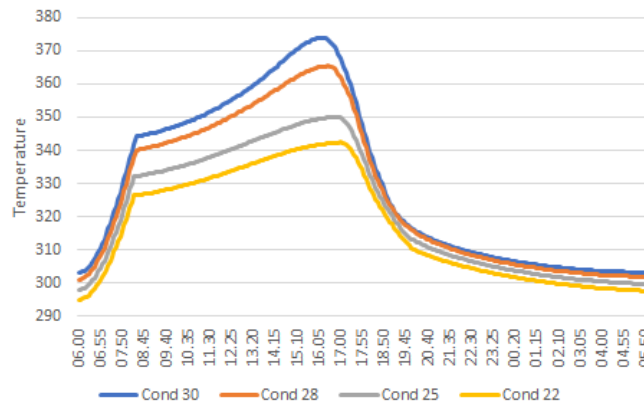


**Figure 8.24:** Condenser/ambient temperature effect on bed temperature

Due to the non-linearity of adsorption and desorption, the amount of ice is not so intuitive as Figure 8.23. In Figure 8.25 the highest condenser temperature start the ice production process first. However, the highest condenser temperature produces the least amount of ice. This is due to the nature of the adsorption and desorption curve, as described earlier.

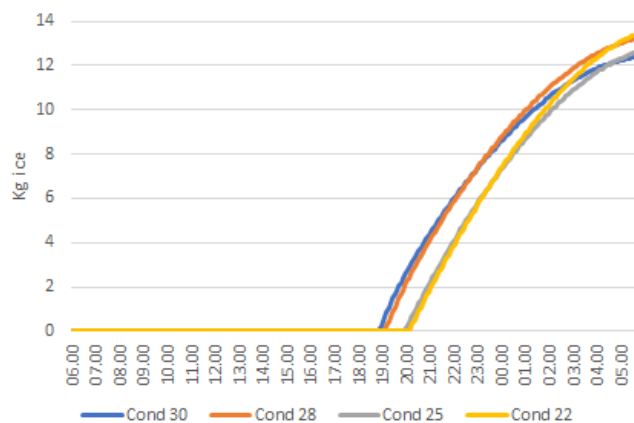


**Figure 8.25:** Condenser/ambient temperature effect ice production

### 8.3.6 Mass flow

The mass flow dimensions the pipes in the system. Figure 8.26 shows the mass flow in and out of the bed. The flow out of the system is defined as negative, and the flow into the system is defined as positive.

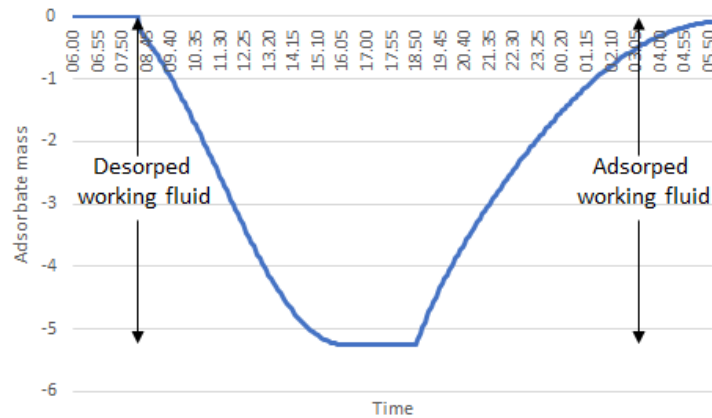


**Figure 8.26:** Desorped and adsorped working fluid through the day

Figure 8.27 shows the mass flow rate in 5 min intervals. The desorption process has almost a constant mass flow rate until it starts to decrease. This is also seen in Figure 8.26 in the linearity of the desorption process. The adsorption process is flow rate much greater at the beginning of the process and steadily decreases.

The maximum mass flow from Figure 8.27 is  $0.10 \text{ kg}/5 \text{ min}$ , which turn out  $\sim 3.33 \times 10^{-4} \text{ kg}/\text{s}$ . Methanols density is depended on temperature at  $70^\circ \text{C}$  is the density  $1.47 \text{ kg}/\text{m}^3$  for methanol and  $1.058 \text{ kg}/\text{m}^3$  for ethanol. Which gives a maximum volume flow of  $0.0005 \text{ m}^3/\text{s}$  for methanol and  $0.00035 \text{ m}^3/\text{s}$ . To minimize the pressure losses in the tubes, the velocity is set to maximum  $0.5 \text{ m}/\text{s}$ , which gives a required cross-section areal of  $0.001 \text{ m}^2$ .

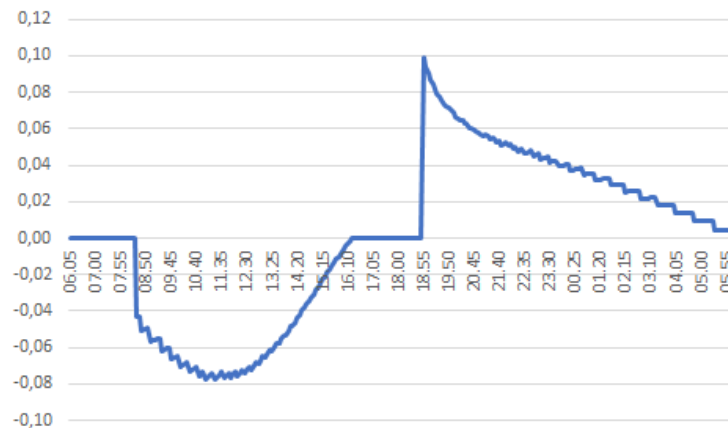


**Figure 8.27:** Mass flow rate through the day

### **8.3.7 Summary of simulation through a day**

The simulation through the day shows that the heating of the bed is in the time period 06:00 to 16:30, which is the period when the bed is pressurized and desorbed. While in the time period 16:30 to 06:00 is the bed first depressurized and then adsorbed. The ice production of the system starts at about 18:30 and is ongoing until 06:00. The simulation indicates the volume flow rates that the system could expect, which will determine the dimensions of the pipes.

## Conclusion and further work

This master thesis explores the cold chain status in India. A two and a half month stay at IIT Kharagpur was completed in cooperation with SINTEFs Refood project. During the stay was some of the different cold chains mapped, such as seafood, dairy, fruit, and vegetable. It is clear that various cold chains have various needs and criteria. Unfortunately, are many of the steps for an efficient and working cold chain not in place in India. However, quality cold chains are required in the export market and high-end product, which are spreading to other products.

A survey at the local market was completed. The participants were fish, meat, fruit and vegetable sellers, as well as students and other academics. The survey revealed that many of the local sellers were aware of the need for cold chain. However, they did not use any form of cooling for the products they sold, nor cared if the food they bought were a part of any cold chain. One of the most important reasons was the lack of accessibility and affordability of cooling. For the cooling demand of some fishermen and rural farmers, a solar-based adsorption ice maker could be a solution. This system has some important advantages for the Indian market. There is no need for electricity and no operation cost because it uses solar heat.

Maxsorb III is currently the best adsorbent on the market and three working fluids (methanol, ethanol, R134a) has been simulated. The simulations are in three parts. Part one carried out a thermodynamic analysis of the most important parameters, part two looks at the thickness of the bed, and part three looks at the operation through a whole day. The calculations are based on climatic data from India and based on energy balances of the components of the system. R134a and Maxsorb III turn out not to be a good combination for intermittent operation, while methanol and ethanol show promising results in the thermodynamic analysis. Methanol is the best working fluid for adsorption temperatures below 28°C and ethanol is the best working fluid for above 28°C. The thickness of the bed is calculated to a maximum of 7.5 cm to have a tolerant cooling time. To sum up, a small scale adsorption ice maker with the dimensions of 1 m<sup>2</sup> solar collector, 20 kg of adsorbent and Indian solar conditions can provide cooling to people who previously did not have access to cooling almost all year round. Giving access to cooling will reduce food waste and use of resources, and using natural working fluids such as methanol and ethanol are critical regarding global warming.

---

## Further work

- The natural next step is to make a prototype of the system and do some field work.
- In this master thesis, the best adsorbent currently on the market was studied. However, there are more affordable adsorbents on the market. To make a more affordable system must either the cost of Maxsorb III go down or other adsorbents considered.
- Most of the research on solar based adsorption system has been on methanol and activated carbon. The results of ethanol and activated carbon shows great potential to be a challenger to methanol. Most of the literature on adsorption based ice maker system is on methanol as adsorbent, and more research should be done on ethanol.
- An aspect of the system is what to do on days with insufficient solar irradiation. One possible solution to explore is a small oven which leads the flue gas to the back side of the bed, thus heating the bed. Wood and other bio waste may be used.



# Bibliography

- Alghoul, M., Sulaiman, M., Azmi, B., Sopian, K., Wahab, M., 2007. Review of materials for adsorption refrigeration technology. *Anti-Corrosion Methods and Materials* 54 (4), 225–229.
- apeda.gov.in, 2019. Fresh fruits & vegetables - agricultural & processed food products export development authority. [http://apeda.gov.in/apedawebsite/six\\_head\\_product/FFV.htm](http://apeda.gov.in/apedawebsite/six_head_product/FFV.htm), [Online; Accessed on 2019-05-18].
- Arduino, G., Carrillo Murillo, D., Parola, F., 11 2013. Refrigerated container versus bulk: evidence from the banana cold chain. *Maritime Policy & Management* 42, 1–18.
- Askalany, A., Saha, B. B., Uddin, K., Miyazaki, T., Koyama, S., 2012a. Adsorption isotherms of r134a and r32 onto activated carbons. *ADSORPTION* 1, 3–8.
- Askalany, A. A., Salem, M., Ismail, I., Ali, A. H. H., Morsy, M., 2012b. Experimental study on adsorption-desorption characteristics of granular activated carbon/r134a pair. *International Journal of Refrigeration* 35 (3), 494 – 498.
- Badia-Melis, R., Carthy, U. M., Ruiz-Garcia, L., Garcia-Hierro, J., Villalba, J. R., 2018. New trends in cold chain monitoring applications - a review. *Food Control* 86, 170 – 182.
- bbc.com, 2015. India 'to overtake china's population by 2022' - un. <https://www.bbc.com/news/world-asia-33720723>, [Online; Accessed on 2019-03-31].
- Bighane, N., 2017. Cold supply chain in india. [https://www.academia.edu/9636882/Cold\\_Supply\\_Chain\\_in\\_India](https://www.academia.edu/9636882/Cold_Supply_Chain_in_India), [Online; Accessed on 2019-03-27].
- Biswas, A. K., 2014. India must tackle food waste. <https://www.weforum.org/agenda/2014/08/india-perishable-food-waste-population-growth/>, [Online; Accessed on 2019-03-20].
- Brijesh K. Tiwari, Tomas Norton, N. M. H., 2013. *Sustainable Food Processing*. Wiley.
- Cantwell, M., 2011. Properties and recommended conditions for the long term storage of fresh fruits and vegetables. <http://postharvest.ucdavis.edu/files/230191.pdf>, [Online; Accessed on 2019-03-20].

- 
- Choudhury, B., Saha, B. B., Chatterjee, P. K., Sarkar, J. P., 2013. An overview of developments in adsorption refrigeration systems towards a sustainable way of cooling. *Applied Energy* 104, 554 – 567.
- Cohen, G., Levin, C., 2011. *Food Storage*. New York: Nova Science Publishers Inc.
- Derens-Bertheau, E., Osswald, V., Laguerre, O., Alvarez, G., 2015. Cold chain of chilled food in France. *International Journal of Refrigeration* 52, 161 – 167.
- Do, D. D., 1998. *Adsorption Analysis: Equilibria and Kinetics : (With CD Containing Computer Matlab Programs)*. Vol. 2. PUBLISHED BY IMPERIAL COLLEGE PRESS AND DISTRIBUTED BY WORLD SCIENTIFIC PUBLISHING CO.
- Duffie, J. A., Beckman, W. A., 2013. *Solar Engineering of Thermal Processes*. John Wiley & Sons, Inc., Hoboken, NJ, USA.
- Eikevik, T. M., 2018. *Heat Pumping Processes and system*. NTNU.
- El-Sharkawy, I., Hassan, M., Saha, B., Koyama, S., Nasr, M., 2009. Study on adsorption of methanol onto carbon based adsorbents. *International Journal of Refrigeration* 32 (7), 1579 – 1586.
- El-Sharkawy, I., Saha, B., Koyama, S., He, J., Ng, K., Yap, C., 2008. Experimental investigation on activated carbon/ethanol pair for solar powered adsorption cooling applications. *International Journal of Refrigeration* 31 (8), 1407 – 1413.
- El-Sharkawy, I. I., Pal, A., Miyazaki, T., Saha, B. B., Koyama, S., 2016. A study on consolidated composite adsorbents for cooling application. *Applied Thermal Engineering* 98, 1214 – 1220.
- El-Sharkawy, I. I., Uddin, K., Miyazaki, T., Saha, B. B., Koyama, S., Miyawaki, J., Yoon, S.-H., 2014. Adsorption of ethanol onto parent and surface treated activated carbon powders. *International Journal of Heat and Mass Transfer* 73, 445 – 455.
- epa.gov, 2019. Understanding global warming potentials - united state environmental protection agency. <https://www.epa.gov/ghgemissions/understanding-global-warming-potentials>, [Online; Accessed on 2019-05-18].
- FAO, 2019. India food availability - food and agriculture organization of the united nations. <http://www.fao.org/faostat/en/#country/100>, [Online; Accessed on 2019-03-31].
- FASAR, 2015. Indian sea food industry : The cold chain perspective (food & agribusiness strategic advisory & research, yes bank). [https://www.yesbank.in/pdf/indian\\_sea\\_food\\_industry\\_the\\_cold\\_chain\\_prospective.pdf](https://www.yesbank.in/pdf/indian_sea_food_industry_the_cold_chain_prospective.pdf), [Online; Accessed on 2019-03-20].
- Fellows, P., 2017. *Food processing technology : principles and practice*.
-

- 
- FN, 2019a. Montrealprotokollen. <https://www.fn.no/Om-FN/Avtaler/Miljoe-og-klima/Montrealprotokollen>, [Online; Accessed on 2019-06-18].
- FN, 2019b. Parisavtalen. <https://www.fn.no/Om-FN/Avtaler/Miljoe-og-klima/Parisavtalen>, [Online; Accessed on 2019-06-18].
- Goyal, P., Baredar, P., Mittal, A., Siddiqui, A. R., 2016. Adsorption refrigeration technology an overview of theory and its solar energy applications. *Renewable and Sustainable Energy Reviews* 53, 1389 – 1410.
- Hamrahi, S. E., Goudarzi, K., Yaghoubi, M., 2018. Experimental study of the performance of a continues solar adsorption chiller using nano-activated carbon/methanol as working pair. *Solar Energy* 173, 920 – 927.
- Hassan, H., Mohamad, A., Alyousef, Y., Al-Ansary, H., 2015. A review on the equations of state for the working pairs used in adsorption cooling systems. *Renewable and Sustainable Energy Reviews* 45, 600 – 609.
- iifiir, 2017. The impact of the refrigeration sector on climate change - international institute of refrigeration. [http://www.iifiir.org/userfiles/file/publications/notes/NoteTech\\_35\\_EN\\_uz7bwths.pdf](http://www.iifiir.org/userfiles/file/publications/notes/NoteTech_35_EN_uz7bwths.pdf), [Online; Accessed on 2019-05-18].
- indiaenergyportal.org, 2018. Renewable energy - solar, india energy portal. <http://www.indiaenergyportal.org/subthemes.php?text=solar>, [Online; Accessed on 2019-03-29].
- James, S., James, C., 08 2010. The food cold-chain and climate change. *Food Research International* 43, 1944–1956.
- John, M., Kimambo, C. Z., Eikevik, T. M., Nydal, O. J., Kihedu1, J., 2017. Potential application of commercial refrigerants as adsorbate in adsorption refrigeration system. ISES Solar World Congress.
- Kaale, L. D., Eikevik, T. M., Rustad, T., Nordtvedt, T. S., 2014. Changes in water holding capacity and drip loss of atlantic salmon (*salmo salar*) muscle during superchilled storage. *LWT - Food Science and Technology* 55 (2), 528 – 535.
- Leygonie, C., Britz, T. J., Hoffman, L. C., 2012. Impact of freezing and thawing on the quality of meat: Review. *Meat Science* 91 (2), 93 – 98.
- Mahajan, P., Caleb, O., Singh, Z., Watkins, C., Geyer, M., 05 2014. Postharvest treatments of fresh produce. *Philosophical transactions. Series A, Mathematical, physical, and engineering sciences* 372, 20130309.
- Mercier, S., Villeneuve, S., Mondor, M., Uysal, I., 05 2017. Time-temperature management along the food cold chain: A review of recent developments: Food preservation along the cold chain. *Comprehensive Reviews in Food Science and Food Safety* 16.
-

- 
- NCCD, 2015. All india cold-chain infrastructure capacity assessment of status & gap (national centre for cold-chain development). [https://www.nccd.gov.in/PDF/CCSG\\_Final%20Report\\_Web.pdf](https://www.nccd.gov.in/PDF/CCSG_Final%20Report_Web.pdf), [Online; Accessed on 2019-03-20].
- NIAEM, 2017. Supply chain management in agriculture ( national institute of agricultural extension management). <http://www.manage.gov.in/studymaterial/scm-E.pdf>, [Online; Accessed on 2019-03-24].
- Paludetti, L. F., Kelly, A. L., O'Brien, B., Jordan, K., Gleeson, D., 2018. The effect of different precooling rates and cold storage on milk microbiological quality and composition. *Journal of Dairy Science* 101 (3), 1921 – 1929.
- Pang, Z., 01 2012. Scenario-based design of wireless sensor system for food chain visibility and safety. *Advances in Computer, Communication, Control and Automation. Lecture Notes in Electrical Engineering* 121, 541–548.
- Passos, E., Escobedo, J., Meunier, F., 1989. Simulation of an intermittent adsorptive solar cooling system. *Solar Energy* 42 (2), 103 – 111.
- Paulrajan, R., Jacob, F., 07 2009. Business models of vegetable retailers in india. *Great Lakes Herald* 4, 31–43.
- Ruiz-Garcia, L., Steinberger, G., Rothmund, M., 2010. A model and prototype implementation for tracking and tracing agricultural batch products along the food chain. *Food Control* 21 (2), 112 – 121.
- Saha, B., El-Sharkawy, I., Chakraborty, A., Koyama, S., 2007. Study on an activated carbon fiberethanol adsorption chiller: Part ii performance evaluation. *International Journal of Refrigeration* 30 (1), 96 – 102.
- Saha, B., El-Sharkawy, I., Chakraborty, A., Koyama, S., Banker, N., Dutta, P., Prasad, M., Srinivasan, K., 2006. Evaluation of minimum desorption temperatures of thermal compressors in adsorption refrigeration cycles. *International Journal of Refrigeration* 29 (7), 1175 – 1181.
- Saha, B. B., Chakraborty, A., Koyama, S., Yoon, S.-H., Mochida, I., Kumja, M., Yap, C., Ng, K. C., 2008. Isotherms and thermodynamics for the adsorption of n-butane on pitch based activated carbon. *International Journal of Heat and Mass Transfer* 51 (7), 1582 – 1589.
- Saha, B. B., Habib, K., El-Sharkawy, I. I., Koyama, S., 2009a. Adsorption characteristics and heat of adsorption measurements of r-134a on activated carbon. *International Journal of Refrigeration* 32 (7), 1563 – 1569.
- Saha, B. B., Habib, K., El-Sharkawy, I. I., Koyama, S., 2009b. Adsorption characteristics and heat of adsorption measurements of r-134a on activated carbon. *International Journal of Refrigeration* 32 (7), 1563 – 1569.
- URL <http://www.sciencedirect.com/science/article/pii/S0140700709000863>
-

- 
- Shashi, Cerchione, R., Singh, R., Centobelli, P., Shabani, A., 2018. Food cold chain management: From a structured literature review to a conceptual framework and research agenda. *The International Journal of Logistics Management* 29 (3), 792–821.
- Shukla, M., Jharkharia, S., 2013. Agrifresh produce supply chain management: a stateoftheart literature review. *International Journal of Operations & Production Management* 33 (2), 114–158.
- Srivastava, N., Eames, I., 1998. A review of adsorbents and adsorbates in solidvapour adsorption heat pump systems. *Applied Thermal Engineering* 18 (9), 707 – 714.  
URL <http://www.sciencedirect.com/science/article/pii/S1359431197001063>
- Subburaj, M., Babu, T. R., Subramonian, B. S., 2015. A study on strengthening the operational efficiency of dairy supply chain in tamilnadu, india. *Procedia - Social and Behavioral Sciences* 189, 285 – 291, operations Management in Digital Economy.
- Thu, K., Kim, Y.-D., Ismil, A. B., Saha, B. B., Ng, K. C., 2014. Adsorption characteristics of methane on maxsorb iii by gravimetric method. *Applied Thermal Engineering* 72 (2), 200 – 205, special Issue: International Symposium on Innovative Materials for Processes in Energy Systems 2013 (IMPRES2013).
- Uddin, K., ISLAM, M. A., Mitra, S., Lee, J., Thu, K., Saha, B., Koyama, S., 09 2017. Specific heat capacities of carbon-based adsorbents for adsorption heat pump application. *Applied Thermal Engineering* 129.
- UN, 2019. Current world population. <http://www.worldometers.info/world-population/>, [Online; Accessed on 2019-03-31].
- von Grebmer, K., Bernstein, J., Hossain, N., Brown, T., Prasai, N., Yohannes, Y., Patterson, F., Sonntag, A., Zimmerman, S.-M., Towey, O., Foley, C., 2017. 2017 global hunger index: The inequalities of hunger. <https://doi.org/10.2499/9780896292710>, [Online; Accessed on 2019-03-20].
- Wang, L., Wang, R., Oliveira, R., 2009. A review on adsorption working pairs for refrigeration. *Renewable and Sustainable Energy Reviews* 13 (3), 518 – 534.  
URL <http://www.sciencedirect.com/science/article/pii/S1364032108000038>
- Wang, R., Li, M., Xu, Y., Wu, J., 2000. An energy efficient hybrid system of solar powered water heater and adsorption ice maker. *Solar Energy* 68 (2), 189 – 195.
- Wang, R., Oliveira, R., 2006. Adsorption refrigerationan efficient way to make good use of waste heat and solar energy. *Progress in Energy and Combustion Science* 32 (4), 424 – 458.
- Younes, M. M., El-Sharkawy, I. I., Kabeel, A., Saha, B. B., 2017a. A review on adsorbent-adsorbate pairs for cooling applications. *Applied Thermal Engineering* 114, 394 – 414.

---

Younes, M. M., El-Sharkawy, I. I., Kabeel, A., Saha, B. B., 2017b. A review on adsorbent-adsorbate pairs for cooling applications. *Applied Thermal Engineering* 114, 394 – 414.

# India

## A.1 Optimal tilt angle of the collector

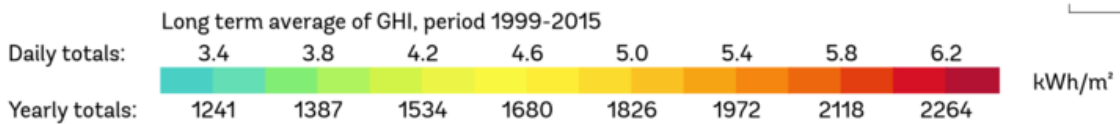
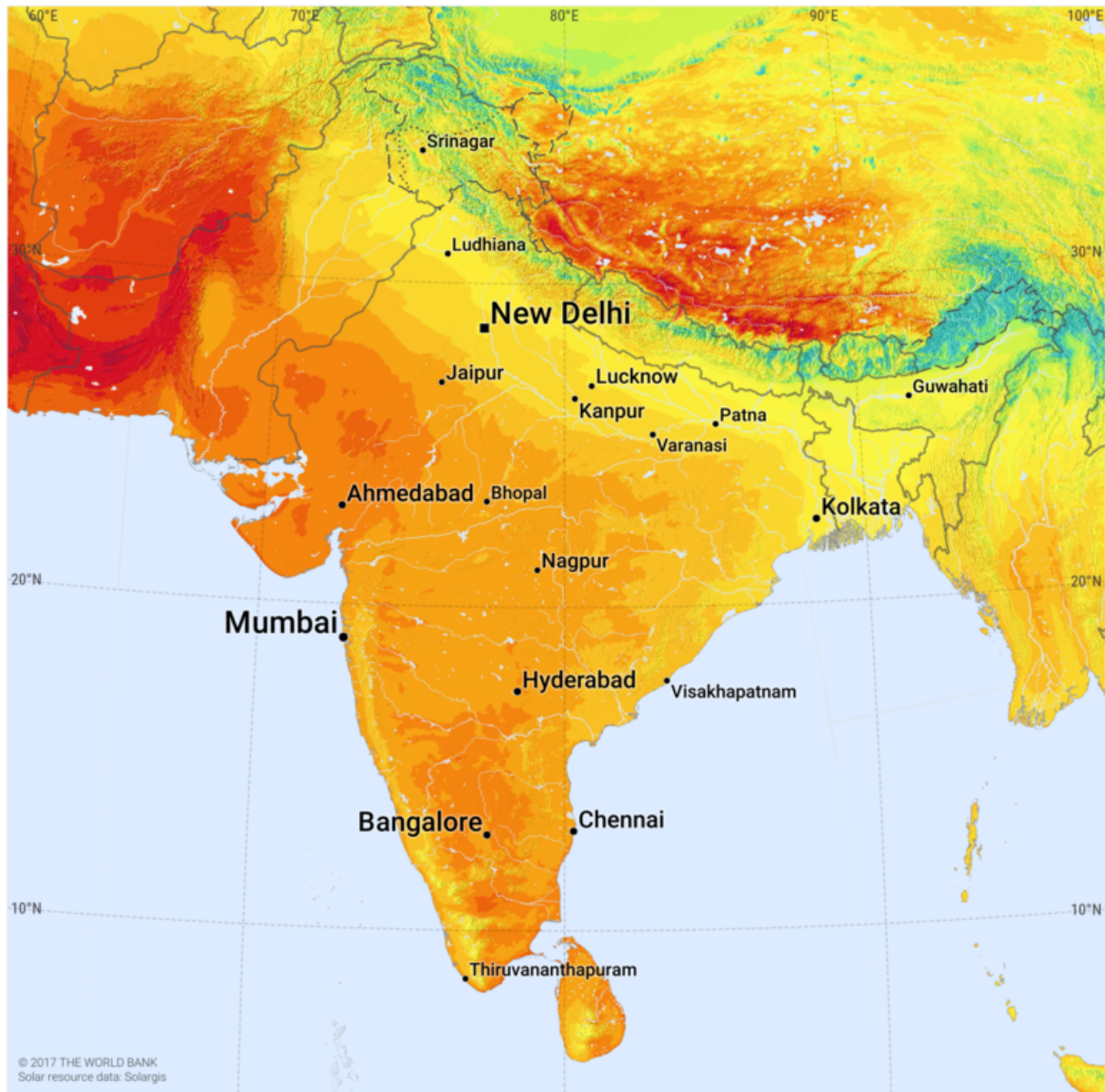
Date	Optimal angle [°] Kolkata	Optimal angle [°] Jaipur
01.jan	45,593	49,981
16.jan	43,702	48,090
31.jan	40,410	44,798
15.feb	35,934	40,322
02.mar	30,572	34,960
17.mar	24,678	29,066
01.apr	18,645	23,033
16.apr	12,871	17,259
01.mai	7,739	12,127
16.mai	3,591	7,979
31.mai	0,700	5,088
15.jun	-0,741	3,647
30.jun	-0,637	3,751
15.jul	1,005	5,393
30.jul	4,076	8,464
14.aug	8,373	12,761
29.aug	13,611	17,999
13.sep	19,443	23,831
28.sep	25,481	29,869
13.okt	31,326	35,714
28.okt	36,589	40,977
12.nov	40,923	45,311
27.nov	44,039	48,427
12.des	45,731	50,119
27.des	45,887	50,275

## A.2 Solar irradiation in India

SOLAR RESOURCE MAP

### GLOBAL HORIZONTAL IRRADIATION

### INDIA



This map is published by the World Bank Group, funded by ESMAP, and prepared by Solargis. For more information and terms of use, please visit <http://globalsolaratlas.info>.



## A.3 Previous system

Summary of various solar adsorption refrigeration systems.

YEAR	REFERENCES	TYPE	WORKING PAIR	SOLAR COLLECTOR TYPE	AREA (m <sup>2</sup> )	SOLAR RADIATIONS (MJ/(m <sup>2</sup> . Day))	APPLICATION	SOLAR COP	ICE MASS PRODUCED
1982	Dalgado et al. [106]	Simulation	Activated carbon-methanol	-	4	-	Ice maker	0.15(syst)	25kg/day
1986	Pons and Guilleminot [74]	Experimental	Activated carbon-methanol	Flat plate	6	16-19 MJ/day	Ice maker	0.10-0.12(net)	6 kg/(m <sup>2</sup> .day)
1986	Sakoda and Suzuki [75]	Simulation	Silica-gel-Water	Flat plate	0.25	-	-	0.2	-
1987	Pons and Grenier [107]	Experimental	Activated carbon-methanol	-	-	19-22 MJ/(m <sup>2</sup> .day)	Ice maker	0.10-0.12(net)	7 kg/ m <sup>2</sup>
1988	Grenier et al. [108]	Experimental	Zeolite -Water	Flat plate	20	17.8-25.3 MJ/ m <sup>2</sup>	Refrigerator	0.10 (net)	-
1990	Lemmini [109]	Simulation	Activated carbon-methanol	Flat plate	-	20 MJ/ m <sup>2</sup>	Refrigerator	0.114	-
1992	Tan et al. [77]	Experimental	Activated carbon-methanol	-	1.1	22MJ/( m <sup>2</sup> .day)	Ice maker	0.09	3kg/day
1993	Exell et al. [110]	Experimental	Activated carbon-methanol	Flat plate w/Tubes	0.97	-	Ice maker	0.1-0.123(net)	4kg /day
1994	Hadley et al. [111]	Experimental	Activated carbon-methanol	CPC	2	26.8MJ / ( m <sup>2</sup> .day)	Ice maker	0.2	1Kg
1995	Iloje et al. [112]	Simulation	CaCl <sub>2</sub> -Ammonia	Flat plate W/tubes	-	-	Ice maker	0.14	-
1995	Boelman et al. [56]	Experimental	Silica gel- water	Solar/ waste heat (40-75°C)	-	-	Chiller	0.4	-
1997	Bansal et al. [82]	Experimental	Sr-Cl <sub>2</sub> -Ammonia	Evacuated tubes	2.1	26 MJ/ m <sup>2</sup>	Refrigerator	0.081	-
1997	Critoph et al. [78]	Experimental	Ammonia	Flat plate w/Tubes	1.4	13.8-19.8 MJ(w/lamp)	-	0.061-0.071	-
1999	Sumathy and Li [79]	Experimental	Activated carbon-methanol	Flat plate	0.92	17-19 MJ/( m <sup>2</sup> .day)	Ice maker	0.1-0.12	4-5 kg /day
2000	Boubakri et al. [76]	Simulation	Activated carbon-methanol	Flat Plate	1	29 MJ/( m <sup>2</sup> .day)	Ice maker	0.19	11.5 Kg/ m <sup>2</sup>
2000	Gurgel et al. [81]	Simulation	Silica-gel-Water	Flat plate w/Tubes	1	23.8 MJ/( m <sup>2</sup> .day)	Water cooler	0.17	-
2001	Saha et al. [126]	Experimental	Silica-gel-Water	55°C source	-	-	Chiller	0.96	-
2002	Zhang and Wang [55]	Simulation	Activated carbon-methanol	Rational Flat Plate	0.4	21.6 MJ /day	Hybrid	0.18	-
2002	Li et al. [113]	Experimental	Activated carbon-methanol	Flat Plate	1.5	28-30 MJ/day(w/lamp)	Ice maker	0.13-0.14	7-10 Kg
2002	Mayor and Dind [83]	Simulation	Silica-gel-Water	Flat Plate W/tubes	1	-	Ice maker	0.10-0.15	-
2003	Anyanwu and Ezekwe [114]	Experimental	Activated carbon-methanol	Flat Plate W/tubes	1.2	-	Water cooler	0.036-0.057	-
2003	Li et al. [84]	Simulation	Zeolite -Water	Evacuated tubes	-	-	Refrigerator	0.25-0.30	-
2004	Khatab [115]	Experimental	Activated carbon-methanol	Glass shell + Reflector	-	17-20 MJ/( m <sup>2</sup> .day)	Ice maker	0.136-0.159	6.9-9.4 kg/ m <sup>2</sup> .day
2004	Aghbalou et al. [116]	Simulation	Activated -carbon-Ammonia	CPC	-	-	-	0.114	-
2004	Hildbrand et al. [117]	Experimental	Silica-gel-Water	Flat plate W/tubes	2	> 20 MJ/( m <sup>2</sup> .day)	Ice maker	0.12-0.23	4.7 kg/( m <sup>2</sup> .day)
2004	Li et al. [118]	Experimental	Activated-carbon-ethanol	Flat plate	0.94	18.2MJ	Ice maker	0.029	0 Kg
2005	Luo et al. [119]	Experimental	Activate-carbon-methanol	Flat Plate	1.2	15-23 MJ/( m <sup>2</sup> .day)	Ice maker	0.083-0.127(net)	3.2-6.5 Kg/ m <sup>2</sup>
2006	Boubakri [120]	Simulation	Activate-carbon-methanol	Flat plate	1	27 MJ/( m <sup>2</sup> .day)	Ice maker	0.14	5.2 Kg /day
2007	Leite et al. [77]	Experimental	Activate-carbon-methanol	Flat plate W/Tubes + Reflector	1(X2)	23.7 MJ/( m <sup>2</sup> .day)	Ice maker	0.085 (net)	6.05 Kg/ m <sup>2</sup>
2007	González and Rodríguez [121]	Experimental	Activate-carbon-methanol	CPC	0.55	19.5 MJ/( m <sup>2</sup> .day)	-	0.096	0Kg
2008	Ogueke and Anyanwu [122]	Simulation	Activated-carbon-methanol	Flat plate W/tubes	1.2	-	Water cooler	0.023(net)	-
2009	González et al. [86]	Simulation	Activated-carbon-methanol	CPC	0.55	-	Ice maker	0.117-0.087	0.06-0.4 Kg/ m <sup>2</sup>
2011	Hassan et al. [89]	Simulation	Activated-carbon-methanol	Flat plate W/tubes	1	900 W/m <sup>2</sup> (max)	-	0.211	-
2012	Suleiman et al. [29]	Simulation	Activated-carbon-methanol	Flat plate	2	-	Hybrid	0.024	-
2012	Omisanya et al. [90]	Experimental	Zeolite -Water	CPC	1	14.7 MJ/m <sup>2</sup>	Water cooler	0.8-1.5(cycle)	-
2013	Hassan [30]	Simulation	Activated-carbon-methanol	Flat tube	2	24.18 MJ/m <sup>2</sup>	Ice maker	0.618 (cycle)	27.82 Kg/day
2013	Abu-Hamdeh et al. [94]	Simulation	Olive waste-Methanol	FTC W/tubes	3.7	56.2 MJ/m <sup>2</sup> (on site)	Refrigerator	0.75(gross)	-
2013	Baju et al. [95]	Experimental	Activated-carbon-methanol	CPC	3	-	Refrigerator	0.196(day)0.335 (night)	-
2014	Santori et al. [123]	Experimental	Activated-carbon-methanol	Flat tube W/tubes	1.2	28.7 MJ/day	Ice maker	0.08 (net)	5 Kg/day

Review of previous solar ice makers (Goyal et al., 2016).

---

## A.4 Potato cold storage

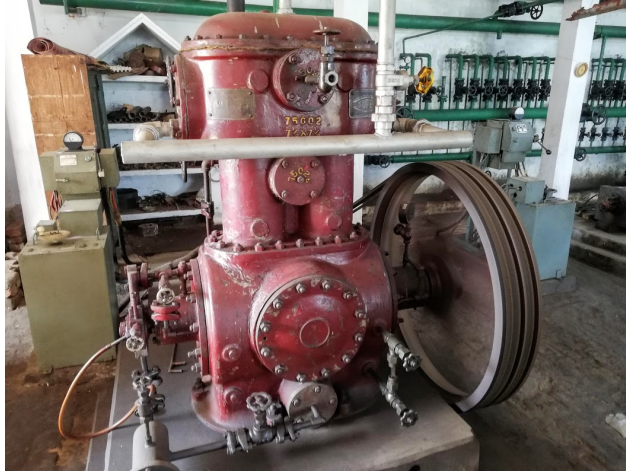
During our stay in Kharagpur, we had the opportunity to visit a potato cold storage. The potato harvest season is at the end of March and beginning of April, so we were able to see the storage after it was filled with potatoes. The following pictures give a glimpse of the Indian cold chain.



There is ice building on the evaporator inside of the cold storage, which suggests the system is running on too low temperatures. The evaporator was placed close to the ceiling, to provide natural circulation. There were also placed regular ceiling fans to provide some forced circulation.



Water is sprayed on the condenser to reduce the temperature. There is some algae growth in the baths, and the same water is circulating on the coils, which is causing the coils to have a green layer with algae.



The motors are placed outside in some form of a shed with simple walls covering it from the weather. There are no safety features, and ammonia is used as working fluid. There was a strong smell of ammonia when we walked into the engine room, and we felt some discomfort of the smell. However, we know that small amounts of ammonia smell strong and are not dangerous.



The front of the cold storage where the potatoes are stored intermediate before stacked in the cold storage. All the stacking is done by hand, and the cold storage was employing many people during the harvesting season.





There are no forms of pre-cooling of the potatoes. So the potatoes get all stacked up as in the picture above. There were three stories of the same height and four rows. The ammonia system was turned on when we were visiting, and the temperature inside had started to decrease. However, due to the amount of product, and no pre-cooling was the pull-down time expected to be one month.

## **A.5 Local fruit and vegetable market & local fish market**



The fish market at campus consisted of about 10 to 15 sellers in the same room. Each seller had the fish and seafood laying in front of them. This way, the buyers could select freely which fish they wanted. There was no form of cooling in the way they display the fish. The buyer pointed out which piece of fish they wanted and how much. The seller used the huge knife in front of them to gut the fish and weigh up the amount of fish the buyer asked for.



Some of the sellers we talked to had some boxes with ice they put the fish during night time. They used plastic and leaves as insulation. However, most of the sellers did not have ice or cooling because they said they only bought the amount of fish they knew they were going to sell. Nevertheless, it seems like they were not able to sell everything.



The fish and vegetable market was only open early and in the evening, during the day it was very hot, and most people did not do any shopping. In the picture above is a typical vegetable vendor. He has all the vegetables in front of him on display, and buyers come by and pick what they want. There is no form of cooling, but some people threw some water on the produce to lower the temperature. There were about ten vegetable vendors selling almost the same product in the same place.



## EES code

### B.1 6-point analysis model

```
$UNITSYSTEM kJ kg K
```

```
"Main program"
```

```
T_eva = -5 [K] +273,15 [K]
```

```
T_iw = 30 [K] +273,15 [K]
```

```
T_ad = 40 [K] +273,15 [K]
```

```
T_con = 30 + 273,15 [K]
```

```
{T_g = 100 [K] +273,15 [K]
```

```
T_sd = T_con*T_ad/T_eva
```

```
T_sa = T_g*T_eva/T_con
```

```
{Evaporation temperature R$ in evaporator}
```

```
{Initial water temperature}
```

```
{Adsorption temperature }
```

```
{Condensation temperature}
```

```
{Maximum generation temperature}}
```

```
{Maxsorb III - Methanol}
```

```
q_st = 1900 [kJ/kg]
```

```
D = 4,022*10(-6)
```

```
x_0 = 1,24 [kg/kg]
```

```
n = 2,0 [-]
```

```
R$ = 'Methanol'
```

```
C_pwf = 2,53 [kJ/kg K]
```

```
"Isosteric heat of adsorption"
```

```
"Maxsorb III"
```

```
"Cp working fluid"
```

```
{Maxsorb III - Ethanol}
```

```
q_st = 1026 [kJ/kg]
```

```
D = 9,265*10(-6)
```

```
x_0 = 1,2 [kg/kg]
```

```
n = 1,8 [-]
```

```
R$ = 'Ethanol'
```

```
C_pwf = 2,57 [kJ/kg K]
```

```
"Isosteric heat of adsorption"
```

```
"Maxsorb III"
```

```
"Cp working fluid"
```

```
Maxsorb III - R134a
```

```
q_st = 210 [kJ/kg]
```

```
D = 2,93*10(-4)
```

```
x_0 = 1,945 [kg/kg]
```

```
n = 1,17 [-]
```

```
R$ = 'R134a'
```

```
C_pwf = 0,88 [kJ/kg K]
```

```
"Isosteric heat of adsorption"
```

```
"Maxsorb III"
```

```
"Cp working fluid"
```

m_AC = 20 [kg]	"AC mass"
m_wall = 5 [kg]	"Collector mass"
m_eva = 4 [kg]	"Evaporator mass"
C_pAC = 0,920 [kJ/kg K]	"Cp AC"
C_pwall = 0,480 [kJ/kg K]	"Cp stainless steel"
C_pw = 4,180 [kJ/kg K]	"Cp water"
C_pice = 1,922 [kJ/kg K]	"Cp ice"
P_con = p_sat(R\$; T=T_con)	{21,39 kPa}
P_eva = p_sat(R\$; T=T_eva)	{2,86 kPa}

"Point 1: isosteric heating"

T[1] = T\_ad  
P[1] = P\_eva  
P\_sat[1] = p\_sat(R\$; T=T\_ad)  
h[1] = enthalpy(R\$; T=T[1]; P=P[1])  
x[1] = X\_0 \* exp(-D\*(T[1]^n \* ln(P\_sat[1]/P\_eva)))

"Point 2: isobaric desorption"

T[2] = T\_sd  
P[2] = P\_con  
P\_sat[2] = p\_sat(R\$; T=T\_sd)  
h[2] = enthalpy(R\$; T=T[2]; P=P[2])  
x[2] = x[1]

"Point 3: Isosteric cooling"

T[3] = T\_g  
P[3] = P\_con  
P\_sat[3] = p\_sat(R\$; T=T\_g)  
h[3] = enthalpy(R\$; T=T[3]; P=P[3])  
x[3] = X\_0 \* exp(-D\*(T[3]^n \* ln(P\_sat[3]/P\_con)))

"Point 4: Isobaric adsorption"

T[4] = T\_sa  
P[4] = P\_eva  
P\_sat[4] = p\_sat(R\$; T=T\_sa)  
h[4] = enthalpy(R\$; T=T[4]; P=P[4])  
x[4] = x[3]

"Find the energy input"

Q\_12 = (T\_sd - T\_ad) \* (C\_pAC\*m\_AC + C\_pwall\*m\_wall + m\_AC\*x[1]\*C\_pwf)  
Q\_23 = (T\_g - T\_ad) \* (C\_pAC\*m\_AC + C\_pwall\*m\_wall + m\_AC\*C\_pwf\*(x[1] + x[3])/2) +  
DeltaX\*m\_AC\*q\_st  
Q\_tot = Q\_12 + Q\_23

"R\$ cycle"

DeltaX = x[1] - x[3]

m\_wfTOT = x[2]\*m\_AC

"Point 5: R\$ high pressure"

T[5] = T\_ad  
P[5] = P\_con  
P\_sat[5] = p\_sat(R\$; T=T[5])  
h[5] = enthalpy(R\$; T=T[5]; x=0)

B<sub>2</sub>\_con = DeltaX \* m\_AC \* (h[2] - h[5])



---

"Point 5: R\$ low pressure"

$T[6] = T_{\text{eva}}$

$P[6] = P_{\text{eva}}$

$P_{\text{sat}}[6] = p_{\text{sat}}(R\$; T=T[6])$

$h[6] = h[5]$

$x_{\text{quality}} = \text{quality}(R\$; h=h[6]; P=p[6])$

$x_{\text{liquid}} = 1 - x_{\text{quality}}$

$h[7] = \text{enthalpy}(R\$; T=273; P=P_{\text{eva}})$

"Ice production"

$Q_{\text{cold}} = \Delta X * m_{\text{AC}} * (h[7] - h[6]) * x_{\text{liquid}}$

$h_{\text{water.ICE}} = \text{enthalpy\_fusion}(\text{Water})$

$m_{\text{ice}} = (Q_{\text{cold}}) / (h_{\text{water.ICE}} + C_{\text{pw}} * (T_{\text{iw}} - 273,15[\text{K}]) + C_{\text{pice}} * (273,15[\text{K}] - T_{\text{eva}}) + (m_{\text{eva}}) * C_{\text{pw}} * (T_{\text{iw}} - T_{\text{eva}}))$

$\text{COP} = Q_{\text{cold}} / (Q_{\text{tot}})$

---

## B.2 Transient analysis model

```
Subprogram findmu (Bi: mu_1; mu_2; mu_3)
y = mu_1/Bi
y = 1/tan(mu_1)
x = mu_2/Bi
x = 1/tan(mu_2)
z = mu_3/Bi
z = 1/tan(mu_3)
End

Procedure singledimensionalanalsis (T_amb; T_bed_avg; T_bed_cen; T_bed_mid; T_bed_edg; j :
T_bed_avg_new; T_bed_cen_new; T_bed_mid_new; T_bed_edg_new )
k = 0,088 "Thermal conductivity vanlig 0,13-0,20"
rho = 281 "Density 281 - 577 kg/m3"
C_p.AC = (200 + 2*T_bed_avg + (3605410)/(T_bed_avg^2)) "Specific heat"
a = k/(C_p.AC * rho) "Thermal diffusivity 0,4 - 1,3 * 10^6"
L = 0,05 "Thickness of bed"
alpha = 5 "External heat transfer coefficient 5-10 for air"
time = 30 "Seconds"

Bi = (alpha * L)/(k)
Fo = (a * j * time)/(L^2)

Call findmu (Bi: mu_1; mu_2; mu_3)
theta_avg1 = ((2*sin(mu_1)^2) / (mu_1^2 + mu_1*sin(mu_1)*cos(mu_1))) * exp(-1*mu_1^2 *Fo)
theta_avg2 = ((2*sin(mu_2)^2) / (mu_2^2 + mu_2*sin(mu_2)*cos(mu_2))) * exp(-1*mu_2^2 *Fo)
theta_avg3 = ((2*sin(mu_3)^2) / (mu_3^2 + mu_3*sin(mu_3)*cos(mu_3))) * exp(-1*mu_3^2 *Fo)

theta_cen1 = ((2*sin(mu_1)) / (mu_1 + sin(mu_1)*cos(mu_1))) * exp(-1*mu_1^2 *Fo) * cos(0)
theta_cen2 = ((2*sin(mu_2)) / (mu_2 + sin(mu_2)*cos(mu_2))) * exp(-1*mu_2^2 *Fo) * cos(0)
theta_cen3 = ((2*sin(mu_3)) / (mu_3 + sin(mu_3)*cos(mu_3))) * exp(-1*mu_3^2 *Fo) * cos(0)

theta_mid1 = ((2*sin(mu_1)) / (mu_1 + sin(mu_1)*cos(mu_1))) * exp(-1*mu_1^2 *Fo) * cos(mu_1*0,5)
theta_mid2 = ((2*sin(mu_2)) / (mu_2 + sin(mu_2)*cos(mu_2))) * exp(-1*mu_2^2 *Fo) * cos(mu_2*0,5)
theta_mid3 = ((2*sin(mu_3)) / (mu_3 + sin(mu_3)*cos(mu_3))) * exp(-1*mu_3^2 *Fo) * cos(mu_3*0,5)

theta_edg1 = ((2*sin(mu_1)) / (mu_1 + sin(mu_1)*cos(mu_1))) * exp(-1*mu_1^2 *Fo) * cos(mu_1)
theta_edg2 = ((2*sin(mu_2)) / (mu_2 + sin(mu_2)*cos(mu_2))) * exp(-1*mu_2^2 *Fo) * cos(mu_2)
theta_edg3 = ((2*sin(mu_3)) / (mu_3 + sin(mu_3)*cos(mu_3))) * exp(-1*mu_3^2 *Fo) * cos(mu_3)

theta_avg_temp = theta_avg1 + theta_avg2 + theta_avg3

If ( theta_avg_temp > 1) Then
theta_avg = 1
Else
theta_avg = theta_avg_temp
Endif

theta_cen_temp = theta_cen1 + theta_cen2 + theta_cen3
```

---

```

If ( theta_cen_temp > 1) Then
theta_cen = 1
Else
theta_cen = theta_cen_temp
Endif

theta_mid_temp = theta_mid1 + theta_mid2 + theta_mid3

If ( theta_mid_temp > 1) Then
theta_mid = 1
Else
theta_mid = theta_mid_temp
Endif

theta_edg_temp = theta_edg1 + theta_edg2 + theta_edg3

If ( theta_edg_temp < 0) Then
theta_edg = 1
Else
theta_edg = theta_edg_temp
Endif

T_bed_avg_new = T_amb + theta_avg*(T_bed_avg - T_amb) "Dimensional analysis"

T_bed_cen_new = T_amb + theta_cen*(T_bed_cen - T_amb)

T_bed_mid_new = T_amb + theta_mid*(T_bed_mid - T_amb)

T_bed_edg_new = T_amb + theta_edg*(T_bed_edg - T_amb)

End

T_amb = 273
T_bed_avg[0] = 373
T_bed_cen[0] = 373
T_bed_mid[0] = 373
T_bed_edg[0] = 373
Time[0] = 0

Duplicate j=1;240
Call singledimensionalanalysis (T_amb; T_bed_avg[j-1]; T_bed_cen[j-1]; T_bed_mid[j-1]; T_bed_edg[j-1]; j;
T_bed_avg[j]; T_bed_cen[j]; T_bed_mid[j]; T_bed_edg[j] )
Time[j] = j*0,5 [min]
End

```

## B.3 Simulation through one day

"Solar irradiance and ambient temperature"

```
Module sun_ambient_temperature(t_hr: I; T_amb)
$COMMON T_amb.max; T_amb.min; timestep; Time_interval
I_max = 660 * Time_interval / 1000           "Max value through the day 900 given in W times
time_interval in sec "
t_sunrise = 6 * timestep                    "Making the right amount of timestep in 1 hr"
t_sunset = 18 * timestep
sun = I_max * cos( (pi*(t_hr-t_sunrise)) / (t_sunset - t_sunrise))
I = if(0; sun; sun ; 0)                    "Only positive values for I, else 0"
T_amb = (T_amb.max + T_amb.min) / 2 + (T_amb.max - T_amb.min) / 2 * cos( (pi*(t_hr-t_sunrise)) / (t_sunset - t_sunrise) )
End
```

Procedure logic (I; Q; P\_bed\_old; T\_bed\_old; x\_eq\_old: P\_bed; T\_bed)

```
$COMMON P_con; P_eva; R$
If ( ( I > Q ) ) Then
  If ( P_bed_old < P_CON ) Then
    Call heating_bed_without_dx(I; Q; T_bed_old; x_eq_old: T_bed; P_bed)
  Else
    Call desorping(I; Q; T_bed_old; x_eq_old: T_bed; P_bed)
  Endif
Else
  If ( P_bed_old > P_EVA ) Then
    Call cooling_bed_without_dx(I; Q; T_bed_old; x_eq_old : T_bed; P_bed)
  Else
    Call adsorbing(Q; T_bed_old; x_eq_old: T_bed; P_bed)
  Endif
Endif
End
```

"Stage 1 -> Pressure increase"

```
Subprogram heating_bed_without_dx(I; Q; T_bed_old; x : T_bed; P_bed)
$COMMON C_p.AC; m_AC; C_p.wall; m_wall; DELTAH; D; R$; Areal; x_0; P_con; C_p.wf; n
I - Q = (C_p.AC*m_AC + C_p.wall*m_wall + C_p.wf*x*m_AC)*(T_bed - T_bed_old)
p_sat = p_sat(R$; T=T_bed)
ln(x/X_0) = -D*(T_bed*ln(p_sat/P_bed))^n
End
```

"Stage 2 -> Temperature increase with reduction in x\_eq"

```
Procedure desorping(I; Q; T_bed_old; x_eq_old: T_bed; P_bed)
$COMMON C_p.AC; m_AC; C_p.wall; m_wall; DELTAH; D; R$; Areal; x_0; P_con; C_p.wf; n
EnergyBalanceLS = I - Q           "Energy balance left side"
P_bed = P_CON
T_bed_guess = T_bed_old + 0,05
P_sat = p_sat(R$; T=T_bed_guess)
x_eq = X_0 * exp(- D*(T_bed_guess*ln(P_sat/P_CON))^n)
dx_temp = x_eq_old - x_eq
EnergyBalanceRS = (C_P.AC*M_AC + C_P.WALL*M_WALL + C_P.WF*x_eq*M_AC)*(T_bed_guess - T_bed_old) + dx_temp*DELTAH*M_AC
```

---

```

    If (EnergyBalanceLS > EnergyBalanceRS ) Then
    Repeat
    T_bed_guess = T_bed_guess + 0,02
    P_sat = p_sat(R$; T=T_bed_guess)
    x_eq = X_0* exp(- D*(T_bed_guess*ln(P_sat/P_CON))^n )
    dx_temp = x_eq_old - x_eq
    EnergyBalanceRS = (C_P.AC*M_AC + C_P.WALL*M_WALL + C_P.WF*x_eq*M_AC)*(T_bed_guess -
T_bed_old) + dx_temp*DELTAH*M_AC
    Until (EnergyBalanceLS < EnergyBalanceRS)
    T_bed = T_bed_guess
    Else
    T_bed = T_bed_guess
    Endif
End

" Stage 3 -> Temperature & pressure decrease without dx"
Subprogram cooling_bed_without_dx(I; Q; T_bed_old; x : T_bed; P_bed)
$COMMON C_p.AC; m_AC; C_p.wall; m_wall; DELTAH; D; R$; Areal; x_0; P_con; C_p.wf; n
I - Q = (C_p.AC*m_AC + C_p.wall*m_wall + C_p.wf*x*m_AC)*(T_bed - T_bed_old)
p_sat=p_sat(R$; T=T_bed)
ln (x/X_0) = -D *(T_bed* ln(p_sat/P_bed))^n
End

"Stage 4 -> Temperature decrease with increase in x_eq"
Procedure adsorbing(Q; T_bed_old; x_eq_old: T_bed; P_bed)
$COMMON C_p.AC; m_AC; C_p.wall; m_wall; DELTAH; D; R$; Areal; x_0; P_con; C_p.wf; n; P_eva
EnergyBalanceLS = - Q "Negative value"
P_bed = P_EVA
P_bed_guess = T_bed_old - 0,01
P_sat = p_sat(R$; T=T_bed_guess)
x_eq =X_0* exp(- D*(T_bed_guess*ln(P_sat/P_EVA))^N )
dx_temp = (x_eq_old - x_eq) "negative value. x_eq is going to be bigger than the old"
EnergyBalanceRS = (C_P.AC*M_AC + C_P.WALL*M_WALL+ C_P.WF*x_eq*M_AC)*(T_bed_guess -
T_bed_old) + dx_temp*DELTAH*M_AC

    If ( EnergyBalanceLS < EnergyBalanceRS ) Then
    Repeat
    T_bed_guess = T_bed_guess - 0,01
    P_sat = p_sat(R$; T=T_bed_guess)
    x_eq =X_0* exp(- D*(T_bed_guess*ln(P_sat/P_EVA))^N )
    dx_temporary = x_eq_old - x_eq
    EnergyBalanceRS = (C_P.AC*M_AC + C_P.WALL*M_WALL+ C_P.WF*x_eq*M_AC)*(T_bed_guess -
T_bed_old) + dx_temporary*DELTAH*M_AC
    Until ( EnergyBalanceLS > EnergyBalanceRS)
    T_bed = T_bed_guess
    Else
    T_bed = T_bed_guess
    Endif
End

```

---

---

```

Procedure heat_loss (I; Q_old; T_bed; T_amb; p_bed : Q)
$COMMON Areal; Time_interval; p_eva
dT = T_bed - T_amb
U_L_backAndSides = 0,81                                "Insulation"
U_L_backwi = 15                                       "Without insulation, natural convection varies from 5-10"
If ( I > Q_old ) Then                                "When the bed is heating up, want min Q"
    U_L_top = u_l_top (T_bed; T_amb)
    U_L = U_L_top + U_L_backAndSides
    Q = (U_L_top*AREAL*dT*TIME_INTERVAL)/1000
Else                                                "When bed is cooling, want max Q"
    If (p_bed > P_EVA) Then
        U_L_top = u_l_top (T_bed; T_amb)
        U_L = U_L_top + U_L_backAndSides
        Q = (U_L_top*AREAL*dT*TIME_INTERVAL)/1000
    Else
        U_L_top = u_l_top (T_bed; T_amb)              "Remove the back cover"
        U_L = U_L_top + U_L_backwi
        Q = (U_L*AREAL*dT*TIME_INTERVAL)/1000
    Endif
Endif

```

**End**

```

Function u_l_top (T_bed; T_amb)
N = 2                                                  "Number of glass covers"
h_w = 10 [W/m^2K]                                    "Wind heat transfer coefficient"
Sigma = 5,67*10^(-8)                                 "Stefan-Boltzmann constant"
beta = 20                                            "Must be in degrees..."
C = 520*(1-0,000051*beta^2)
e = 0,430*(1-(100/T_bed))                            "Mean plate temperature... sjekk seksjon 6.9"
eps_g = 0,88                                         "Emmittance of glass"
eps_p = 0,95                                         "Emmittance of plate"
f = (1+0,089*h_w-0,1166*h_w*eps_p)*(1+0,07866*N)
A = (C/T_bed)*((abs(T_bed-T_amb))/(N+f))^e
B = Sigma*(T_bed+T_amb)*(T_bed^2 + T_amb^2)
B_2 = (eps_p + 0,00591*N*h_w)^(-1)
B_3 = (2*N+f-1+0,133*eps_p)/eps_g
If (A = 0 ) Then                                    "Get division by 0..."
    U_t = (1/h_w)^(-1) + B/(B_2+B_3 -N)
Else
    U_t = (N/A + 1/h_w)^(-1) + B/(B_2+B_3 -N)        "Correct format"
Endif
u_l_top = U_t
End

```

```

Procedure massflow (x_eq_old; x_eq; T_bed_old; T_bed; mass_tot_old : mass; mass_tot)
$COMMON C_p.AC; m_AC; C_p.wall; m_wall; DELTAH; D; R$; Areal; x_0; P_con; C_p.wf; n; P_eva
If ( T_bed_old > T_bed ) Then
    mass_des = (x_eq - x_eq_old)*M_AC
Else
    mass_des = (x_eq - x_eq_old)*M_AC
Endif
mass_tot = mass_tot_old + mass_des
mass = mass_des

```

---

**End**



---

```

Procedure icemaking (mass ; Q_cold_tot_old; m_ice_tot_old : Q_cold_tot; m_ice_tot)
$COMMON C_pw; C_pice; h_con; x_quality; x_liquid; DELTAh_vap; T_iw; T_eva
If ( mass > 0 ) Then
Q_cold_dot = DELTAH_VAP* X_LIQUID*mass
m_ice_dot = (Q_cold_dot) / (enthalpy_fusion(Water) + C_PW*(T_IW - 273,15[K])+ C_PICE*(273,15[K] -
T_EVA) )
Q_cold_tot = Q_cold_tot_old + Q_cold_dot
m_ice_tot = m_ice_tot_old + m_ice_dot
Else
mass = 0
Q_cold_dot = DELTAH_VAP* X_LIQUID*mass
m_ice_dot = (Q_cold_dot) / (enthalpy_fusion(Water) + C_PW*(T_IW - 273,15[K])+ C_PICE*(273,15[K] -
T_EVA) )
Q_cold_tot = Q_cold_tot_old + Q_cold_dot
m_ice_tot = m_ice_tot_old + m_ice_dot
Endif
End

"CONSTANTS"
R$ = 'Ethanol'
T_eva = -5 [K] +273 [K]           {Evaporation temperature working fluid in evaporator}
T_con = +30 [K] + 273 [K]
P_eva = p_sat(R$; T= T_eva) {Evaporation pressure working fluid in evaporator}
P_con = p_sat(R$; T= T_con)
T_iw = 30 [K] +273,15 [K]           {Initial water temperature}

"ENERGY BALANCE CONSTANTS"
C_p.wall = 0,480 [kJ/kg K]           "Stainless steel"
C_p.AC = 0,930 [kJ/kg K]           "Maxsorb"

"EXPERIMENTAL DATA FOR MAXSORB III - WORKING FLUID"
"METHANOL - MAXSORB"
DELTAH = 1900 [kJ/kg]           "Isosteric heat of adsorption"
D = 4,022*10^(-6) [1/K]           "Maxsorb III"
x_0 = 1,24 [kg/kg]
n = 2,0 [-]
C_p.wf = 2,53 [kJ/kg K]           "Cp working fluid"

"ETHANOL - MAXSORB"
DELTAH = 1026 [kJ/kg]           "Isosteric heat of adsorption"
D = 9,265*10^(-6)           "Maxsorb III"
x_0 = 1,2 [kg/kg]
n = 1,8 [-]
C_p.wf = 2,57 [kJ/kg K]           "Cp working fluid"

"ICEMAKING"
C_pw = 4,180 [kJ/kg K]           "Cp water"
C_pice = 1,922 [kJ/kg K]           "Cp ice"
h_con = enthalpy(R$; T=T_con ;x=0)           "Enthalpy after the condenser"
x_quality = quality(R$; h=h_con; P=p_eva)           "Quality after throttling"

x_liquid = 1 - x_quality
DELTAh_vap=enthalpy_vaporization(R$; T=T_eva)

```

---

---

"SYSTEM DESIGN"

Areal = 1 [m<sup>2</sup>] {1 square meter area}  
m\_AC = 30 [kg]  
m\_wall = 5 [kg]

"TIME"



Time\_interval = 300 [s] {5 min intervals}  
Timestep = 3600/ Time\_interval  
T\_amb.max = 35 +273 [K]  
T\_amb.min = 25 +273 [K]

"MAIN PROGRAM"

T\_bed[0] = 30 +273  
p\_sat[0]=p\_sat(R\$ ; T=T\_bed[0])  
x\_eq[0] = X\_0\* exp(- D\*(T\_bed[0]\*ln(P\_sat[0]/P\_eva))^n )  
P\_bed[0] = p\_eva  
Q[0] = 0  
mass\_tot[0]= 0  
Q\_cold\_tot[0] = 0  
m\_ice\_tot[0] = 0  
l\_tot[0] = 0  
  
*Duplicate* j = 1; 288  
t\_hr[j] = j\*5 /60  
*Call* sun\_ambient\_temperature(j: l[j]; T\_amb[j])  
l\_tot[j] = l[j]/3600 + l\_tot[j-1]  
*Call* logic (l[j]; Q[j-1]; P\_bed[j-1]; T\_bed[j-1]; x\_eq[j-1]: P\_bed[j]; T\_bed[j])  
*Call* heat\_loss (l[j]; Q[j-1]; T\_bed[j]; T\_amb[j]; p\_bed[j] : Q[j])  
p\_sat[j]=p\_sat(R\$ ; T=T\_bed[j])  
x\_eq[j] = X\_0\* exp(- D\*(T\_bed[j]\*ln(P\_sat[j]/P\_bed[j]))^n )  
*Call* massflow (x\_eq[j-1]; x\_eq[j]; T\_bed[j-1]; T\_bed[j]; mass\_tot[j-1]: mass[j]; mass\_tot[j])  
*Call* icemaking (mass[j] ; Q\_cold\_tot[j-1]; m\_ice\_tot[j-1] : Q\_cold\_tot[j]; m\_ice\_tot[j])  
*End*



# Hazardous activity identification process

NTNU	Hazardous activity identification process	Prepared by	Number	Date	
		HSE section	HMSRV2601E	09.01.2013	
HSE		Approved by		Replaces	
		The Rector		01.12.2006	

Unit: Department of Energy and Process Engineering

Date: 28.01.2019

Line manager: Trygve Magne Eikevik

Participants in the identification process: Trygve Magne Eikevik (Norwegian supervisor) and Souvra Mitra (Indian supervisor)

Short description of the main activity/main process: Master project for student Erling Vingelsgård. Project title: *Design and simulation of a sorption based solar ice maker.*

Is the project work purely theoretical? (YES/NO): NO

Answer "YES" implies that supervisor is assured that no activities requiring risk assessment are involved in the work. If NO, briefly describe the activities below.

Signatures:

Responsible supervisor:  Dr. Souvra Mitra

Student:  Erling Vingelsgård

ID nr.	Activity/process	Responsible person	Existing documentation	Existing safety measures	Laws, regulations etc.	Comment
1	Transport in India	Erling Vingelsgård		Seat belts, travel insurance		
2	Recreational activities	Erling Vingelsgård		Don't walk alone, listen to local students, use common sense		
3	Food and water	Erling Vingelsgård		Drink bottled water and be careful with hygiene		
4	Disease and general health	Erling Vingelsgård		Vaccines, travel insurance and common sense		
5	Visiting local farmers/cold storages	Erling Vingelsgård		Careful with hygiene, travel insurance, common sense		
6						

	<h2 style="margin: 0;">Risk assessment</h2>	Prepared by	Number	Date	
		HSE section	HMSRV2803E	04.02.2011	
		Approved by The Rector		Replaces 01.12.2008	

Unit: Department of Energy and Process Engineering

Date: 28.01.2019

Line manager: Trygve Magne Eikevik

Participants in the identification process: Trygve Magne Eikevik (Norwegian supervisor) and Maddali Ramgopal (Indian supervisor)

Short description of the main activity/main process: Master project for student Tom André Bredesen. Project title: *Design and simulation of a small cold storage with NH<sub>3</sub> refrigeration system and CO<sub>2</sub> as indirect cooling loop for storing of fresh fruits and vegetables*

Signatures: Responsible supervisor:

Student:

Activity from the identification process form	Potential undesirable incident/strain	Likelihood:	Consequence:			Risk Value (human)	Comments/status Suggested measures
		Likelihood (1-5)	Human (A-E)	Environment (A-E)	Economy/material (A-E)		
Transport in India	Traffic accident	3	C	C	C	3C	See hazardous activity identification form
Recreational activities	Injuries, crime	2	A	A	A	2A	See hazardous activity identification form
Food and water	Food poisoning	4	A	A	B	4A	See hazardous activity identification form
Disease and general health	Disease, other health issues	4	A	A	B	4A	See hazardous activity identification form
Visiting local farmers/cold storages	Injury, disease	3	B	A	B	3B	See hazardous activity identification form

Likelihood, e.g.:

1. Minimal
2. Low
3. Medium
4. High
5. Very high

Consequence, e.g.:

- A. Safe
- B. Relatively safe
- C. Dangerous
- D. Critical
- E. Very critical

Risk value (each one to be estimated separately):

- Human = Likelihood x Human Consequence  
 Environmental = Likelihood x Environmental consequence  
 Financial/material = Likelihood x Consequence for Economy/material

 NTNU HSE/KS	<h2 style="margin: 0;">Risk assessment</h2>	Prepared by	Number	Date	
		HSE section	HMSRV2603E	04.02.2011	
		Approved by		Replaces	
		The Rector		01.12.2006	

**Potential undesirable incident/strain**  
 Identify possible incidents and conditions that may lead to situations that pose a hazard to people, the environment and any materiel/equipment involved.

**Criteria for the assessment of likelihood and consequence in relation to fieldwork**  
 Each activity is assessed according to a worst-case scenario. Likelihood and consequence are to be assessed separately for each potential undesirable incident. Before starting on the quantification, the participants should agree what they understand by the assessment criteria:

**Likelihood**

Minimal 1	Low 2	Medium 3	High 4	Very high 5
Once every 50 years or less	Once every 10 years or less	Once a year or less	Once a month or less	Once a week


**Consequence**

Grading	Human	Environment	Financial/material
<b>E</b> Very critical	May produce fatality/ies	Very prolonged, non-reversible damage	Shutdown of work >1 year.
<b>D</b> Critical	Permanent injury, may produce serious serious health damage/sickness	Prolonged damage. Long recovery time.	Shutdown of work 0.5-1 year.
<b>C</b> Dangerous	Serious personal injury	Minor damage. Long recovery time	Shutdown of work < 1 month
<b>B</b> Relatively safe	Injury that requires medical treatment	Minor damage. Short recovery time	Shutdown of work < 1week
<b>A</b> Safe	Injury that requires first aid	Insignificant damage. Short recovery time	Shutdown of work < 1day

The unit makes its own decision as to whether opting to fill in or not consequences for economy/materiel, for example if the unit is going to use particularly valuable equipment. It is up to the individual unit to choose the assessment criteria for this column.

**Risk = Likelihood x Consequence**  
 Please calculate the risk value for "Human", "Environment" and, if chosen, "Economy/materiel", separately.

**About the column "Comments/status, suggested preventative and corrective measures":**  
 Measures can impact on both likelihood and consequences. Prioritise measures that can prevent the incident from occurring; in other words, likelihood-reducing measures are to be prioritised above greater emergency preparedness, i.e. consequence-reducing measures.

NTNU	Risk matrix	prepared by	Number	Date	
		HSE Section	HMSRV2604	8 March 2010	
HSE/IKS		approved by	Page	Replaces	
	Rector	4 of 4	9 February 2010		

### MATRIX FOR RISK ASSESSMENTS at NTNU

CONSEQUENCE	Extremely serious	E1	E2	E3	E4	E5
	Serious	D1	D2	D3	D4	D5
	Moderate	C1	C2	C3	C4	C5
	Minor	B1	B2	B3	B4	B5
	Not significant	A1	A2	A3	A4	A5
		Very low	Low	Medium	High	Very high
		LIKELIHOOD				

Principle for acceptance criteria. Explanation of the colours used in the risk matrix.

Colour	Description
Red	Unacceptable risk. Measures must be taken to reduce the risk.
Yellow	Assessment range. Measures must be considered.
Green	Acceptable risk Measures can be considered based on other considerations.